

Geologic Map of the Mount Taylor Volcano Area, New Mexico

Geologic Map 80

Fraser Goff, Shari A. Kelley, Cathy J. Goff,
David J. McCraw, G. Robert Osburn, John R. Lawrence,
Paul G. Drakos, and Steven J. Skotnicki



New Mexico Bureau of Geology and Mineral Resources
A research division of New Mexico Institute of Mining and Technology

Socorro 2019

Geologic Map of the Mount Taylor Volcano Area, New Mexico

Fraser Goff, Shari A. Kelley, Cathy J. Goff, David J. McCraw,
G. Robert Osburn, John R. Lawrence, Paul G. Drakos, and Steven J. Skotnicki

Copyright © 2019

NEW MEXICO BUREAU OF GEOLOGY AND MINERAL RESOURCES

CARTOGRAPHY

David J. McCraw
Phil L. Miller
Mark M. Mansell

PROJECT EDITING, LAYOUT, & DESIGN

David J. McCraw
Phil L. Miller
Gina D'Ambrosio
Brigitte Felix

GRAPHICS

David J. McCraw
Stephanie Chavez
Phil L. Miller

Dr. Nelia W. Dunbar, *Director and State Geologist*
Dr. J. Michael Timmons, *Associate Director for Mapping Program and Deputy Director*

A research division of

NEW MEXICO INSTITUTE OF MINING AND TECHNOLOGY

Dr. Stephen G. Wells, *President*

801 Leroy Place
Socorro, NM 87801
(575) 835-5145

BOARD OF REGENTS

Ex Officio

Michelle Lujan Grisham, Governor of New Mexico
Kate O'Neill, Secretary of Higher Education

Appointed

Deborah Peacock, President, 2011–2022, Corrales
Jerry A Armijo, Secretary/Treasurer, 2015–2020, Socorro
Dr. Yolanda Jones King, 2018–2024, Socorro
David Gonzales, 2015–2020, Farmington
Veronica Espinoza, Student Member, 2018–2020, Albuquerque

New Mexico Bureau of Geology and Mineral Resources

First Printing 2019

Published by Authority of State of New Mexico, NMSA 1953 Sec. 63–1–4
ISBN 978-1-883905-44-6

Available from New Mexico Bureau of Geology and Mineral Resources
801 Leroy Place, Socorro, NM 87801
geoinfo.nmt.edu

Geologic Map of the Mount Taylor Volcano Area, New Mexico

Fraser Goff¹, Shari A. Kelley², Cathy J. Goff³, David J. McCraw²,
G. Robert Osburn⁴, John R. Lawrence⁵, Paul G. Drakos⁶, Steven J. Skotnicki⁷

¹*Department of Earth and Environmental Science, New Mexico Institute of Mining and Technology, Socorro, NM 87801*

²*New Mexico Bureau of Geology and Mineral Resources, New Mexico Institute of Mining and Technology, Socorro, NM 87801*

³*Independent Consultant, 5515 Quemazon, Los Alamos, NM 87545*

⁴*Earth and Planetary Science, Washington University, St. Louis, MO, 63130*

⁵*Lawrence GeoServices Ltd. Co., 2321 Elizabeth St. NE, Albuquerque, NM 87112*

⁶*Glorieta Geoscience Inc., P.O. Box 5727, Santa Fe, NM 87502*

⁷*Independent Consultant, 281 W. Amoroso Dr., Gilbert, AZ 85233*



Looking WSW from near the east edge of the map area across Laguna Bandeja maar toward Mount Taylor volcano: CP = Cerro Pelón area trachybasalt flows and cones, LM = La Mosca trachydacite, and SP = Spud Patch trachydacite dome and flow complex. Ridge line east (left) of La Mosca is composed of many unnamed domes and flows of trachydacite and trachyandesite. Hills in the middle foreground are various unnamed trachybasalt scoria cones on southern Mesa Chivato.

Introduction

This map is a 1:36,000 compilation of six recently published 1:24,000 quadrangles (2008–2014) that encompass Mount Taylor and surrounding mesas and basins (Cover photo, Figs. 1 and 2). Our final field checking, edge matching, and sampling for this map resulted in the presentation of more geologic details than depicted on the earlier maps. Mount Taylor is an extinct composite volcano and is New Mexico's second largest volcano after the Valles caldera and Jemez Mountains (e.g., Price, 2010, p. 51). The volcano is part of a northeast-trending volcanic field that includes Mesa Chivato and comprises one of many volcanic fields along the Jemez volcanic lineament (Mayo, 1958). Mount Taylor forms a conspicuous topographic feature roughly 20 km northeast of Grants. The peak is named in honor of President Zachary Taylor, a major general who became U.S. president in March 1849 and died prematurely in office in July 1850 (Simpson, 1850). The volcano and surroundings were inhabited by pre-Columbian Indian cultures (Paleo-Indian, Archaic, and ancestral Puebloan, Fig. 3a) and the region is sacred to at least four Native American tribes who have inhabited the region, some for many centuries (Acoma, Laguna, Navajo and Zuni,

e.g., <http://www.manataka.org/page2469.html>). The Mount Taylor region was well known to early Spanish explorers who entered the region after the mid-1500s. The oldest Spanish settlement in the map area is Seboyeta established in 1746 (<http://voiceofthesouthwest.org/2014/04/23/a-history-of-the-old-mining-missions-in-cibola-county-nm>). Around 1820 Mexican settlers came and American settlers arrived after 1848 (Fig. 3b; see Appendix 1 for English translations of Spanish words). All inhabitants left an indelible mark on the landscape.

Many researchers have studied volcanic rocks at Mount Taylor. Dutton (1885) wrote the first accurate description of these rocks and provided a rough geologic map. Johnson (1907) first described the volcanic necks east of Mesa Chivato. Hunt (1938) published a detailed discussion of the geology and structure of the Mount Taylor "volcanic field," and published a generalized color geologic map of the volcano and surroundings (1 inch = 2 miles). Coal, uranium, perlite, and geothermal investigations since the 1950s resulted in several more geologic maps covering various parts of Mount Taylor volcano (Moench, 1963; Santos, 1966; Chapman et al., 1974; Lipman et al., 1979; Dillinger, 1990), but except

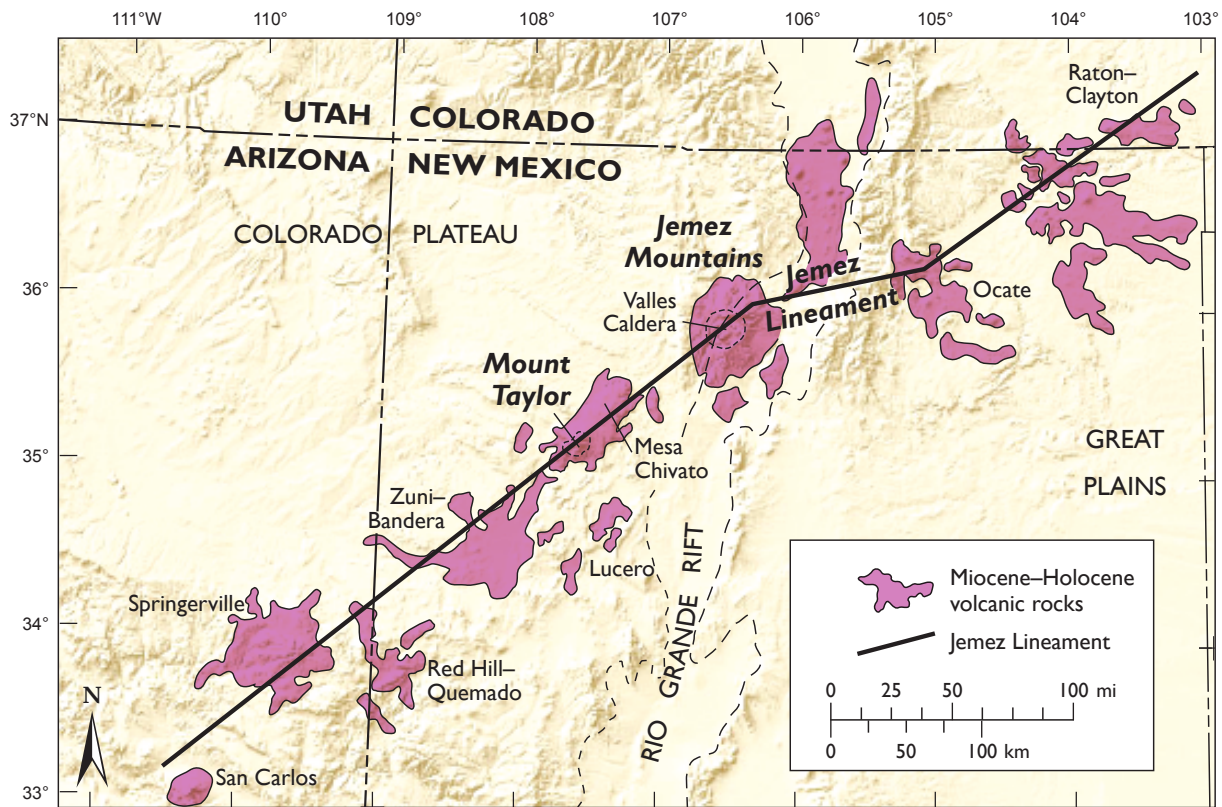


FIGURE 1. Map showing location of Mount Taylor with respect to other volcanic fields of the Jemez lineament and to basins of the Rio Grande rift (modified from Goff and Gardner, 2004, fig. 1).

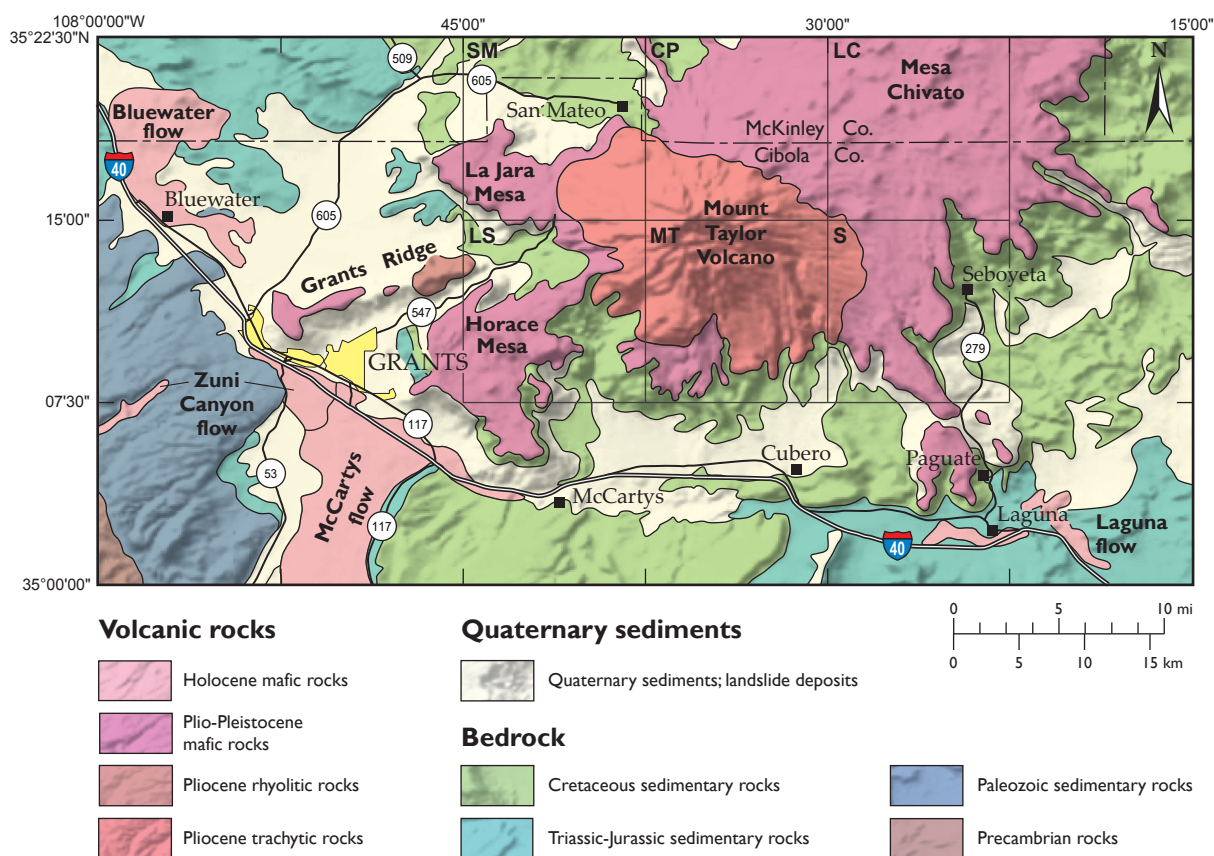


FIGURE 2. Map of Mount Taylor volcano area showing simplified geology and the locations of six recently completed 1:24,000 quadrangles: CP=Cerro Pelón (Goff et al., 2012), LC=Laguna Cañoneros (Goff et al., 2014a), LS=Lobo Springs (Goff et al., 2008), MT=Mount Taylor (Osburn et al., 2010), S=Seboyeta (Skotnicki et al., 2012), and SM=San Mateo (McCraw et al., 2009).

for the map by Lipman et al., the volcanic rocks are highly generalized. Several reports have provided modern petrologic evaluations, chemical and limited isotopic analyses and/or radiometric dates of Mount Taylor rocks: Hunt (1938), Bassett et al. (1963), Kerr and Wilcox (1963), Baker and Ridley (1970), Lipman and Moench (1972), Lipman and Menhart (1979), Crumpler (1980a, 1980b, 1982), Perry et al. (1990), Laughlin et al. (1993) and Hallett et al. (1997). Perry et al. also include a magmatic model based on chemical and isotope results and a geologic map of the Mount Taylor Amphitheater and the southwest flank of the volcano (0.8 in = 1 km). The only volcanic rock of economic importance, other than local materials for road construction, has been minor perlite extraction from the Grants Ridge center (Kerr and Wilcox, 1963). However, southern Mesa Chivato ("Red Mesa") now generates electricity from wind (Fig. 3c).

The Mount Taylor region is also well known for the Mesozoic rocks exposed in the canyons and valleys around the flanks of the volcanic field and for the coal and uranium deposits hosted within them (e.g., Schrader, 1906; Shimer and Blodgett, 1908, Gardner, 1909; Sears et al., 1941; Kelley, 1963; Moench and Schlee, 1967; Santos, 1970). Transgressive-regressive cycles of marine sedimentation are superbly expressed in Upper Cretaceous rocks beneath the volcano (Sears et al., 1941; Molenaar, 1974; Owen and Owen, 2003). Coal was mined west of Horace Mesa until the 1960s and is still extracted from several mines in the Ambrosia Lake district about 15 km northwest of San Mateo. Until the 1980s,

the Grants district was the largest uranium producing area in the United States and probably 4th worldwide (Kelley, 1963; Chapman et al., 1974; Reise, 1977, 1980; McLemore et al., 1986; 2013; McLemore, 2011). Several hundred boreholes were drilled by mining companies through volcanic rocks north of Mount Taylor to trace uranium-bearing Jurassic strata between large mines on the volcano flanks at San Mateo and Laguna Pueblo. Thus, this geologic map can be used to advance research in Mesozoic stratigraphy, geohydrology, coal/uranium extraction, and seismic hazards, although the primary focus of our work has been the evolution of Mount Taylor volcano and surrounding volcanic centers.

Appendices 1, 2, and 3 are included with this report; Appendices 2 and 3 are available in digital form in repository <https://geoinfo.nmt.edu/repository/index.cfm?rid=20190001>.

Physical Setting and Access

Mount Taylor summit is located 20 km northeast of the small city of Grants (population about 9,200 in 2016) in west-central New Mexico (Fig. 2). The volcano forms a broad conical highland (Cover photo) cresting at an elevation of 3,445 m (11,301 ft) and is surrounded by several lava-capped mesas at elevations of roughly 2,440 m (8,000 ft). Lowest elevations are located along the Río Paguete at 1,838 m (6,030 ft) near the southeast corner of the map. Ponderosa pine, blue spruce, white pine, and aspen forest characterize the higher elevations, which can receive several meters of snow in winter.

Piñon-juniper forest, sagebrush, and chamisa (rabbitbrush) are most common at lower elevations. Watercourses contain cottonwood and sycamore. The mountain areas are home to black bear, cougar, and elk, whereas deer, coyote, feral horses, and rattlesnakes are more common on the mesas and basins. While the regional climate is semi-arid, Mount Taylor and Mesa Chivato, however, are classified as boreal or warm temperate with high humidity and warm summers. Summer monsoons bring thunder, lightning, and bursts of rain from late June through August. Average yearly precipitation in Grants from weather records is 267 mm/year (10.5 in/year) while the Mount Taylor summit and Amphitheater receive more than 800–900 mm/year (31–35 in/year; Meyer et al., 2014).

The largest mesa is Mesa Chivato, which extends beyond the northeast corner of our map, but other significant mesas include La Jara to the west and Horace to the southwest. Mesa Chivato can be divided into several smaller mesas herein named Seboyetita Mesa, Chupadero Mesa, Silver Dollar Mesa and Encinal Mesa. The mesas are flanked or cut by several basins and canyons that expose primarily Cretaceous and older strata, but which also may expose capping layers of lavas and beds of silicic tuffs. The most significant canyon flanking the volcano is Water Canyon. It holds the largest perennial stream, which drains the eastern end of Mount Taylor Amphitheater before turning south. On the west is the basin that includes the village of San Mateo and the San Mateo (or Mount Taylor) uranium mine. Coal Mine basin and Lobo Canyon lie to the southwest between La Jara and Horace mesas. Rinconada basin and Rinconada Canyon lie to the south-southwest. Several smaller but relatively deep canyons such as Seco and Two Mile canyons also drain to the south. Encinal, Bear, Paguete, and Seboyeta canyons drain the southeast side of the volcanic highland. The only basin to the north is San Lucas Valley, which is normally dry.

Access to Mount Taylor volcano is highly variable (Fig. 4). Much of the west side of the volcano, including Mount Taylor summit, “La Mosca,” and the western Amphitheater, belong to the Cibola National Forest, Mount Taylor Ranger District headquartered in Grants. These lands can be entered via paved NM Hwy 547 from Grants, and then traversing several Forest Service roads (shown in Fig. 4). However, there is a significant portion of southern Horace Mesa that belongs to Acoma Pueblo (permission to enter is required). Portions of Lobo Canyon are under private ownership, much by owners with small land holdings. Portions of the area around San Mateo are also privately owned by the Lee Ranch, the San Mateo Springs land grant, and the current owner of the inactive uranium mine. The most difficult area to access in the western Mount Taylor area is the south and southeast rim of the Amphitheater because of the lack of roads, steep tree- and brush-covered terrain, and long walks to and from convenient parking areas.

The eastern side of Mount Taylor volcano and southwestern Mesa Chivato are impossible to access without formal permission. Laguna Pueblo owns the eastern Amphitheater, and adjoining mesas to the south, Water Canyon, Encinal Mesa, and Silver Dollar Mesa, which are patrolled by Laguna Police. The Elkins Ranch (headquarters in Grants, NM) owns a large area of land northeast of the Amphitheater. Areas around Seboyeta Canyon are controlled by the Seboyeta Land and Cattle Association. The extreme southeastern end of Mesa Chivato (informally named Red Mesa) is owned by the Lobo Ranch (of Scottsdale, AZ) and is controlled by the



FIGURE 3a. Pre-Puebloan cliff house ruin hidden within a grotto in Cretaceous sandstone, in an unnamed canyon of the Rinconada basin, south of Mount Taylor (exact location omitted for archeological reasons).



FIGURE 3b. Casa Fria, an old trading post east of Mount Taylor, was active into the early 1900s. The log cabin is located on the north end of Silver Dollar Ranch (presently owned by Laguna Pueblo). Cabin location UTM and UTM's for other photos are available in Appendix 3 and in digital form in the repository (<https://geoinfo.nmt.edu/repository/index.cfm?rid=20190001>).



FIGURE 3c. The view looks east-southeast across the head of Seboyeta Canyon toward “Red Mesa,” an arm of southern Mesa Chivato displaying some of the many windmills installed for electric power generation.

Red Mesa Wind Farm. Most of the northeast side of the volcano and Mesa Chivato is owned by the Lee Ranch (Fernandez Company of San Mateo). Locked gates and fences block entry into these lands.

Geologic Background

Mount Taylor volcano is one of many Miocene to Quaternary volcanic fields that have been emplaced along the northeast-trending Jemez volcanic lineament (JVL, Fig. 1; Mayo, 1958; Laughlin et al., 1982; Luedke and Smith, 1978; Smith and Luedke, 1984). Mount Taylor also lies in a transition zone of extension between the Colorado Plateau to the northwest and the Rio Grande rift (RGR) to the east (Olsen et al., 1979; 1987; Thompson and Zoback, 1979; Aldrich and Laughlin, 1984). A recent interpretation of 3D seismic structure beneath the RGR to a depth of 200 km (Sosa et al., 2014) suggests that the transition zone is a broad low-velocity region and that an upwelling, broad, sheet or linear bulge of hot mantle material underlies the JVL. This sheet has probably fed the volcanic centers along the lineament including Mount Taylor and Mesa Chivato. Presence of an upwelling zone along the JVL during the last 4 Myr is supported by the incision and denudation history of the Río San Jose just south of our map area (Channer et al., 2015).

Mount Taylor overlies the southeast margin of the Laramide-age San Juan Basin and the western flank of the northeast-striking McCarty syncline of Hunt (1938). An east-dipping monoclinical ridge along the northwest edge of the map marks the western edge of the McCarty syncline (Goff et al., 2008; McCraw et al., 2009). The effect of this monoclinical ridge is to drop the Mesozoic rocks a thousand meters or more beneath Mount Taylor and southwest Mesa Chivato. Several low amplitude folds that strike northwest to northeast in the Lobo Canyon area are superimposed on the large-scale synclinal structure (Dillinger, 1990). These folds do not affect the overlying volcanic rocks and are presumably Laramide in age.

Major formations of Cretaceous rocks interfinger with each other and pinch out at various locations (see Fig. 5a and rock descriptions). The upper Cretaceous section (Figs. 5a, 6 and 7) is a regressive sequence, recording a gradual transition from open marine conditions (Mancos Shale) to marginal marine environments (Gallup Sandstone, Stray and Dalton Sandstone members of the Crevasse Canyon Formation) to deltaic settings (Dilco and Gibson Coal members of the

Crevasse Canyon Formation). The Mancos Shale is interbedded with the Gallup Sandstone, the Crevasse Canyon Formation, and the Mesaverde Group. The Point Lookout Sandstone (Hosta Tongue), exposed in the southeast and northwest parts of the map, was deposited during a marine transgression. The Satan Tongue of the Mancos Formation overlies the Point Lookout and underlies a variety of lava flows capping southwest Mesa Chivato. Photographs of the Cretaceous rocks are presented in several of our recent quadrangle maps (Goff et al., 2008, 2012; McCraw et al., 2009; Skotnicki et al., 2012). The report by Skotnicki et al. (2012, p. 54–68) contains 21 measured sections of Cretaceous strata from the Satan Tongue down to the Dakota Sandstone and a diagram correlating the sections.

The upper Cretaceous sequence in the Mount Taylor region was folded, uplifted, and eroded in early- to mid-Cenozoic time forming part of the greater Colorado Plateau. Cretaceous rocks were partially eroded during a period of base level stability and pedimentation in west-central New Mexico that lasted from approximately 4 to 2.5 Ma. Mount Taylor volcanics erupted onto this pediment surface. Bryan and McCann (1938) suggested that the erosion surface underlying Mount Taylor was correlative with the Ortiz surface located in the Rio Grande rift. Beginning in the early Pliocene (roughly 3.8 Ma), volcanism ensued in the region, filling shallow valleys and a few ravines. Eventually, a composite intermediate composition stratovolcano formed at Mount Taylor flanked by mesas covered with basaltic lavas and scoria cones. This volcanism more or less ceased at about 1.25 Ma.

The Plio-Pleistocene transition (about 2.50 Ma) was a period of rapid erosion through the mesas flanking Mount Taylor (Lipman and Mehnert, 1979), in part due to a wetter climate (Zachos et al., 2001). For example, Love and Connell (2005) have documented about 250 m of downcutting between 2.93 and 2.39 Ma in the Rio San Jose drainage system south of Mount Taylor. Using these measured values translates to an erosion rate of 460 m per million years. Between 2.39 Ma and 170 ka, the erosion rate slowed to an average of 68 m per million years.

Classification and Petrology of Volcanic Rocks

Previous work

Mount Taylor volcanic rocks have been given many names, particularly the intermediate composition rocks. Hunt (1938) recognized that Mount Taylor rocks are alkalic (relatively rich in $\text{Na}_2\text{O} + \text{K}_2\text{O}$) and used the terms olivine basalt, porphyritic andesite, porphyritic trachyte and latite, and rhyolite (tuffs and lava). Hunt presented five chemical analyses of poorly located samples collected and analyzed around the turn of the previous century (Clark, 1910). In modern terminology (Le Bas et al., 1986), one analysis is of basalt, one is of trachybasalt (hawaiite), and three are of trachydacite composition.

Baker and Ridley (1970) wrote a later report on magmatic origins of Mount Taylor volcanic products but used the following terms: basalt, basaltic andesite, andesite, dacite, and rhyolite. They called Mount Taylor volcanic rocks “calc-alkaline,” which in modern terminology they are not, and failed to reference Hunt (1938). These authors recognized

that a few of the early mafic lavas are basanite and noticed the fairly conspicuous “big feldspar” basalts (more recently called “plagioclase” basalts) within the volcano. However, their chemical analyses (Baker and Ridley, 1970, table 1) are averages of petrologic rock types, suitable for generalizations on magma genesis, but not suitable for mapping purposes.

Lipman and Moench (1972) studied basaltic rocks mostly in the southern portions of the Mount Taylor volcano area. They broke the basalts into four groups: Early basalts or basanites (similar to Baker and Ridley), basalts of high mesas, basalts of low mesas, and late basalts. This later group corresponds with mafic lavas south of Grants and near Laguna Pueblo (i.e. El Malpais) and does not appear on our geologic map. Analyses of rocks in the first three groups (Lipman and Moench, 1972, table 1) are of high quality and useful for mapping purposes. Later on, Lipman and Mehnert (1979) used the new terms lower basalt for early basalt, and upper basalt for basalts of high mesas. The latter unit is loosely equivalent to unit Q_{Tub} on our geologic map (Fig. 5b; pages 8 and 9).

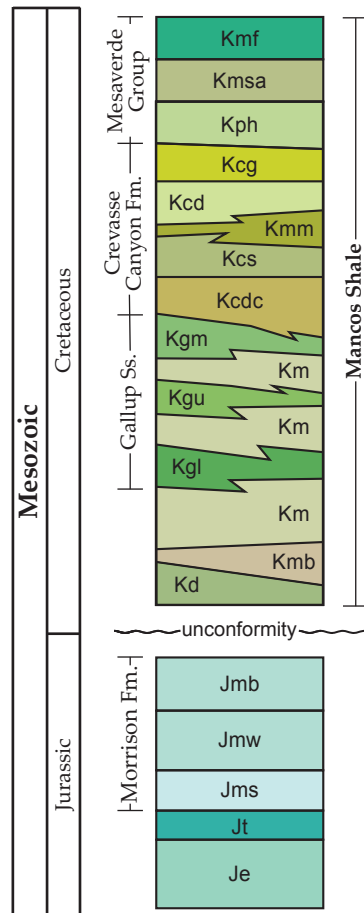


FIGURE 5a. Correlation of Mesozoic bedrock map units beneath Mount Taylor volcano and surrounding areas.

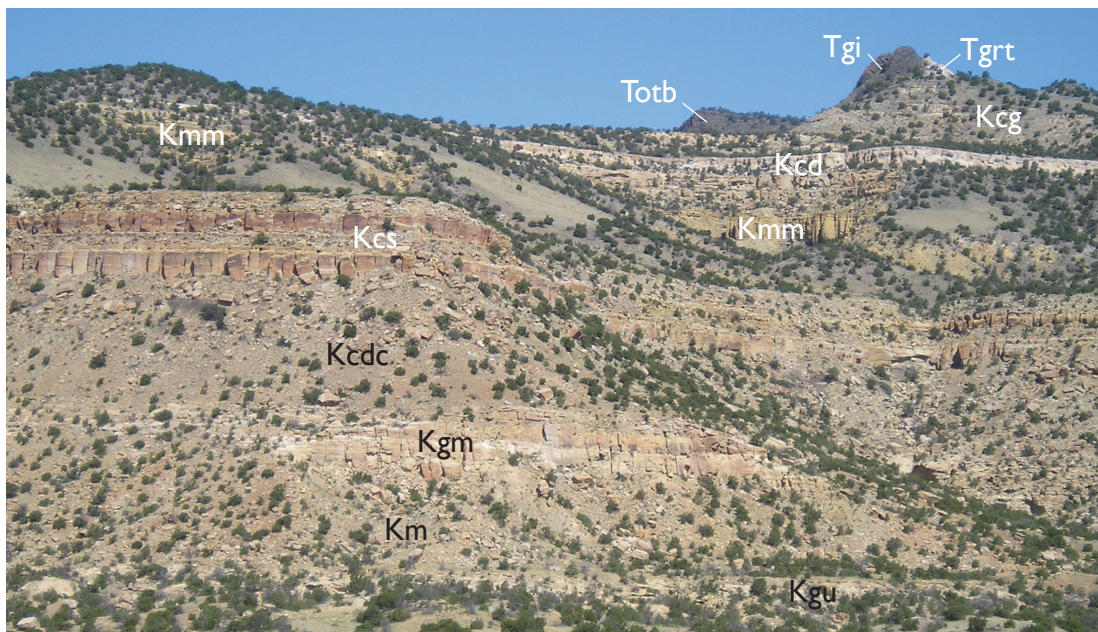
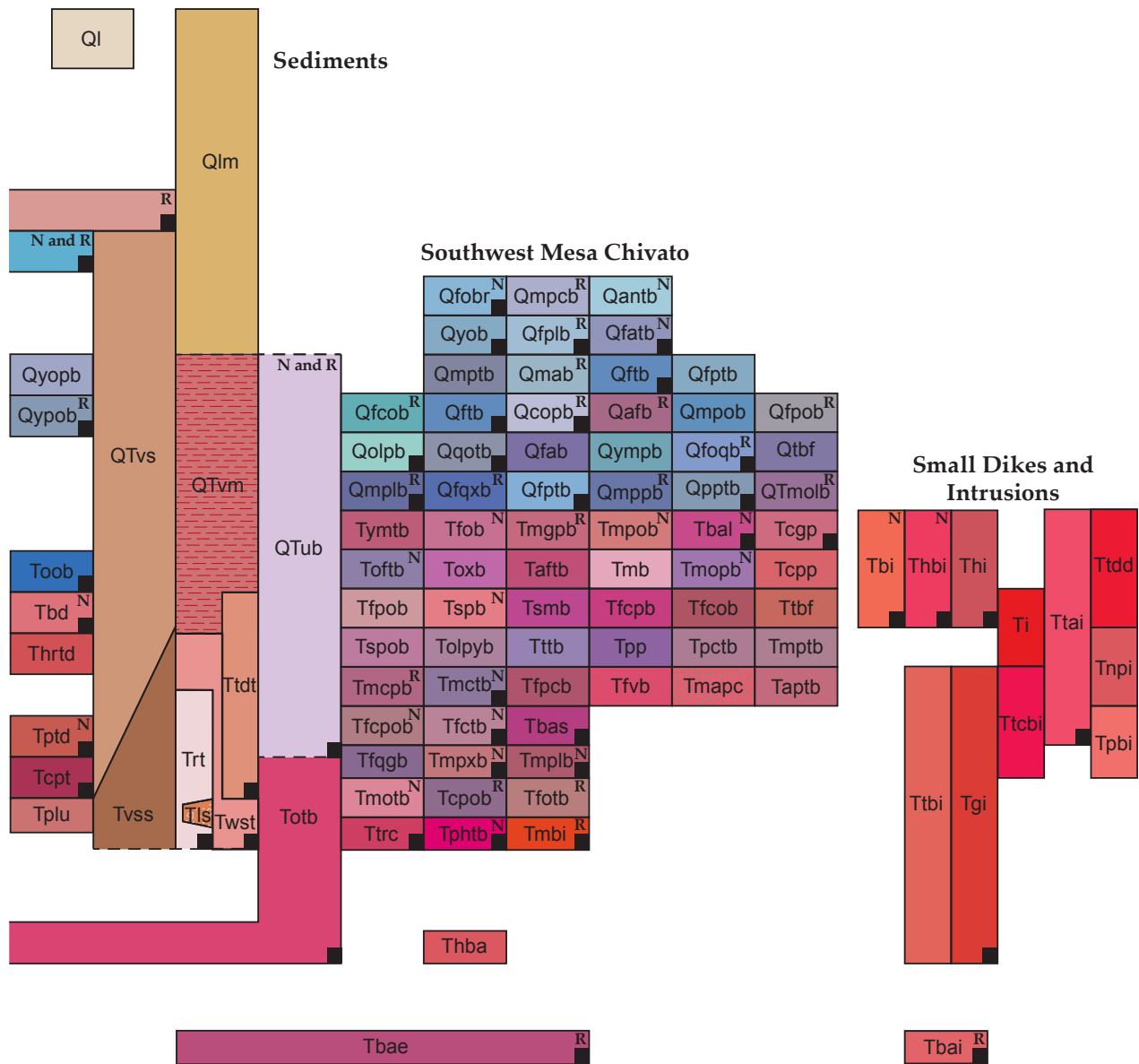


FIGURE 6. Cretaceous rocks exposed on the west wall of Rinconada Canyon near the south edge of the map; **Kgu**–upper Gallup Sandstone, **Km**–Mancos Shale, **Kgm**–Main body, Gallup Sandstone, **Kcdc**–Dilco Coal Member, **Kcs**–Stray Sandstone (a distinct doublet sandstone), **Kmm**–Mulatto Member, Mancos Shale, **Kcd**–Dalton Sandstone, **Kcg**–Gibson Coal Member, **Tgrt**–Grants Ridge rhyolite tuff (≈ 3.3 Ma), **Tgi**–monzodiorite plug, and **Totb**–older trachybasalt lava.



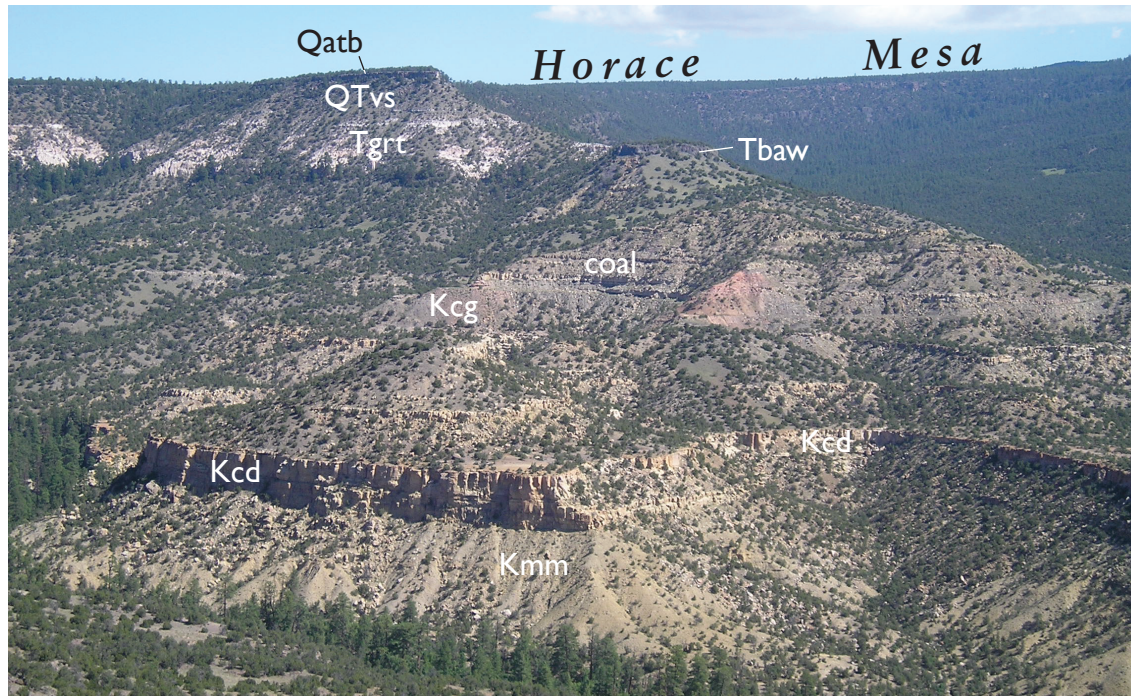


FIGURE 7. The view looks north at the west side of Guadalupe Canyon in the Rinconada basin toward Horace Mesa; **Kmm**—Mulatto Member, Mancos Shale, **Kcd**—Dalton Sandstone, **Kcg**—Gibson Coal Member, a mixture of mudstone, siltstone, sandstone, and some coal (one coal horizon shown), **Tbaw**—west olivine basanite (3.64 Ma), **Tgrt**—Grants Ridge rhyolite tuff (≈ 3.3 Ma), **QTvs**—volcaniclastic sediments interlayered with various Mount Taylor tuffs, **Qatb**—aphyric trachybasalt (1.80 Ma).

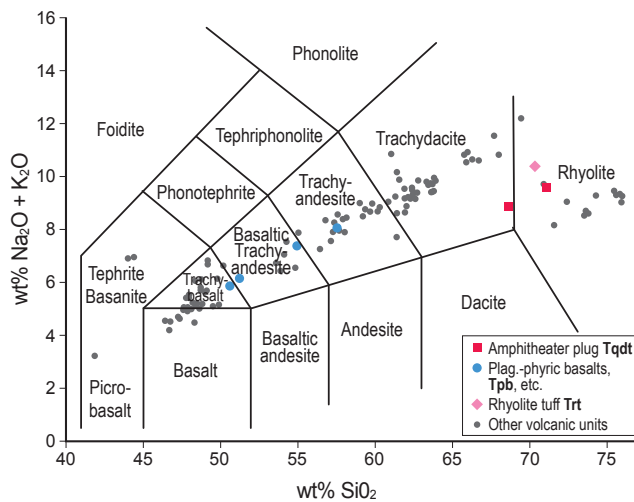


FIGURE 8. Total alkali-silica diagram of Le Bas et al. (1986) with chemical analyses of Mount Taylor region volcanic rocks (small gray circles) published by Fella (2011). Plug=c.a. 2.55 Ma intrusion within the Mount Taylor Amphitheater, Plag-phyric basalts="plagioclase or big feldspar basalts" described by previous researchers; Tuff=rhyolitic fall deposit (3.08 Ma) on the cliff east of La Mosca Canyon south of San Mateo.

Crumpler (1980a, 1980b) worked on Mesa Chivato rocks immediately northeast of our map area, noting their distinctive alkalic chemistry and calling them an alkali basalt through trachyte suite. He also compared chemical compositions of Mount Taylor rocks to many alkalic rocks at Hawaii. His analyses (Crumpler, 1980b, table 3) are useful for correlating units across the northeast edge of our map.

The most comprehensive geochemical and petrologic study of Mount Taylor proper was published by Perry et al. (1990). These authors also recognized the alkalic chemistry of the rocks but used the older terms—basanite—hawaiite—latite—quartz latite—rhyolite as per Irvine and Baragar (1971). Rock chemistry presented by Perry et al. (1990, table 2) is very useful for identifying and correlating units on our geologic map.

Present study

Most volcanic rocks in the Mount Taylor area are truly alkalic (Fella et al., 2009; Fella, 2011; Fig. 8), not calc-alkalic. For our map, we use the internationally accepted classification scheme of Le Bas et al. (1986), previously published chemical analyses, and our chemical analyses (Appendix 2) to rename and categorize the volcanic units. Thus, most alkali basalts (hawaiites) are called trachybasalts, basaltic andesites (muergerites) are called basaltic trachyandesites, andesites (latites) are called trachyandesites, and quartz latites are called trachydacite. The only volcanic rocks with no name changes are rhyolites and basanites, although we reserve the name trachyte for a few exceptionally alkali-rich trachydacitic rocks. We also note that many of the Mount Taylor mafic rocks are "true" basalts using the classification scheme of Le Bas et al. (1986) in that they have ≤ 5.00 wt% $\text{Na}_2\text{O} + \text{K}_2\text{O}$ and 45–52 wt% SiO_2 normalized to 100% on a loss-on-ignition (LOI) free basis. Mineralogically, the phenocrysts in Mount Taylor products (Table 1) are similar to those in alkali-rich volcanic terrains erupted in or near continental rifts (see figure 11.12 in Wilson, 1989). Augite and plagioclase are present in practically all rocks, including most of the rhyolites. Hypersthene is present in some of the intermediate composition rocks. Hornblende and titaniferous biotite are

TABLE 1. Phenocryst mineralogy of volcanic rocks, Mount Taylor volcano area, New Mexico.

Mineral	Basanite	Basalt	Trachybasalt (Hawaiiite)	Trachyandesite	Trachyte	Trachydacite	Rhyolite
Olivine	●	●	●	●		○	
Analcime	●						
Augite	●	●	●	●	●	●	●
Hypersthene			●	●		●	
Hornblende			●	●	●	●	●
Biotite			○	●	●	●	●
Plagioclase	●	●	●	●	●	●	●
Potassium Feldspar				●	●	●	●
Quartz				○		●	●

● = major, ● = minor, ○ = trace

present in a couple of the trachybasalts. Hornblende and biotite are common in the more evolved rocks. Primary quartz is only abundant in the rhyolites and a couple of trachydacites. Generally, olivine displays minor to severe iddingsite alteration. Most of the mafic and intermediate composition rocks contain visible apatite microphenocrysts. All rocks generally contain Fe-Ti oxides, but we did not attempt to determine relative percentages between magnetite and ilmenite.

Three types of textures dominate within the volcanic suite. First, all rocks except basanites tend to be porphyritic; trachyandesites and trachydacites are commonly highly porphyritic with large complexly zoned plagioclase and sanidine phenocrysts. Second, the high alkali content of most of the magmas, particularly Na, causes the growth of abundant groundmass plagioclase aligned during post-eruptive flow. In thin section, most of the trachybasalts and intermediate composition rocks have pronounced pilotaxitic or trachytic texture (Williams et al., 1954, p. 23). Freshly broken surfaces often display a felty appearance caused by tiny aligned feldspar crystals, usually plagioclase. Felty, trachytic mafic rocks are often exceptionally hard to break with a rock hammer. Felty textures provide a robust means to distinguish trachybasalt from true basalt. Third, weathered surfaces of many trachybasalts and basanites show faint to prominent, white to pale gray spotting (or small “eyes”) caused by the growth of ocellar plagioclase and/or analcime (Williams et al., 1954, p. 24). Ocellar analcime is found only in basanites (see Lipman and Moench, 1972). The spots are usually 1–2 mm in diameter.

Some obsidian has formed in the rhyolites, particularly on the northeast side of the Grants Ridge rhyolite center. Obsidian lithic fragments are also abundant in the upper ignimbrite of the Grants Ridge tuff. Consequently, artifacts are common on mesa top edges underlain by the tuff, primarily Horace and La Jara mesas (see also Shackley, 1998). We found scant spherulitic obsidian in the west rhyolite within the Mount Taylor Amphitheater. Occasional outcrops of black glassy rock are found within some of the trachydacite dikes in the central part of the Amphitheater. This material is easily confused with

rhyolitic obsidian and can only be distinguished as trachydacite by thin section and chemistry.

Fused Grants Ridge tuff was identified at the margins of three mafic intrusions. The most spectacular outcrop is adjacent to the southeast margin of the Horace Mesa dike (Goff et al., 2013a, fig. 5B) where thin selvages (2–5 cm thick) of gray to black glassy tuff have been fused by intruding trachybasalt (unit **Qatd**). Additional fused tuff is found next to a dike of basalt (**Toed**) about 1 km southeast of the Grants Ridge rhyolite center, and next to the plug of trachybasalt (**Tomtb**) on the south margin of La Jara Mesa.

Many intermediate to silicic rocks contain mafic enclaves, blobs or clots of mafic magma injected into and quenched within an intermediate to silicic host magma (Eichelberger, 1980; Bacon, 1986; Stimac and Pearce, 1992). Perry et al. (1990) noted mafic clots in their Mount Taylor “Type B latites and quartz latites.” These enclaves generally have finer-grained texture than the enclosing host rock and are sometimes highly vesiculated. Typically, they consist of plagioclase and hornblende ± augite and biotite. Our chemical analyses (not included in Appendix 2) show that the enclaves are usually basalt to trachyandesite in composition.

A few of the trachybasalts and basalts also contain peridotite, dunite, norite, troctolite, anorthoclase, and/or rare crustal xenoliths. Peridotite (spinel lherzolite) xenoliths were noted by Perry et al. (1990) in some Mount Taylor “nepheline normative hawaiiites.” Baldrige et al. (1996) mentioned spinel lherzolite xenoliths in a trachybasalt west of Mount Taylor (our unit **Qyxtb**). This lava and the peridotite xenoliths were further described by Goff and Goff (2013), and the gabbroic xenoliths in several other lavas were documented by Goff et al. (2013b). Many of the mafic lavas contain quartz xenocrysts with or without clinopyroxene reaction rims (Iddings, 1888; Nicholls et al., 1971) and they are particularly common in a group of younger trachybasalts that flank Mount Taylor (our unit **Qfqtb**). Although the quartz was considered primary by some early researchers, isotope studies show that the quartz is a crustal contaminant (e.g., Baldrige et al., 1996).

Volcanic History

We obtained 107 $^{40}\text{Ar}/^{39}\text{Ar}$ dates from the New Mexico Geochronology Research Laboratory (New Mexico Tech) for the volcanic and intrusive units in the map area, which are included with each rock description on the map. All dates from samples collected during 2007–2013 quadrangle mapping projects used the Fish Canyon Tuff sanidine neutron flux interlaboratory monitor (FC-2) with an assigned age of 28.02 Ma. Fourteen fill-in samples collected in 2014 for the Mount Taylor compilation map used FC-2 sanidine with an assigned age of 28.201 Ma (Kuiper et al., 2008). We also obtained 216 major and trace element chemical analyses of volcanic rocks using a combination of XRF and ICP-MS methods. Of these, 166 samples were analyzed by the GeoAnalytical Lab at Washington State University (WSU) of which 154 analyses appear in Fella (2011). J. Wolff (WSU; see Fella, 2011 for analytical methods) provided twelve additional analyses. Fifty more samples were analyzed for major and trace element chemistry by ALS Minerals in Reno, Nevada (ALS, 2014). A selection of 84 analyses that show the chemistry of important map units is listed in Appendix 2. Details of the geochronology and geochemistry will be presented in another paper.

In addition to providing more refined ages for previously dated units and determining the age range of volcanism, the

new data were used to verify if Mount Taylor volcano began with eruption of silicic rocks (trachyte and rhyolite) and ended with trachyandesite (porphyritic andesite of Hunt, 1938; latite of Perry et al., 1990). Our work shows that this is not the case. During our dating campaign, we initially found that the trachyandesites were the most difficult rocks to date. Toward the end of our study, we dated the groundmass concentrate of the trachyandesites rather than potassium-rich minerals such as sanidine and biotite.

We also measured the magnetic polarity of many samples by handheld (portable) fluxgate magnetometer (all rock types) and Brunton™ compass (basaltic rocks only) to help constrain our geochronology (Table 2). We used a $\mu\text{MAG}^{\text{TM}}$ digital magnetometer built by MEDA, Inc. (Dulles, VA). Many volcanic rocks at Mount Taylor and southwest Mesa Chivato were erupted during the magnetic flip from the Gauss Normal Chron to the Matayama Reverse Chron at 2.581 Ma (Gee and Kent, 2007, table 3). Unfortunately, our magnetic polarity measurements started late in the mapping campaign and many hard to access locations were not revisited. Note that our map uses the Plio–Pleistocene boundary of about 2.58 Ma in accordance with recent international stratigraphic changes (Cohen et al., 2013).

TABLE 2. Comparison of latest magnetic polarity subchrons from Gee and Kent (2007).

<u>Chron Name</u>	<u>Age range (Ma)</u>	<u>Normal polarity subchron</u>	<u>Reverse polarity subchron</u>
Brunhes	0.000–0.780	C1n	
Matayama	0.780–0.990		C1r.1r
	0.990–1.070	C1r.1n	
	1.070–1.201		C1r.2r
	1.201–1.211	C1r.2r-1n	
	1.211–1.770		C1r.2r
	1.770–1.950	C2n	
	1.950–2.140		C2r.1r
	2.140–2.150	C2r.1n	
	2.150–2.581		C2r.2r
Gauss	2.581–3.040	C2An.1n	
	3.040–3.110		C2An.1
	3.110–3.220	C2An.2n	
	3.220–3.330		C2An.2r
	3.330–3.580	C2An.3n	
Gilbert	3.580–4.180		C2Ar
	4.180–4.290	C3n.1n	
	4.290–4.480		C3n.1
	4.480–4.620	C3n.2n	
	4.620–4.800		C3n.2r
	4.800–4.890	C3n.3n	
	4.890–4.980		C3n.3r

The ages are in agreement with the FC-2 monitor age of 28.02 Ma.

Mount Taylor is a very complex stratovolcano composed of mafic to silicic domes, flows, intrusions, and minor tuffs (Fig. 9; see map). A large east-west-trending erosional amphitheater that drains to the east occupies the center of the volcano. Our dates indicate that the main edifice was built from about 3.2–2.5 Ma, more or less in agreement with previous researchers, but different in many details (Lipman and Mehnert, 1979; Perry et al., 1990). Thus, construction of Mount Taylor volcano was essentially complete by the end of the Pliocene, but erosion since that time has decapitated the highest points of the original complex.

Our schematic cross section in Fig. 9 shows the evolution of Mount Taylor volcano. Mount Taylor is surrounded by and interlayered with mostly basaltic lava flows, scoria cones, and a few centers of more silicic composition. Overall, the most common mafic rock is trachybasalt (hawaiite). Basanites and basalts are most common in the earlier eruptions

while trachybasalt is highly predominant in later eruptions (Appendix 2). The number of mafic flows and concentration of scoria cones is focused along the northeast-trending axis of Mesa Chivato (Fig. 2). As a result, the thickness of the mafic stack is greatest along the axis, and the younger eruptions mostly flow to the west-northwest or south-southeast away from this linear axis of higher elevation. This characteristic is much less pronounced on Horace and La Jara mesas, southwest of Mount Taylor. Our dates and those of others show that the peripheral volcanism in the Mount Taylor area began at about 4.5 Ma (Picacho Peak basanite plug and dikes; Hallett, 1994; Hallett et al., 1997) and ended at about 1.25 Ma (Cerro Pelón trachybasalt cone and flow). Again, this age range generally agrees with previous researchers (e.g., Lipman and Mehnert, 1979), but the details are considerably different. In the discussions that follow, “older” mafic units are those with ages >2.50 Ma.

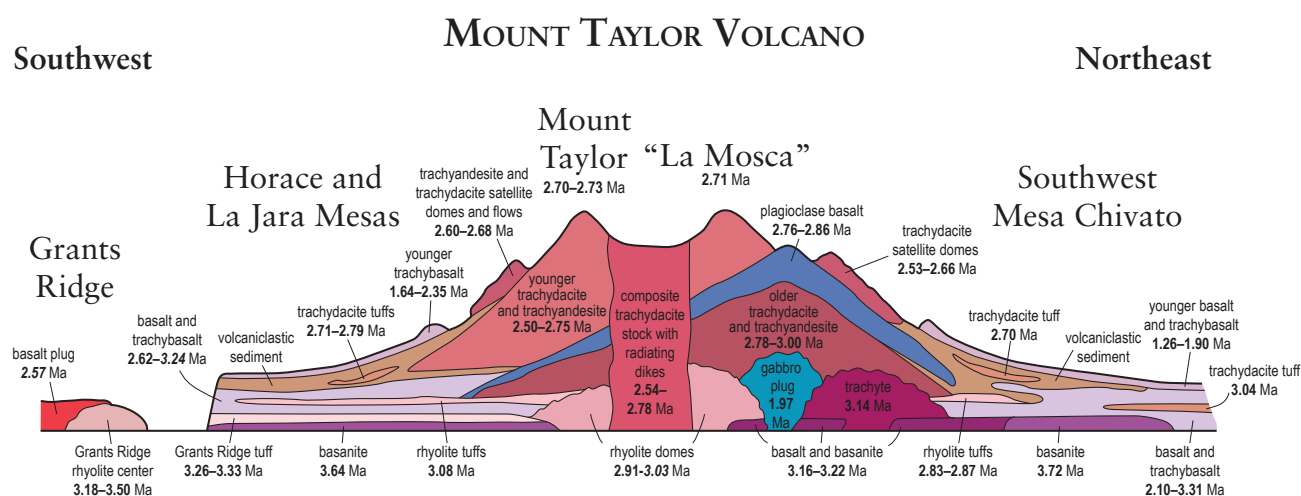


FIGURE 9. Conceptual cross section (not to scale) through Mount Taylor composite volcano showing ages of various units and their relative stratigraphic positions. This cross section is based on concepts developed during our recent quadrangle mapping. Dates were obtained from the New Mexico Geochronology Research Laboratory at New Mexico Tech except for three dates (in italics): trachybasalt plug at Grants Ridge (Keating et al., 2008); old trachybasalt lava on Horace Mesa (Laughlin et al., 1993); and west rhyolite in Amphitheater (Perry et al., 1990). Section is modified from Plate 15 in Zeigler et al. (2013).

Construction of Mount Taylor Volcano

Phase I, the volcano floor (3.72–2.91 Ma)

Phase I volcanism began with the eruption of mesa basanites (units *Tbac* and *Tbaw*, 3.72–3.64 Ma, respectively) as documented by previous workers (Perry et al., 1990). Conveniently, Grants Ridge tuff (unit *Tgrt*, 3.26 and 3.33 Ma, discussed later) forms a distinctive white layer that overlies mesa basanite in the Horace Mesa and Rinconada Basin areas southwest of the volcano. Next came the eruption of a trachyandesite dome exposed in the bottom of upper Rinconada Canyon (unit *Tbhtd*; not shown schematically in Fig. 9). The date for this eruption (3.26±0.20 Ma) has a relatively large error but the magnetic polarity is normal, suggesting an age <3.22 Ma (Table 2). Following dome emplacement, another eruption of basanite occurred (unit *Tbaa*, 3.22 Ma), as well as a younger alkali basalt (unit *Toab*, 3.21 and 3.16 Ma), now exposed in upper Rinconada Canyon and in the bottom of the central to eastern Amphitheater. The flow of alkali basalt in Rinconada Canyon overlies Grants Ridge tuff, as do several older trachybasalt flows (unit *Totb*) in the Horace Mesa

area. Within Mount Taylor, a trachyte dome (unit *Ttr*, 3.14 Ma) was erupted in what is now the eastern Amphitheater followed by emplacement of rhyolite domes and intrusions in the western and central Amphitheater (units *Trw* and *Tre*, 3.03 and 2.91 Ma, respectively). Small volume rhyolite and trachyandesite ignimbrite and fall deposits (units *Trt*, 3.08 Ma, and *Twst*, ranging from 3.04–2.74 Ma) began to fill early paleocanyons and paleoravines, particularly in Water and San Mateo canyons, and to cover mesa tops around the volcano sporadically (Dunbar et al. 2013; Kelley et al., 2013). Individual pyroclastic eruptions are <1 km³ in volume originating from dome eruptions. No caldera has been identified at Mount Taylor. The sequence of events recorded in Phase I are visible in Figs. 7, 10, 11, 12, and 13.

Phase II, the stratovolcano grows (2.90–2.75 Ma)

During phase II, the growing stratovolcano erupted a mixture of trachyandesite, trachyandesite, and trachyte lavas and domes, and associated small volume ignimbrites and tuffs. Two

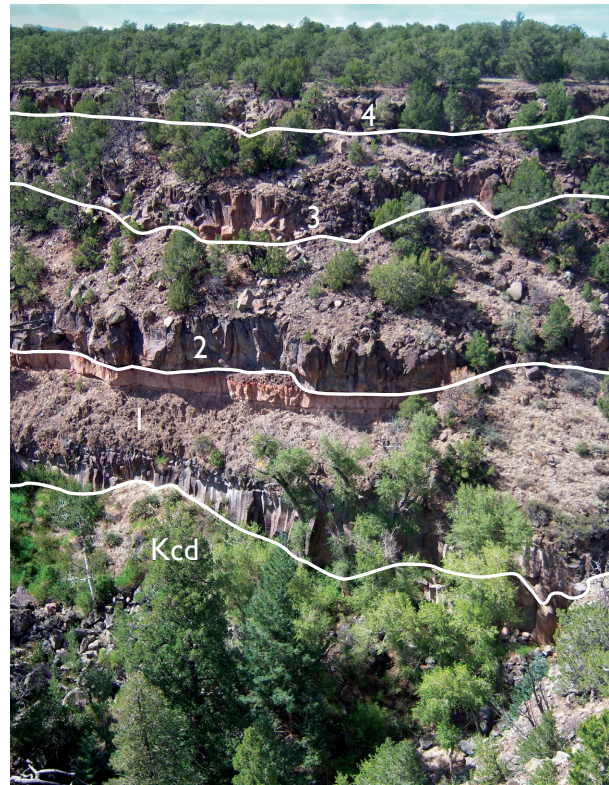


FIGURE 10. The stratigraphy exposed in Bear Canyon, east of Silver Dollar Mesa shows Dalton Sandstone (**Kcd**) overlain by several lava flows: 1) the east olivine basanite (**Tbae**, 3.72 Ma) overlain by volcaniclastic sandstone mixed with tuffs (**Tvss**, undated at this location but probably about 3.0 Ma), 2) a trachybasalt (**Tmotb**), 3) a younger, fine-grained augite-phyric trachybasalt (**Tfctb**, 2.65 Ma), and 4) a quartz-bearing olivine trachybasalt (**Qqotb**, 2.32 Ma). About 10–15 m of volcaniclastic gravels (**QTVs**) form a layer between flows 3 and 4.



FIGURE 11. The stratigraphy exposed in the east wall of La Mosca Canyon shows Menefee Formation (**Kmf**) overlain by a thick sequence of pyroclastic fall deposits, soils, and small-volume ignimbrites capped by lava. For clarity, the pyroclastic sequence is shown as a single unit (**Trt**) on the geologic map but a detailed section can be found in McCraw et al. (2009, Appendix A; see also Fig. 13 of this report). **Tgrt** is the Grants Ridge rhyolite fall/surge beds (3.33 Ma), **Trt** is a single rhyolite pumice fall (3.08 Ma), **Tplta** is a coarse-grained plagioclase trachyandesite lava (2.86 Ma).

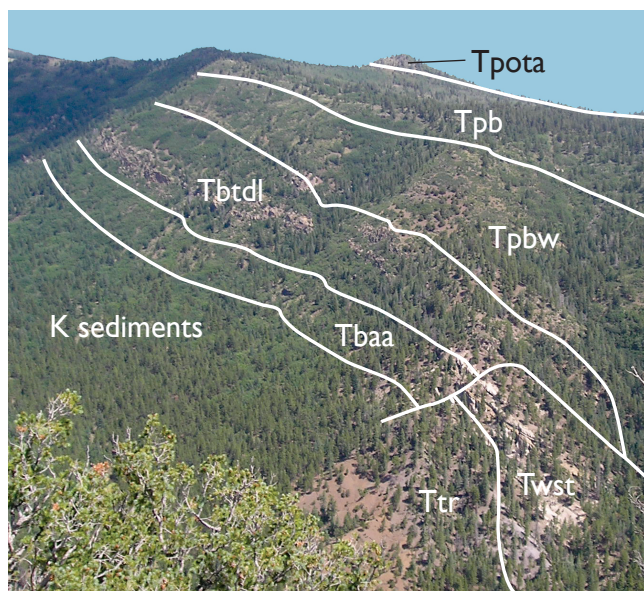


FIGURE 12. The stratigraphy exposed in the northeast wall of Mount Taylor Amphitheater shows scattered outcrops of Cretaceous sediments (Satan Tongue; Hosta Tongue, Point Lookout Sandstone) overlain by **Tbaa** (olivine basanite, 3.22 Ma) and intruded by **Ttr** (trachyte, 3.14 Ma). These early Phase I “floor” eruptions are overlain by rhyolitic tuffs (**Twst**, roughly 2.87 Ma), a thick biotite trachydacite (**Tbt**), plagioclase basalt of Water Canyon (**Tpbw**), “classic” plagioclase basalt (**Tpb**, 2.79 Ma), and a satellite eruption of porphyritic olivine trachyandesite (**Tpot**, 2.67 Ma).

previously unrecognized trachytes (**Tbht** and **Tcpt**; the former in Appendix 2) were dated at 2.83 and 2.82 Ma, respectively. The latter unit is so porphyritic it weathers like syenite. The porphyritic trachyte is overlain by a thick enclave-bearing trachydacite (unit **Tpetd**) dated at 2.81 Ma. Field relations and other dates bracket these dome eruptions between 3.0 and 2.78 Ma. The tuffaceous deposits (e.g., an ignimbrite in unit **Ttdt** dated at 2.79 Ma, Appendix 2) continued to fill in preexisting ravines and depressions but are also found in scattered outcrops around the volcano interlayered with trachybasalt and minor basalt lavas, and with early volcanoclastic rocks (unit **QTvs**) shed off the developing volcano.

The defining units ending Phase II result from eruptions of a series of “plagioclase” or “big feldspar” mafic rocks (Figs. 9, 12 and 14; units **Tpb**, **Tpbs**, **Tpbw**, **Tpbm**, 2.86–2.75 Ma). Although these lavas include trachybasalt as defined in Fig. 8 on page 10 (“classic” plagioclase basalt, Appendix 2), most of the flows are basaltic trachyandesite to trachyandesite. The classic varieties are among the latest of this group to erupt but these rocks are interlayered within the uppermost intermediate flows making up Phase II (e.g., unit **Tptd** dated at 2.78 Ma). “Plagioclase basalt” is most common in the central and eastern parts of the stratovolcano, in canyons cutting the southern flank of the stratovolcano, and on the large bluff of volcanic rocks south of San Mateo.

Phase III, the final stratovolcano eruptions (2.75–2.50 Ma)

Continued effusion of intermediate composition lavas and domes from 2.75–2.50 Ma characterizes volcanic activity for Phase III. These eruptions originate in part from a composite stock generating radial dikes that developed beneath the

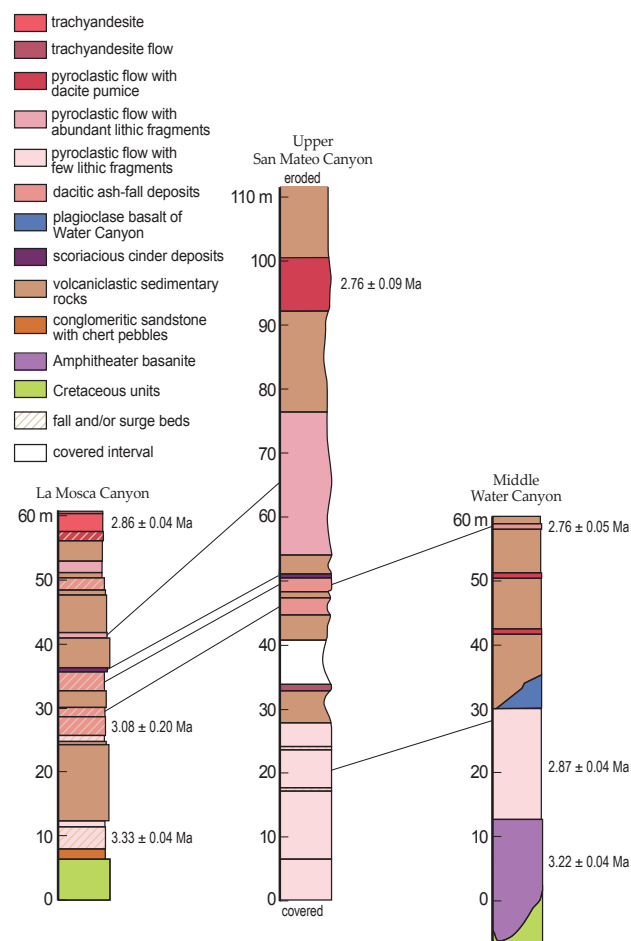


FIGURE 13. Measured sections of pyroclastic rocks exposed northwest and east-southeast of Mount Taylor volcano. The La Mosca Canyon section is shown in Fig. 11. The upper San Mateo Canyon section is a composite that first appeared in Goff et al. (2012, fig. 6). The middle Water Canyon section is a composite that first appeared in Kelley et al. (2013).



FIGURE 14. Photograph, with a dime for scale, showing the texture of classic “plagioclase or big feldspar basalt,” actually trachybasalt (unit **Tpb**, Appendix 2). Until our mapping project, this widespread unit was never successfully dated. A similar sample from the south flank of the Amphitheater yielded an age of 2.76 Ma.

central to western Amphitheater. Our new dates and chemical analyses show that trachyandesite and trachydacite are coeval in time and space. For example, what is now Mount Taylor summit (3,445 m, Fig. 15) is built of successive flows of trachyandesite (units **Thta** and **Thtas**, 2.73–2.70 Ma) erupted from a buried or obliterated vent in the westernmost Amphitheater. “La Mosca” (3,365 m; Fig. 16) is constructed of a small intrusion exposed in the northwest Amphitheater wall (unit **Tpbti**, 2.71 Ma, almost a trachyte; Appendix 2) that produced a thick flow of trachydacite (**Tpbtd**). These are presently the two highest peaks of the volcano, but due to subsequent erosion, the edifice was perhaps two hundred meters or so higher than it is now.

During this period, eruption of pyroclastic rocks ceased. A trachydacite ignimbrite at the head of Lobo Canyon (unit **Ttdt**) previously identified by Lipman and Mehnert (1979) was dated at 2.71 Ma. The youngest we found were relatively thin trachydacite to alkali rhyolite fall deposits east and northeast of the volcano (e.g., unit **Trt**, 2.70 Ma). A few dome collapse breccias (glowing avalanche deposits?) are recorded in the larger dome eruptions (i.e., Sugary enclave trachydacite, unit **Tsetdu**), but such deposits appear to be a minor component of the volcano. In contrast, rapid erosion of the growing volcano formed large aprons and fans of water-transported debris flows and other volcanic sediments (unit **QTvs**) interlayered with lava flows. These deposits radiate in all directions away from the volcano but are thickest to the east and southeast.

Toward the middle to end of Phase III (2.68–2.53 Ma), a series of satellite domes and flows erupted on the margins and flanks of the volcano (e.g., unit **Tpota**, Fig. 12). These eruptions are mostly trachydacite (Appendix 2) and match the chemistry and age of radial dikes exposed within and on the margins of the Amphitheater (Fig. 17). The last magmatic events related to the composite stock are: 1) intrusion of a trachydacite to alkali rhyolite plug in the southwest Amphitheater (unit **Tqtd**, 2.58–2.54 Ma, Fig. 18); 2) eruption of the Spud Patch trachydacite satellite dome on the north flank of the volcano

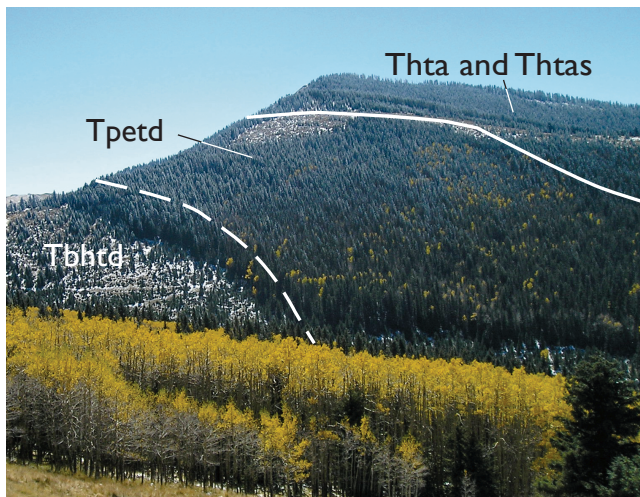


FIGURE 15. The view looks to the south at the summit of Mount Taylor in October 2008; **Thtas** and **Thta** are a stack of hornblende trachyandesite flows (2.70–2.73 Ma) that originated from obliterated vents in the western Amphitheater (left side of photograph). **Tpetd** is an extremely porphyritic enclave-bearing trachydacite (2.81 Ma). **Tbhtd** is a lumped unit (undated at this location) that forms part of the northwest Amphitheater wall.

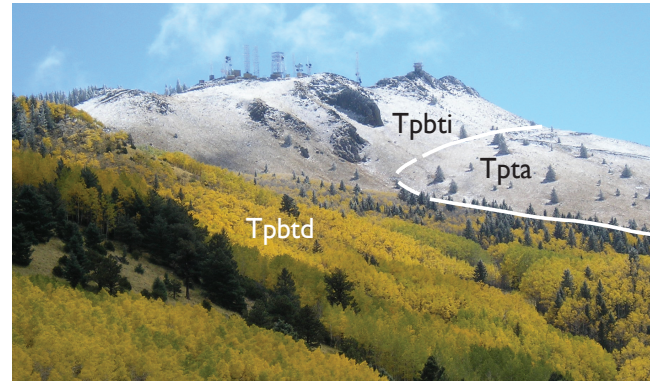


FIGURE 16. The view looks to the south-southeast of “La Mosca” in October 2008; the communication towers stand on biotite trachydacite intrusive (unit **Tpbti**, 2.71 Ma, chemically almost a trachyte, Appendix 2) that fed a large flow of similar trachydacite (**Tpbtd**). These units cut and overlie an earlier porphyritic trachyandesite (**Tpta**, undated at this location).

(unit **Tsptd**, 2.53 Ma); and 3) emplacement of an enclave-rich trachyandesite intrusion and flow on the southwest margin and flank of the volcano (unit **Teta**, 2.50 Ma, borderline trachydacite, Appendix 2).

The last three magmatic events have reverse magnetic polarity, whereas older Phase III rocks have normal polarity. Thus, the youngest magmatism of the stratovolcano captures the major change from normal to reverse magnetic polarity at 2.58 Ma (Gee and Kent, 2007).

Phase IV, terminal mafic volcanism (2.50–1.26 Ma)

Although the formation of the Mount Taylor volcano ceased at 2.5 Ma, various mafic flows, cones, and plugs continue to erupt afterward. A small, eroded cone and flow of basaltic trachyandesite sits just off the north margin of the Amphitheater (unit **Qbta**). Although we did not date this



FIGURE 17. The view looks north at the “south wall dike,” (Goff et al., 2013a), a 1-km-long dike of biotite trachydacite (unit **Tbi**, 2.69 Ma) cutting older trachydacite (**Ttdu**, undated) on the south flank of the Amphitheater. Some dike fins are more than 30 m tall. Note the en echelon behavior of the dike, a common characteristic of Mount Taylor radiating dikes.

unit, we speculate the age is around 2.2 Ma based on its stratigraphic position and state of preservation. Within the eastern Amphitheater, a large circular plug of fine-grained olivine gabbro was emplaced (Figs. 18–19; unit **Qxgi**, 1.97 Ma) that uplifted adjacent Cretaceous rocks. It is not clear if this magma breached the surface to produce a flow. The top of the plug is somewhat vesiculated (Hunt, 1938), but any flow that erupted from this intrusion has been completely eroded. The gabbro contains xenoliths of norite and peridotite, and compositionally the gabbro resembles “true” basalt (≤ 5 wt% total alkalis). This is the youngest magmatic event within the Amphitheater.

Several more cones and flows erupted on the upper flanks of the volcano. A group of xenolith-bearing cones and flows (unit **Qyxtb**, 1.74–1.85 Ma) vented from sites northwest, north and northeast of Mount Taylor. One of these is the Quarry Basalt (Baldrige et al., 1996; Crumpler and Goff,

2012, stops 4 and 8). The xenoliths are largest and most abundant within and near the cones. Because of their density, the xenoliths settle out distally near flow bottoms (Goff and Goff, 2013).

Two aphyric trachybasalts erupted on the north flank of the volcano (**Qyh** and **Qatb**, 1.73 Ma and 1.76 Ma, respectively), which overlie xenolith-bearing units. These were followed by a group of distinctive fine-grained quartz-bearing trachybasalts that vented around the volcano from 1.64–1.53 Ma (unit **Qfqtb**). This group includes Cerro Ortiz (1.56 Ma, Lipman and Mehnert, 1979). The youngest flank eruption we could identify is the cone and flow of Cerro Pelón (Fig. 20, unit **Qyatb**, 1.26 Ma). This aphyric lava is distinctive, containing sparse small olivine phenocrysts, very rare quartz xenocrysts, and tiny groundmass titaniferous biotite, the latter identifiable only in thin section.



FIGURE 18. The view looks east into the Amphitheater toward upper Water Canyon showing late intrusions: **Tqdt** is quartz-bearing trachydacite to alkali rhyolite plug (2.58–2.54 Ma); **Qxgi** is xenocrystic olivine gabbro plug (1.97 Ma). Surmounting the southeast wall is a coarse porphyritic biotite trachydacite (unit **Ttdc**, 2.70 Ma), an early satellite dome. Above the northeast wall is a porphyritic olivine trachyandesite (unit **Tpota**, 2.67 Ma) that overlies classic “plagioclase basalt” (unit **Tpb**, 2.79 Ma at this location). Most contacts are omitted for clarity.

Other Volcanic Centers

Grants Ridge Rhyolite center

An impressive northeast-trending exposure of silicic lava, with associated obsidian and tuffs, towers above the landscape of Coal Mine Basin at the northeast end of Grants Ridge (Fig. 21). Several researchers mentioned previously have worked on the Grants Ridge rocks. The prevailing wisdom about the rhyolite complex is that the eruptions began with a significant pyroclastic phase and terminated with the intrusion of lava (see WoldeGabriel et al., 1999). An early whole-rock K/Ar date of 3.34 Ma on the rhyolite lava was previously reported by Lipman and Mehnert (1979). Just off our map to the southwest, rhyolite tuffs from the Grants Ridge center are intruded and overlain by a trachybasalt plug and lava flow dated at 2.57 Ma (Thaden et al., 1967; Laughlin et al., 1993), and the intrusive relations with tuff have been extensively studied as an analog for certain types of eruptions and intrusions that could disrupt a nuclear waste repository (Keating and Valentine, 1998; WoldeGabriel et al., 1999; Keating et al.,

2008). The rhyolite dome and flow complex at Grants Ridge is massive to flow-banded and weakly porphyritic; containing sparse phenocrysts of sanidine, plagioclase, quartz, and minor biotite barely visible with a hand lens. The northwest side of the complex is partially overlain by sparsely porphyritic obsidian containing tiny sanidine. The east side of the body near NM 547 is famous for deuteritic alteration and mariolitic cavities hosting small euhedral crystals of quartz, tridymite, alkali feldspar, almandine, hematite, and topaz (Crumpler and Goff, 2012, stop 2; Crumpler and Goff, 2013, stop 1). Thus, Grants Ridge rhyolite is often referred to as a “topaz rhyolite” (Christiansen et al., 1983). Our date of the obsidian glass from the northwest flank of the intrusive complex is 3.50 Ma. Surprisingly, our date on the flow-banded rhyolite from a knob just above the “topaz” collecting locality is 3.18 Ma, indicating that the rhyolite was emplaced in at least two events, not a single event. The magnetic polarity of the flow-banded rhyolite is normal (two different sites), which fits the polarity subchron values reported by Gee and Kent (2007).

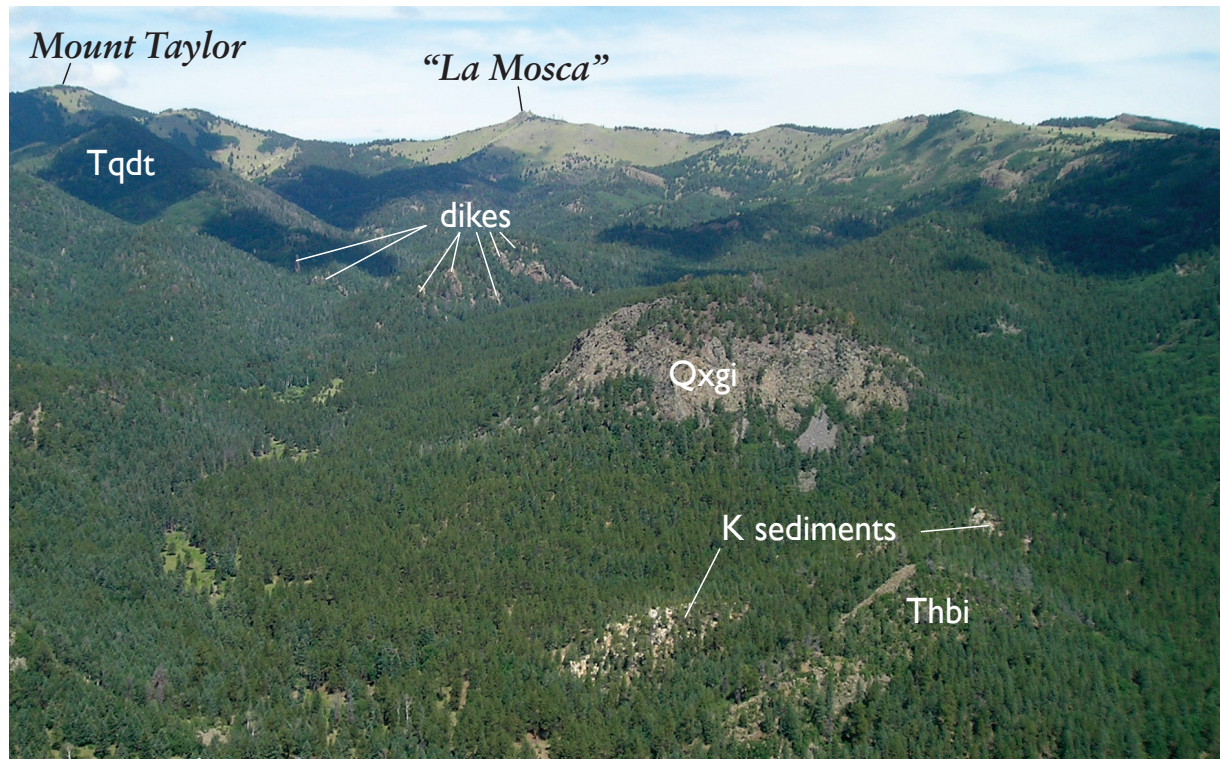


FIGURE 19. The view looks to the west-northwest toward Mount Taylor and “La Mosca” showing the young olivine gabbro plug (**Qxgi**, 1.97 Ma) in the eastern Amphitheater. The gabbro has uplifted and altered Cretaceous sediments (K sediments, see discussion below). An earlier north-south-trending dike also intrudes the Cretaceous rocks (**Thbi**, 2.64 Ma, magnetic polarity is normal). In the middle distance, several radiating dikes of various compositions can be seen. Beyond the dikes is the trachydacite to alkali rhyolite plug (**Tqdt**, 2.54–2.58 Ma).



FIGURE 20. The view looks to the south-southwest at Cerro Pelón, an eroded scoria cone that is the source of the youngest lava flow in the map area (**Qyatb**, 1.26 Ma).



FIGURE 21. The view looks to the west at the internal structure of younger rhyolite in the Grants Ridge volcanic center. The X marks the outcrop that was dated (Tgro, 3.18 Ma, magnetic polarity is normal), which overlooks the topaz-garnet-sanidine-hematite-quartz mineral collecting area (Crumpler and Goff, 2012, stop 2; Crumpler and Goff, 2013, stop 1).

Superb exposures of white Grants Ridge rhyolite tuff (unit Tgrt) can be seen in the upper cliffs of the mesas surrounding Coal Mine Basin and basins beyond. In most exposures, the tuff overlies Cretaceous rocks and discontinuous thin beds of Pliocene gravels, and underlies basaltic rocks. However, beneath upper and middle Horace Mesa, the tuff beds rest on the west basanite (Tbaw) mentioned previously (Fig. 7).

We have obtained four measured sections of the tuff at locations north-northwest, northwest and west of the Grants Ridge center (Keating and Goff, unpub. data, 2008; J. R. Lawrence, Appendix B in McCraw et al., 2009). At these locations, the tuff consists of three separate subunits: a lower ignimbrite, a middle pyroclastic fall and surge package, and an upper ignimbrite (Fig. 22). Our lower ignimbrite probably corresponds with the poorly exposed basal ignimbrite shown by Keating and Valentine (1998, fig. 3), and their central ignimbrite is equivalent to our upper ignimbrite. A key characteristic of the middle fall/surge package is the presence of accretionary lapilli in the wet ashy surge layers (Fig. 23). Locally, a 2-m-thick soil has formed at the top of the fall/surge package (Fig. 22; McCraw et al., 2009, appendix B, fig. B4). We also observed a pronounced angular unconformity between the base of the fall/surge package and the lower ignimbrite in exposures of Grants Ridge tuff beneath the east side of Horace Mesa (Fig. 24). Glass from an aphyric obsidian lithic clast removed from the upper ignimbrite was dated at 3.26 Ma,

whereas tiny sanidine separated from fine pumice in the fall/surge package was dated at 3.33 Ma. Although analytically indistinguishable when considering the uncertainties of the analyses, the two dates are suggestive of a time break in pyroclastic activity. For these reasons, we believe the rhyolite lavas and tuffs were not emplaced as one magmatic event. Instead, they were erupted as several small pulses ($\leq 1 \text{ km}^3$) spanning a considerable length of time (0.32 m.y.).

From chemical analyses on major elements (Appendix 2), there is little difference between Grants Ridge lava, obsidian, and pumice samples, although Shackley (1998) has observed differences in trace element chemistry between obsidian in lava and obsidian in tuff. However, one characteristic of all Grants Ridge samples is their relatively high fluorine contents, averaging 0.32–0.42 ppm F in fresh samples (Christiansen et al., 1983; WoldeGabriel et al., 1999). This is 2–4 times the value of other rhyolites in the region. They are also chemically different than the younger West and East rhyolites and rhyolite tuffs within and outside of Mount Taylor by generally having more SiO_2 , less Al_2O_3 , and less total Fe.

In summary, rhyolitic volcanism from Grants Ridge was relatively long-lived and predates growth of Mount Taylor stratovolcano. The types of erupted products are varied but are the most chemically evolved volcanic rocks in the region (see Appendix 2). The latest intrusive products are also the most mineralogically interesting volcanic rocks in the region.

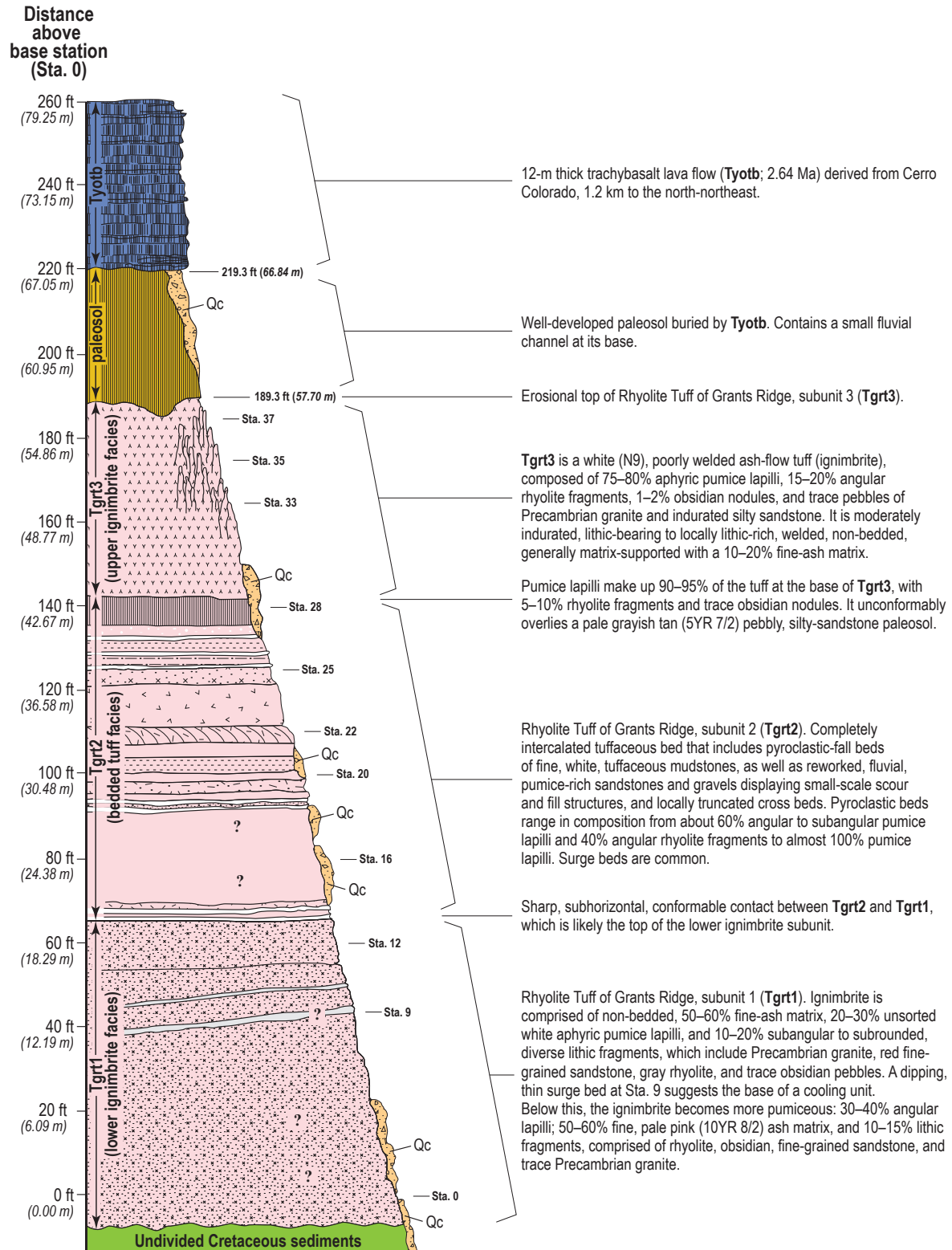


FIGURE 22. Measured section of Grants Ridge rhyolite tuff (unit **Tgrt**) exposed in cliffs of La Jara Mesa 1.2 km south of Cerro Colorado. The top of the section is located at UTM NAD27 025188/390485. Station numbers, figures II-2, II-3, B-4, B-5, B-7, B-8, and B-9, symbol explanations, and detailed lithologic descriptions can be found in Appendix B of McCraw et al. (2009). The complete tuff sequence consists of a lower ignimbrite (**Tgrt1**), a middle interval dominated by fall and surge beds (**Tgrt2**), and an upper ignimbrite (**Tgrt3**). Sanidine in pumice from **Tgrt2** was dated at 3.33 Ma whereas obsidian lithic in **Tgrt3** was dated at 3.26 Ma. **Qc** is Quaternary alluvium. Figure is modified from J.R. Lawrence in Appendix B, McCraw et al. (2009).



FIGURE 23. Accretionary lapilli (≤ 6 mm in diameter) in muddy rhyolitic surge bed from the approximate center of **Tgrt2**, on the east side of Horace Mesa. The muddy layer overlies a dry surge bed.



FIGURE 24. Dramatic angular unconformity exposed in Grants Ridge tuff, on the east side of Horace Mesa. Horizontal beds are the bottom of the fall/surge package (**Tgrt2**, Fig. 22) and underlying dipping beds are the lower ignimbrite (**Tgrt1**). The hammer handle (46 cm long) lies across the unconformity.

Trachydacite of San Jose Canyon

An interesting intrusive complex of porphyritic hornblende trachydacite (unit **Tphtd**, 2.63 Ma) is emplaced near the south-central margin of the map east of Rinconada Basin (formerly called Porphyry of San Jose Canyon; Lipman et al., 1979). The magma intrudes Cretaceous rocks (Fig. 25) and overlying flows of “plagioclase basalt” and megacrystic trachybasalt (units **Tpb** and **Tomtb**, respectively), the latter dated at 2.79 Ma. Lipman et al. (1979) imply that the source magma for the trachydacite underlies the San Fidel Dome complex (a structural dome), but we suggest that the dome may be caused by an underlying gabbro intrusion (see below). In any event, the age and major/trace element chemistry of the trachydacite (Appendix 2) resemble those of some other late Phase III domes on the margin of the Amphitheater in Mount Taylor (e.g., **Tbhtd**, 2.66 Ma). Thus, it is conceivable that a hidden 10-km-long radial dike fed the trachydacite from the stock within Mount Taylor.

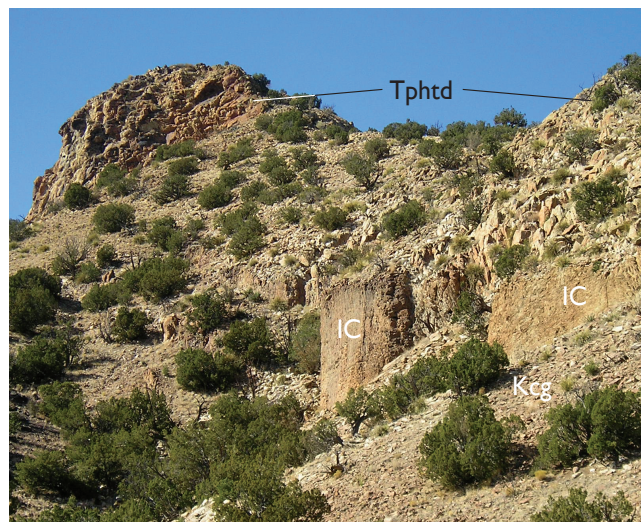


FIGURE 25. A near-vertical intrusive contact (IC) between the porphyritic hornblende trachydacite of San Jose Canyon (**Tphtd**, 2.63 Ma) and the Gibson Coal Member of the upper Cretaceous (**Kcg**, mostly covered by colluvium).

Hill south of San Mateo

About 4 km south of San Mateo stands a broad mesa and hill composed of two intermediate composition lavas cut by an intrusion. The earliest lava is a coarse porphyritic trachyandesite (unit **Tplta**, 2.86 Ma) that forms a mesa cap overlying an impressive sequence of pyroclastic rocks (Fig. 11). This was followed by an eruption of “plagioclase basalt” (unit **Tpbm**, actually a basaltic trachyandesite, Appendix 2) that forms a hill on top of the mesa. Last, a linear intrusion of olivine trachyandesite (unit **Ttai**, 2.79 Ma) cuts both lavas. These eruptions correspond in time and composition with late Phase II lavas forming the stratovolcano of Mount Taylor but lie more than 5 km northwest of the Amphitheater. Early volcanoclastic sediments (**QTvs**) form a discontinuous layer between the two flows but the complex is partially buried on the south-southeast by a later wedge of volcanoclastic sediments eroding off Mount Taylor. A trachydacite ignimbrite interlayered within these later sediments is dated at 2.79 Ma (**Ttdt**).

Southwest Mesa Chivato

Southwest Mesa Chivato contains several small volcanic centers that correspond in chemistry and age with Phase I and II rocks at Mount Taylor proper. The big difference between the two locations is the relative lack of intermediate and silicic composition rocks at Mesa Chivato. It appears that magmatism beneath Mesa Chivato developed a floor similar to Mount Taylor, but could never create a stratovolcano of more evolved rocks.

Crumpler (1977) mapped two 1:24,000 quadrangles north and northeast of our map. His mapping style generally agrees with ours, and his four dates fall into the range we have determined for the area (Crumpler, 1982, table 1). Crumpler (1980b) also obtained a considerable number of chemical analyses, some of which we normalized and plotted on a total alkali versus silica plot following Le Bas et al. (1986). His data are not included with ours in Appendix 2 but they fall along the same trend as ours. We note that his “basanitoid” becomes basanite, his mugearite and benmorite become trachyandesite,

and a couple of his trachytes become more like trachydacite when the data are replotted.

Our dating effort in southwest Mesa Chivato focused on the oldest, youngest, and/or unusual eruptions. Volcanism began with the eruption of trachybasalt and minor basanite lavas that provide isolated snapshots of initial activity. A distinctive hornblende trachybasalt (unit **Tphtb**, 3.16 Ma) is exposed just east of the Cerro Pino and Campo Grande areas. Faulting has uplifted this lava, showing that it underlies most of the volcanic pile in this area. At about the same time the trachyte dome of Cerro Chivato formed (Fig. 26, unit **Ttrc**, 3.16 Ma), which is surrounded by younger lavas. Cerro Chivato is similar in age to the “white trachyte” of Crumpler (1982; 3.22 Ma) that erupted several kilometers north of our map area. A basanite with hackly texture and sparse quartz xenocrysts (unit **Tbal**, 2.58 Ma) forms a 10-m-high ledge along the western shore of Laguna Cañoneros (Fig. 26). This lava has normal magnetic polarity and erupted near the boundary between major polarity reversals (Gee and Kent, 2007). The youngest date we obtained in the northeasternmost part of the map was from the Campo Grande volcanic center (unit **Tcgl**, 2.52 Ma), but slightly younger lavas vented to the southeast and east of Campo Grande.

Older volcanism is also preserved in southern Mesa Chivato at the head of Seboyeta Canyon where an ancient northeast-trending valley is filled with three lava flows and volcanoclastic sediments (Fig. 27). The oldest flow (**Totb**, 2.83 Ma, magnetic polarity is normal) sits on Cretaceous rocks and is overlain by volcanoclastic sandstone mixed with silicic fall deposits (unit **Tvss**). The latter layer is overlain by medium-grained, plagioclase-phyric trachybasalt (**Tmplb**, 2.70 Ma, magnetic polarity is normal) that is overlain by fine-grained basalt with conspicuous megacrysts of augite (**Tfcpob**).

Although undated, the upper flow has normal magnetic polarity, suggesting an age of <2.70 Ma but >2.58 Ma.

Isolated exposures of “big plagioclase” basaltic trachyandesite (unit **Tplta**) were found northwest of Cerro Aguila, which are largely covered by young Quaternary deposits. Although we did not date this unit, it chemically resembles similar rocks around Mount Taylor (Appendix 2). Thus, we surmise it is roughly 2.75 Ma. Part of the trachyandesite is overlapped by a fine-grained trachybasalt flow (unit **Qftb**, 2.28 Ma) and covered by scoria deposits of Cerro Aguila (**Qfoqd**; 2.27 Ma).

We dated several young fine-grained, rather aphyric trachybasalts. An extensive flow on the northern edge of the map (**Qfptb**, 2.13 Ma, the magnetic polarity is reverse) surrounds Laguna Blanca and extends for roughly a kilometer to the north (unit **Qba4** of Crumpler, 1977). Just to the southwest, the Cerro Cuate flow is dated at 2.18 Ma (unit **Qatb**). A large circular flow and faulted cone south of Cerro Chivato (**Qfatb**, 2.14 Ma, the magnetic polarity is normal) conveniently overlies or abuts against nine different older units.

We also dated three phenocryst- and/or megacryst-rich basalts (Appendix 2). Porphyritic olivine basalt (Fig. 28, unit **Qolpb**, 2.41 Ma) forms a small cone and flow just south of the northeast edge of the map. It is equivalent to part of unit **Qba2** of Crumpler (1977). A 6-km-long flow of augite megacrystic basalt (**Qcopb**, 2.31 Ma, the magnetic polarity is reverse) extends west from the axis of volcanism on Mesa Chivato. The youngest basalt, Cerro Redondo, is olivine-rich (possibly from disaggregated peridotite) and forms an impressive scoria cone nearly two hundred meters high (**Qfocr**; 1.90 Ma, magnetic polarity is normal). It is also the youngest unit we dated on southwest Mesa Chivato.

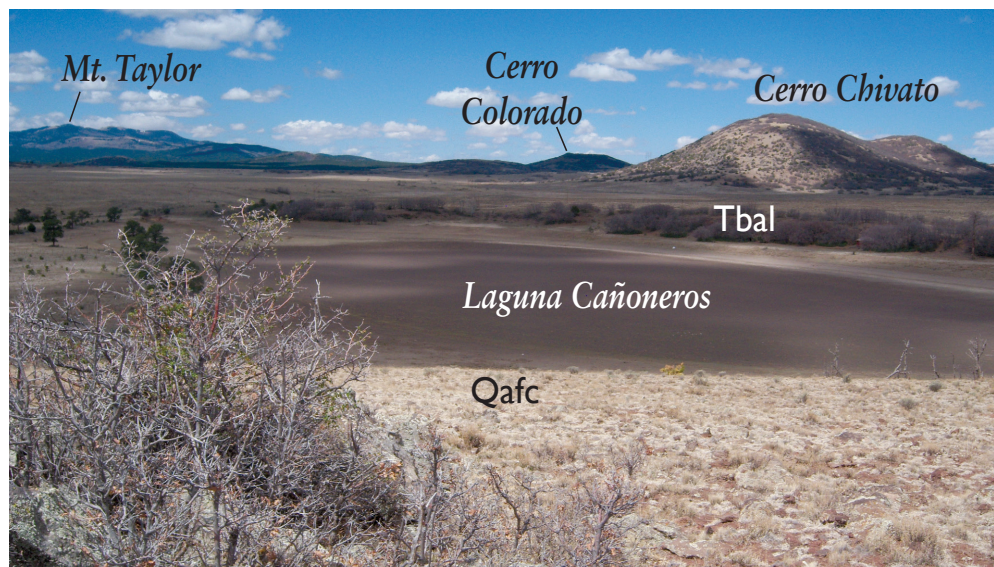


FIGURE 26. The view looks to the southwest to the Cerro Chivato trachyte dome (**Ttrc**, 3.16 Ma) west of Laguna Cañoneros maar. The maar deposits are bracketed between 2.70 and 2.58 Ma. The west shore of the maar is composed of quartz-bearing olivine basanite (**Tbal**, 2.58 Ma). The bluff flanking the east side of the maar (**Qafc**, undated) is an eroded scoria cone that overlies the basanite. Another scoria cone, Cerro Colorado (**Qmppc**, undated) is seen beyond Cerro Chivato. Mount Taylor volcano appears in left background.

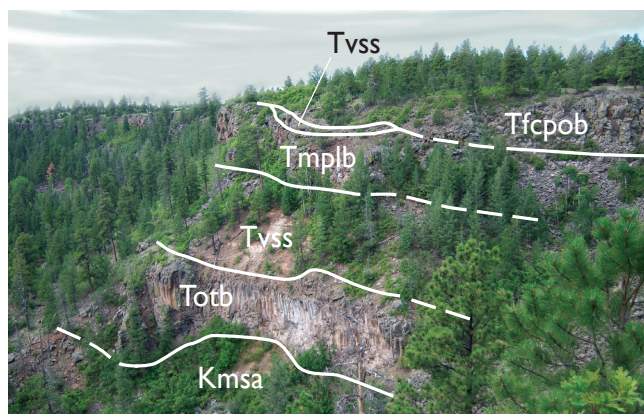


FIGURE 27. A view of the west wall of upper Seboyeta Canyon showing volcanic sequence filling a paleovalley cut into Satan Tongue of Mancos Shale (**Kmsa**). **Totb** is a lumped unit of older fine-grained aphyric trachybasalt (2.83 Ma, the magnetic polarity is normal at this location) overlain by volcanoclastic sediments with interlayered silicic fall deposits (**Tvss**). **Tmplb** is medium-grained plagioclase-phyric trachybasalt (2.70 Ma, the magnetic polarity is normal) overlain by discontinuous exposures of volcanoclastic sandstone (**Tvss**). The sequence is capped with fine-grained augite-phyric trachybasalt (**Tfcpcb**, undated, the magnetic polarity is normal) suggesting the uppermost flow is greater than 2.58 Ma.



FIGURE 28. The photograph shows the phenocryst texture of olivine-rich basalt (**Qolpb**; 2.41 Ma); virtually every phenocryst is olivine although there are a few black-augite and white-plagioclase phenocrysts. Many of the "true" basalts (see Appendix 2) have extremely abundant phenocrysts of olivine \pm augite \pm plagioclase.

Erosion of the Volcano

Our dates allow us to assess the beginning, duration, and end of a massive erosion event that coincided with the growth of Mount Taylor volcano. This erosion is mostly recorded in units **Tvss** and **QTvs**. The former unit consists primarily of bedded volcanic sandstone (Fig. 29), minor conglomerate and interlayered intermediate to silicic tuffs, mostly fall deposits (Figs. 10, 27). The age of the early, bedded deposits (**Tvss**) is between about 3.1 and 2.7 Ma, depending on location. One of the best places to examine them is east of Water Canyon and on the southern end of Encinal Mesa.

The two types of volcanoclastic deposits overlap in time (Fig. 5b), but by about 2.9–2.8 Ma, the coarser and more massive unit (**QTvs**) becomes more dominant. **QTvs** consists of 70–80% water-deposited debris flows containing large boulders of intermediate composition volcanics (Figs. 30a, 30b). Many boulders and cobbles display intense low-grade hydrothermal alteration. The remaining 20–30% of the deposits consist primarily of hyperconcentrated flow and typical streamflow deposits that often form broad channels and become more prevalent away from the volcano (Fig. 31). Beds and lenses of tuffs and reworked tuffs are interlayered in the debris flows at all intervals of the unit (Fig. 32).

Formation of **QTvs** deposits ceased at about 1.5 Ma. For example, at La Jara Mesa and the western flank of Mount Taylor, the Quarry trachybasalt (1.74 Ma; Goff and Goff, 2013) overlies all but a small patch of debris flow deposits found on top of this lava. The majority of the thick **QTvs** debris flows cover mafic lava dated at about 2.9 Ma and are interlayered with various lavas dated at 2.8–2.6 Ma. North of Mount Taylor, distal poorly exposed deposits of **QTvs**

overlie older trachybasalt (**Totb**, 3.2 Ma). Distal deposits are well exposed in middle Colorado Canyon (Fig. 31) where they are overlain by trachybasalt lava dated at 1.79 Ma. In turn, patches of **QTvs** overlie this trachybasalt. East, northeast and southwest of Mount Taylor, **QTvs** underlies quartz-bearing trachybasalts (mentioned above), the youngest of which is dated at 1.53 Ma.

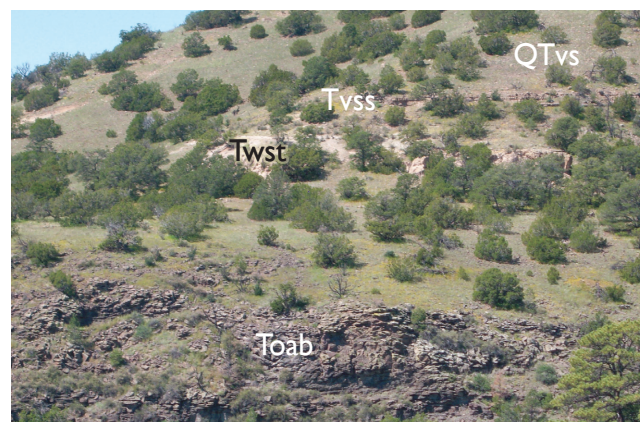


FIGURE 29. The east end of Water Canyon shows older alkali basalt (**Toab**, 3.16 Ma) overlain by a trachydacitic pyroclastic flow that partially lines the upper walls (**Twst**, 2.87 Ma, see Fig. 13). The pyroclastic rocks are overlain by up to 10 m of bedded volcanic sandstones and gravels (**Tvss**) that are in turn overlain by thick volcanic debris flow deposits (**QTvs**).



FIGURE 30a. Massive debris flow deposits (QTvs) exposed along FS-239 west of Mount Taylor (Crumpler and Goff, 2012, stop 7). Most of the boulders are porphyritic trachydacite and trachyandesite.



FIGURE 30b. Debris flow deposit (QTvs) exposed along FS-501 south of Mount Taylor. Note the matrix of gray, fine-grained, ash-rich, volcanic sandstone. Many of the debris flows are matrix supported, but exposures showing this texture are rare. Most deposits are covered by a lag of trachydacite and trachyandesite boulders.

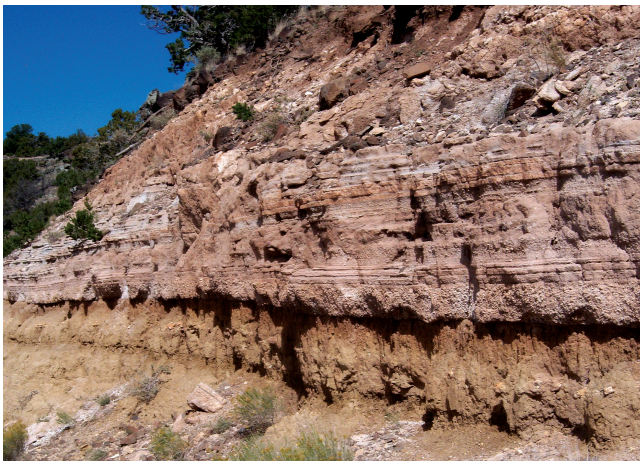


FIGURE 31. Distal deposits of QTvs exposed along middle Colorado Canyon north of Mount Taylor (Crumpler and Goff, 2012, stop 15). These layers contain less gravel and more sandstone than most proximal deposits and also contain beds of pumice and reworked pumiceous sandstone. They are overlain by trachybasalt dated at 1.79 Ma (located in the upper left of the photograph).



FIGURE 32. Pumice blocks in trachydacite ignimbrite exposed as a layer and/or small channel fill within QTvs near head of Lobo Canyon, south of Mount Taylor (Lipman and Mehnert, 1979; Crumpler and Goff, 2012, stop 5). The pumice was dated at 2.71 Ma.

Origin of the Amphitheater

Most previous workers have stated that the Mount Taylor Amphitheater is erosional and was not initially created by a large explosion (Hunt, 1938, Lipman and Menhert, 1979; Perry et al., 1990). There is no widespread apron of late-stage pyroclastic rocks or ignimbrite that surrounds the volcano. The most voluminous pyroclastic material is associated with Phase I rhyolitic volcanism ending around 2.9 Ma. Since that time, pyroclastic eruptions were consistently less voluminous and primarily of a trachydacite composition. We dated no pyroclastic eruptions later than 2.70 Ma. However, the stratovolcano continued to evolve until 2.50 Ma. Additionally, we could not identify any large debris avalanche deposits in unit QTvs. Thus, we concur with most others that the Amphitheater is an erosional feature, perhaps developed along preexisting structures (Fig. 33).

It is our interpretation that late stage emplacement of the radiating dikes and the trachydacite-alkali rhyolite plug (2.54 Ma), and coinciding magma-induced hydrothermal alteration destabilized the core of the volcano causing accelerated erosion along an east-west axis. The eastern core of the Amphitheater was further destabilized by intrusion of the gabbro plug (1.97 Ma). Consequently, the debris from the original cone formed a huge fan east and southeast of the volcano (see map). Starting around 1.5 Ma, stream incision along ravines and the margins of various mesas focused deposition at the mouths of developing canyons such as the Qf3 fan at the mouth of Water Canyon.

In contrast, Crumpler (1982, p. 294) has suggested that the Amphitheater may have resulted from a Mount St. Helens-type lateral blast (sector collapse with simultaneous magmatic explosion). However, our mapping has not identified blast-type pumice deposits or ignimbrites to the east of the volcano in the QTvs section or elsewhere, nor have we identified the hummocky landslide and debris flow deposits characteristic of catastrophic stratovolcano sector collapse (e.g., Hoblitt et al., 1981; Voight et al., 1981).

Another interpretation for the existence of the Amphitheater is Pleistocene glaciation (Ellis, 1935), but the evidence for this view is very sparse. We found no glacial deposits such as moraines anywhere in and around Mount Taylor, although they could possibly be hidden in the large mass of QTvs that formed prior to 1.5 Ma east and southeast of Water Canyon. Additionally, the Amphitheater is certainly not U-shaped with a flat floor like classic glacially carved valleys (Figs. 18, 19, 33). Hunt (1956) also stated that no moraines were found at Mount Taylor, yet several researchers have restated Ellis's concept that the Mount Taylor amphitheater hosted Pleistocene glacial ice (e.g., Pierce, 2004). Recently, Meyer et al. (2014) attempted to find evidence for glaciation at Mount Taylor. Their work suggests that the "cirques" northeast of "La Mosca" may have held short-lived glaciers or rock glaciers, but their evidence is not conclusive. On the other hand, Meyer et al. (2014) state that glaciation was "unlikely to have occurred for any significant period in the eastern Amphitheater of the mountain where it was previously inferred."

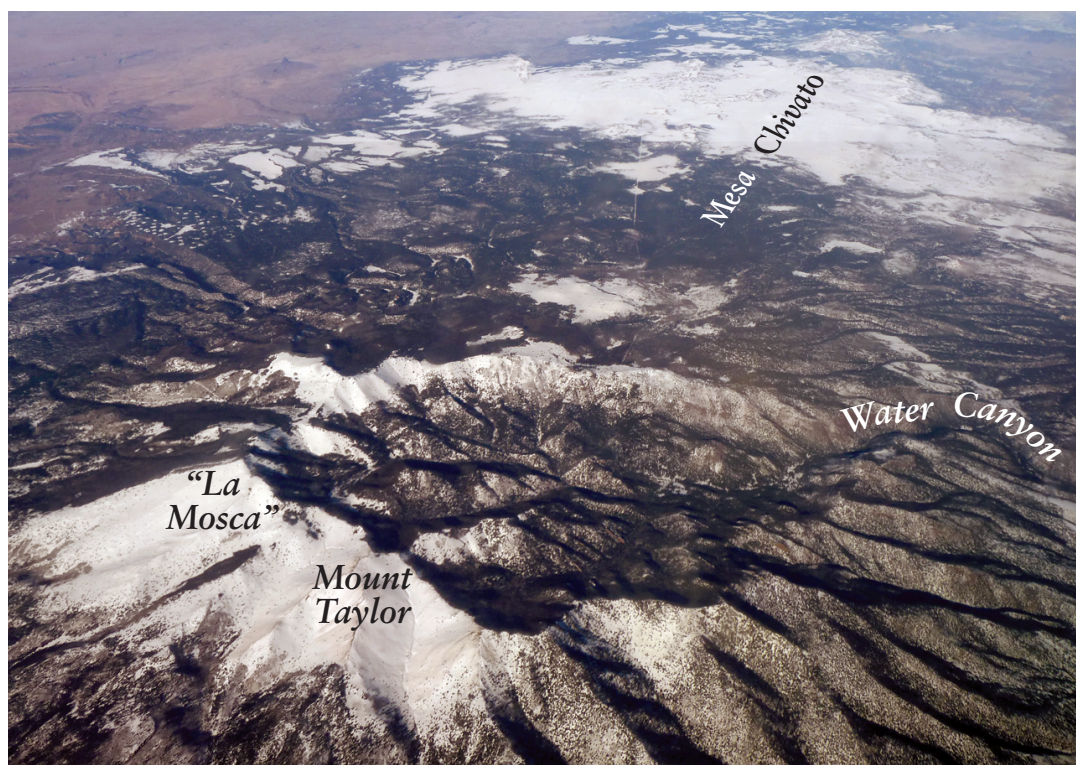


FIGURE 33. Oblique aerial photograph with a view looking northeast across the Amphitheater of Mount Taylor toward southwest Mesa Chivato in winter 2008. The Amphitheater has not evolved into a classic glacially-carved valley with flat-bottomed U-shape. Rather, it is an elongate east-facing bowl exposing eroded volcanic flows, dikes and plugs (see Fig. 19). *Photo courtesy of Kirt Kempter.*

Structural Geology

Folds

The only significant fold in the map area is the north-south striking, unnamed monocline on the western edge between the drainage of Lobo Canyon (south) and La Jara Mesa (north). The monocline dips sharply to the east and plunges south disappearing beneath Grants Ridge but joins a similar structure to the south, slightly west of the map area. Mancos Shale is exposed at the bottom of the monocline, whereas Stray Sandstone is exposed at the top (Fig. 34). The Mulatto Member of the Mancos Shale is exposed across a north-trending valley to the east. The monocline is cut by an east-trending dike of augite-megacrystic trachybasalt (**Ttcbi**) that was emplaced along a small fault (Goff et al., 2013a, fig. 3a). The monocline also appears north of La Jara Mesa and is clearly visible north of NM Highway 605 where it dips gently east.



FIGURE 34. East-dipping bed of Stray Sandstone at the crest of an unnamed monocline on the west edge of the map; Shari Kelley standing here for scale. Note the layers of black manganese oxides deposited along preferential bedding planes.

As mentioned above, this monocline is west of the McCarty syncline of Hunt (1938), and both are Laramide in age (roughly 80–55 Ma; English and Johnston, 2004). According to Hunt (1938, p. 74 and fig. 4), the McCarty syncline is best expressed about 25 km south of Grants. The syncline trends northeast toward the amphitheater of Mount Taylor and disappears beneath the volcanic field. However, drilling intercepts and our mapping shown in cross sections (A–A' and B–B') indicate that the syncline essentially terminates in the Rinconada Basin area south of Mount Taylor. We have observed that Cretaceous rocks are gently warped and folded throughout the Mount Taylor area and that the Cretaceous section is uplifted and deformed by intrusions within the Amphitheater.

Young structural domes

At least four structural domes or broad uplifts, most likely resulting from underlying igneous intrusions (Goff et al., 2013b) occur in the map area. The first three of these features described below were initially recognized by Hunt (1938): the San Fidel Dome, the Devil Canyon Dome, and the exposed gabbro plug (unit **Qxgi**) located in the eastern Amphitheater, which uplifted and displaced Cretaceous beds 500 m or more.

By far the most spectacular is the San Fidel dome near the south edge of the map east of Rinconada Canyon (Fig. 35). It is a 3 x 2 km northeast-trending elliptical dome. The north side and crest of the dome are capped by deformed older megacrystic trachybasalt dated at 2.78 Ma (e.g., lumped unit **Tomtb**, see map). The vent for this lava lies to the west (**Tomtc**) and is not uplifted. The scoria contains blocks of olivine monzogabbro dated at 3.24 Ma (Goff et al., 2013b). An olivine-rich nephelinite dike trending N80°E cuts flat-lying Cretaceous rocks west of the dome but terminates abruptly at the dome margin faults (Goff et al., 2013a, fig. 3c). About 0.5 km southeast of the dome, flows and intrusive rocks of San Jose Canyon trachydacite are exposed (**Tphtd**, 2.63 Ma discussed previously). No dikes or intrusive rocks are exposed in the eroded southern core of the dome, but the folded and uplifted Cretaceous rocks display significant low-grade hydrothermal alteration discussed below.

The southern portion of the dome is deeply eroded by a few hundred meters into the Mancos Shale forming a steep-walled valley. High-angle faults separate flat-lying Cretaceous rocks surrounding the dome from folded and faulted rocks within it. Rocks exposed along these high-angle faults display prominent slickensides (Fig. 36). Maximum uplift is 370 m determined by the difference in elevation between uplifted lava at the crest and non-deformed lava beneath the scoria. In addition, several normal faults with displacements ≤ 100 m appear to trend radially away from the exposed core of the dome. Four of these “radial” faults form small graben-like structures.

The dome was explored for oil in the 1940s, and the State 36-1 oil test was drilled to about 900 m (2,953 ft), spudded in the southern core of the structure. The well did not encounter any igneous rocks but did intersect a repeated section of Cretaceous rocks that we interpret as thrust faulting caused by the magmatic intrusion (Fig. 37). The well penetrated the Jurassic Todilto and Entrada Formations; thus cross section B–B' extends deeper into the Jurassic than cross section A–A'.

Previously, both Hunt (1938) and Lipman et al. (1979) indicated that relatively shallow emplacement of magma caused uplift of the dome. Furthermore, Lipman et al. suggested the intrusion is part of their Porphyry of San Jose Canyon. Our work shows that the intrusion occurred later than 2.78 Ma, but because of the gabbro bombs, mafic dikes and several mafic eruptions in the area, we suggest the causative body is probably gabbro. Alternatively, the uplift could be caused by the combined or sequential intrusion of trachybasalt and trachydacite magmas.

Several researchers have conducted experiments to study faults and fault patterns resulting from magmatic intrusion (magmatic overpressure) into cold country rocks (Komuro et al., 1984; Marti et al., 1994; Walter and Troll, 2001; Acocella et al., 2001). Many of these studies were focused on intrusions

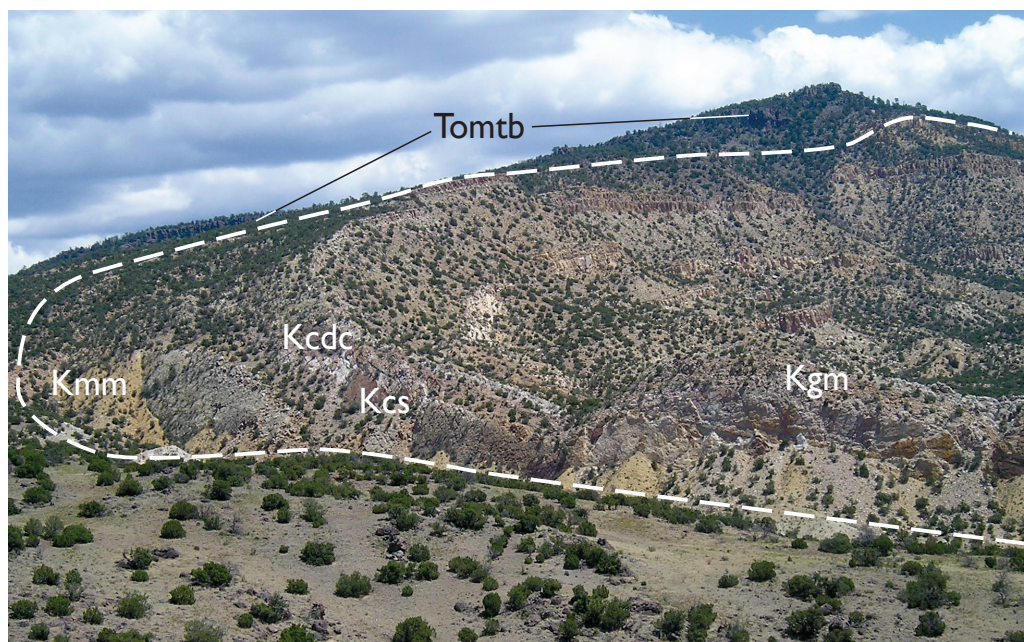


FIGURE 35. The view looks to the north-northeast across the eroded southern core of the San Fidel dome composed of uplifted and deformed Cretaceous rocks (**Kmm**–Mulatto Tongue of Mancos Shale, **Kcs**–Stray Sandstone, **Kcdc**–Dilco Coal, **Kgm**–Main body of the Gallup Sandstone). White dashed line is used to accentuate the domal uplift. **Tomtb** is uplifted older megacrystic trachybasalt lava dated at 2.78 Ma at crest and west flank of dome.



FIGURE 36. Vertically-standing Cretaceous rocks along the west margin of the San Fidel dome contain many slickenside marks from slip along bedding planes.

that form resurgent domes in calderas. All experiments form domal uplifts, but the style of faulting is dependent on experimental materials and parameters. Radial and circular concentric faults are common. The circular faults are very high-angle normal to a variety of reverse faults. The reverse faults often interconnect at depth. Typically, a small shallow graben or depression forms near the top of the dome due to stretching (extension) of the intruded materials. After San Fidel Dome grew, erosion of soft Mesozoic strata in a summit depression or graben may have resulted in the circular steep-walled valley we see today.

Devil Canyon Dome is located about 5 km north of San Fidel Dome in upper Rinconada Basin. The dome is about 1.5 km in diameter and is characterized by an arcuate

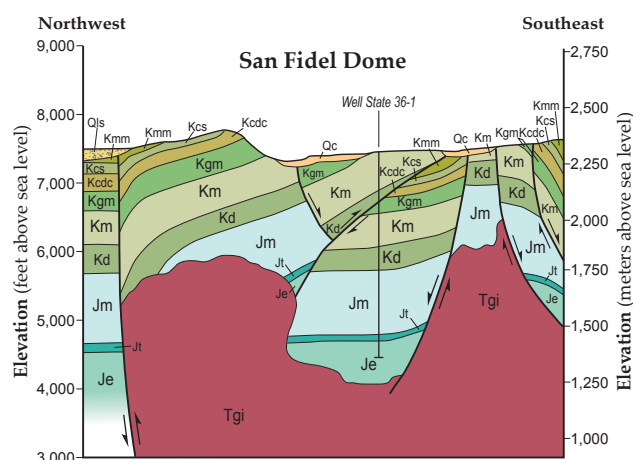


FIGURE 37. Shortened view of the east end of northwest-southeast cross section B-B', Lobo Springs quadrangle (Goff et al., 2008; 2013b) showing the subsurface interpretation of the structure beneath the southern part of the San Fidel dome. **Tgi** is a possible gabbroic intrusion that we believe is the cause of the uplift (but see Lipman et al., 1979 for another interpretation). The western-boundary fault of the uplift has displayed alternating normal to reverse faulting through time: **K** are Cretaceous and **J** are Jurassic rocks (see Goff et al., 2008 for complete descriptions).

uplift of locally faulted Cretaceous strata that superficially resembles a south-plunging monocline. Several mafic dikes with different strike directions cut across the northeast crest of the dome and some of the Cretaceous rocks display weak, low-grade hydrothermal alteration. We suspect that emplacement of shallow gabbro, possibly related to Mount Taylor volcanism, formed the dome, dikes, and alteration. A relatively low amplitude (± 20 gammas), 400-m-wide positive aeromagnetic anomaly, coincident with the Devil Canyon

dome (GeoMetrics, 1979; line 242, p. AL53), supports the interpretation of a magnetite-bearing mafic intrusion at depth (R.M. Chamberlin, NMBGMR, written comm., 2013).

The eastern Mount Taylor Amphitheater contains a gabbro plug (unit Qxgi, 1.97 Ma) that uplifted strata of the Mesa Verde Group, the Gibson Coal Member, and the overlying Satan Tongue of the Mancos Shale (Fig. 38). On the east margin of the intrusion, the beds dip as much as 55° southeast and display considerable low-grade hydrothermal alteration. The dip on these strata is only 15° east roughly 0.3 km east of the intrusion. Cretaceous strata are not uplifted in this manner north and south of the gabbro plug. Although Hunt (1938, p. 75) mentions these deformed strata, he does not specifically tie their deformation to the intrusion. Lipman et al. (1979) lumped all the Cretaceous rocks within the Amphitheater as undivided and did not mention any association between the steeply dipping beds next to the gabbro and igneous intrusion. Further west, the Cretaceous section appears to be down-dropped by a fault. Although exposures are poor, we found coal in some of the beds in this area, which we correlate with the Gibson Coal Member. Possibly the gabbro intruded along preexisting faults (see map and cross section).



FIGURE 38. The view looks to the north at the east-dipping Cretaceous sandstone beds east of the gabbro plug (Qxgi) in Mount Taylor Amphitheater. The elk fence marks the boundary between U.S. Forest Service land (left, west) and Mount Taylor Ranch (owned by Laguna Pueblo, Fig. 4).

American Canyon uplift is located about 7 km north of the amphitheater of Mount Taylor at a sharp west bend of the namesake canyon. The uplift is defined by two, north-trending, down-to-the-west faults that expose over 75 m of volcanoclastic sediments along the south wall of the canyon. Two scoria cones and associated flows cover the north wall. The eastern cone erupted flows containing gabbroic xenoliths, which are dated at 2.30 Ma (Goff et al., 2013b). The sediments south of the canyon are ultimately capped by an aphyric lava flow dated at 1.76 Ma. Both of the dated flows are offset by the easternmost fault mentioned above. This area is unusual because no other place north of Mount Taylor displays such a thick section of sediments surrounded and capped by relatively young, faulted flows. We suspect that emplacement of a small gabbroic intrusion <1.76 Ma has caused uplift of the sediments and flows in this area, and caused the abrupt change in the direction of the creek.

Faults

We identified about 100 faults in the map area. Most are normal faults with displacements of <50 m and the predominant trend is north-northeast to northeast (Fig. 39). Many, but certainly not all, faults are shown on the map of Dillinger (1990). Many of Dillinger's faults in the volcanic rocks on the mesas are located approximately correctly, but we often found the displacement directions are opposite to ours (Fig. 40). Very few faults are shown on the map of Lipman et al. (1979), most around San Fidel dome. However, we found two faults cutting either side of the Amphitheater walls, both trending northeast, down to the southeast. We also found two north- to northwest-trending faults within the core of the Amphitheater probably related in part to intrusions. It is our opinion that the east-west alignment of the youngest intrusions coupled with later faults mentioned above has created structural weakness within the Amphitheater.

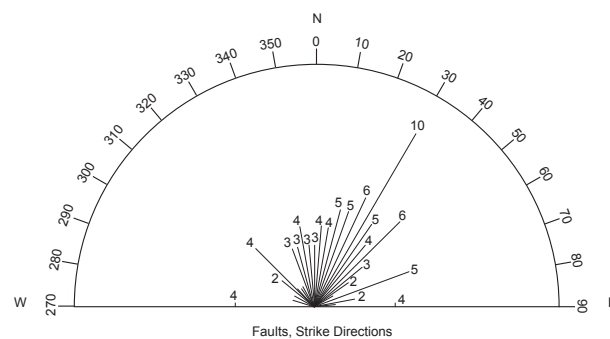


FIGURE 39. Rose diagram showing strike directions of 94 faults measured to the nearest 5° in the Mount Taylor region. The orientation trend ranges from N10°E-N45°E. Curving faults were broken into segments to obtain major strike directions.



FIGURE 40. The view looks to the west at a downthrown-to-the-southeast normal fault cutting lava and underlying Cretaceous rocks at the extreme southern end of Horace Mesa (south edge of the map). This fault is incorrectly shown down to the northwest on the map of Dillinger (1990). Displacement in Cretaceous rocks is greater than in the lava proving that this fault was active before volcanism.

Faults with large displacements occur in the Cretaceous strata indicating that major northeast-trending faulting began before volcanism (Fig. 41; Hunt, 1938). We identified a northeast-trending, shallow graben in the vicinity of Lagunas Cuatas (herein named the Cuatas Graben) in southwest Mesa Chivato. It is bordered on the southeast by a normal fault skirting the highlands of Cerro Pino and Campo Grande. The northwest edge of the graben is defined by a pair of normal faults, one of which was a fissure, dike and spatter system for the eruption of olivine trachybasalt (**Qyob**, about 2.2 Ma). The fissure system resembles the aligned pyroclastic vents described in the Rosa basalt flow in Washington and Oregon (Brown et al., 2014). Cuatas Graben apparently extends northeast into the area mapped by Crumpler (1977), who also identified northeast-trending fault-controlled scoria cones (i.e., Cerros de Alejandro, Crumpler, 1980b, fig. 2). The graben cannot be traced to the southwest beyond Cerro Redondo (1.90 Ma) because relatively young lava flows bury it.



FIGURE 41. The view looks to the northeast at a down-to-the-northwest fault cutting Dalton Sandstone (**Kcd**) and overlying Cretaceous beds in western part of Rinconada Basin. We could not detect any offset in Tertiary volcanic rocks at either end of the fault.

Mafic Dikes

We found several mafic dikes cutting Cretaceous rocks in the basins and mesas surrounding Mount Taylor (Goff et al., 2013a, fig. 3), but mafic dikes are most common as linear ribs of vertically standing lava, spatter and agglutinate within scoria cones (Fig. 42). We measured the strike directions of 127 mafic dikes, and their preferred trend is N30°E–N45°E (Fig. 43). Many of the dikes are curving so an average strike direction was made for these. The preferred direction of mafic dike trends is more or less parallel to the trend of the Jemez volcanic lineament. We did not attempt to characterize the strike directions of mafic dikes as a function of their age, chemistry or mineralogy.

Radial Dikes

Radial dikes are a characteristic feature of the western Mount Taylor Amphitheater and volcano flanks (Hunt, 1938; Lipman et al., 1979; Perry et al., 1990; Crumpler and Goff, 2012, stop 9; Crumpler and Goff, 2013, stop 5; Goff et al., 2013a). As mentioned above, a very high percentage of these dikes post-date the emplacement of trachyandesite lavas forming



FIGURE 42. The view looks to the east at a northeast-trending dike of agglutinate and lava in the summit area of scoria cone (**Qfcd**, undated) south-southeast of Cerro Redondo.

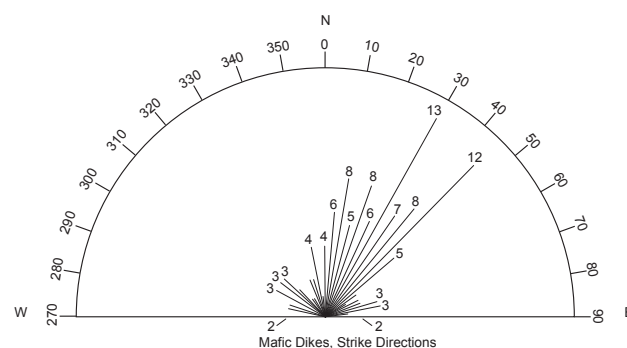


FIGURE 43. Rose diagram showing strike directions of 127 mafic dikes measured to the nearest 5° in the Mount Taylor region. The orientation trend ranges from N30°E–N45°E. Curving dikes were broken into segments to obtain major strike directions.

the summit of Mount Taylor or the trachydacite plug and flow forming “La Mosca,” i.e., mostly younger than 2.70 Ma. Compositionally, there are four major types: trachyandesite (unit **Ttai**), biotite trachydacite (**Tbi**), hornblende-biotite trachydacite (**Thbi**), and hornblende trachydacite (**Thi**). No attempt was made to determine if the composition is somehow related to age. Most dikes are a few hundred meters in length or less, but a few are over a kilometer long. Many have echelon segments. They tend to be 10–30 m wide; some are as much as 30 m tall in outcrop (Fig. 17). We measured the strike direction of 148 radial dikes, and their preferred trend is N55°W (305°, Fig. 44) with most between N60°W–N25°W (300–335°). This orientation is approximately perpendicular to the preferred trends of faults and mafic dikes in the region (compare Figs. 39, 43, and 44). Interestingly, the preferred trend of radial dikes is more or less similar to the trend of the Amphitheater, roughly N60°W (300° azimuth).

Goff et al. (2013b) compared the radial dikes at Mount Taylor to those at Summer Coon volcano in Colorado (about 33 Ma). Summer Coon contains hundreds of radiating basaltic andesite dikes but only about 20 radiating silicic dikes. The latter are 2–7 km long, typically 50 m wide and 20 m high. Poland et al. (2008) have found that silicic dikes tend to

become wider at greater distances from the central vent and have postulated that these wide dikes were feeders to distal eruptions on the flank of the volcano. In this respect, Mount Taylor and Summer Coon are similar in that we have observed that the later flank and rim eruptions at Mount Taylor have the same age and composition of the associated radiating dikes (see Fig. 44). In fact, we observed that the spectacular South Wall dike has an enlarged bud or bulb at the point where the dike crosses the Amphitheater rim (Fig. 45). We believe this bulb was actually the feeder or plug for a now eroded dome that originated from magma in the dike.

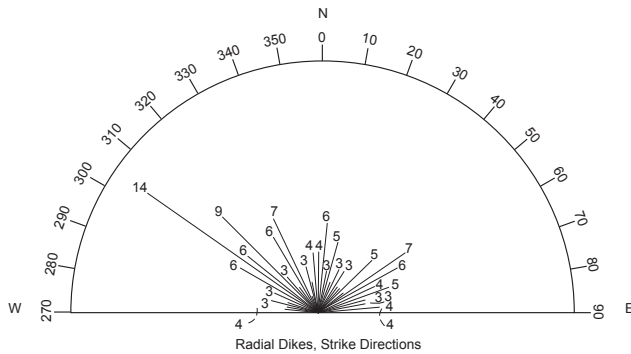


FIGURE 44. Rose diagram showing strike directions of 148 radial dikes measured to the nearest 5° in and around the Mount Taylor Amphitheater. The orientation trend ranges from N65°W–N25°W (295–335°) or nearly opposite to the orientation trends of the measured faults and mafic dikes.



FIGURE 45. The view looks to the north at a bulb at the apex of South Wall dike where it crosses the Amphitheater wall; the slope, on the right, in the background is inside of the north Amphitheater wall. Note the complex cooling joints in the bulb including radial joints (R). This bulb is probably the exposed feeder plug for a now eroded dome (from Goff et al., 2013a).

Maar Volcanoes and Diatremes

One of the defining characteristics of southwest Mesa Chivato is the presence of numerous shallow volcanic depressions or “maars” (Aubele et al., 1976; Goff et al., 2014a, b; Table 3) that have implications regarding the paleohydrology of the area. We have also identified a probable maar on Horace Mesa. Maars were previously described northeast of our map in the region studied by Crumpler (1977). Maars form from the explosive interaction of magma with shallow groundwater producing phreatomagmatic (or hydromagmatic) eruptions and deposits (Fisher and Schmincke, 1984). Maar volcanoes are circular to elongate volcanic craters with encircling tephra ramparts (tuff rings) possessing an interior vent that cuts through preexisting country rock (Fisher and Schmincke, 1984, p. 258). The maar volcanoes in the Mount Taylor region are basaltic and small shallow lakes or lagunas (see Appendix 1) occupy many vents and/or interior depressions. The only maar in the map area currently possessing a real lake is Laguna Redonda; however, in this case, the lake is fed by a nearby well.

For this map, unit **Qlm** is defined as maar crater-fill deposits consisting primarily of poorly exposed, organic-rich, eolian-derived clay and silt filling the circular vent; during wet periods the vent area may contain a shallow lake. We identified 27 maar vents and other depressions of various sizes (Table 3; see below); most are ≤ 1 km in diameter. Unit **QTvm** consists of poorly exposed hydromagmatic deposits that form around the vent area. The best exposures of **QTvm** on southwest Mesa Chivato occur in the modified drainage at the south end of Laguna Cañoneros maar (Fig. 26), where deposits consist primarily of plane-parallel base surge beds containing a mixture of quenched basaltic (hydroclastic) shards and

fragments, sideromelane, yellow-brown palagonite, and lithic fragments (Fig. 46). Colluvium primarily buries other deposits of **QTvm** which are recognized by a lag of poorly sorted and rounded gravel of foreign lithic fragments. Maximum observed thickness of **QTvm** is about 5 m.

A good exposure of maar deposits (unit **Thytb**, undated) is found along the southeast margin of Horace Mesa adjacent to Rinconada Basin (Fig. 47). The deposits overlie trachydacite tuffs (ca. 2.75 Ma) and are overlain by **QTvs**. The source of the hydromagmatic deposits appears to be an unnamed shallow crater to the north that is surrounded by younger lava (**Qfqtb**, 1.64 Ma).

Some “lagunas” or small craters in the Mount Taylor region are probably not maars but are instead shallow areas between lava flow lobes, along lava flow boundaries, or along faults (sag ponds). Examples in order include Laguna Telesfor and Blanquita, Laguna del Padre, and Laguna de Frances, respectively. Two puzzling small circular depressions about 320 m in diameter have very uncertain origins because they are isolated on top of flat lava flows: Laguna Fria and the unnamed depression north of Cerro Colorado (southwest Mesa Chivato). Perhaps they are collapse features resulting from compaction of underlying soil or gravel, or from the collapse of lava tubes.

Exact ages of the various maar vents and deposits are generally unknown but most seem to be late Pliocene to early Pleistocene. The hydromagmatic deposits exposed in the south drainage of Laguna Cañoneros (Fig. 46) are too altered to date without considerable sample preparation. However, the age of the deposits (and thus the eruption) is

TABLE 3. Maar volcanoes and other strange "lagunas," in the Mount Taylor volcano area, New Mexico.

Name, quad ^a	Dimensions (m)	QTvm deposits, comments	Maar?
Laguna Chute, LC	960 x 1600	lag gravel beneath scoria cones, N edge of map	yes
Laguna Blanca, LC	800 x 1300	none obvious	yes
John Nelson Tank, LC	950 x 2000	none obvious; present on east end (?), modified vent	yes
Laguna Piedra, LC	800 x 1100	ring of boulders around vent	yes
Unnamed vent, LC	320 x 650	small ring of boulders around vent, pond NE of L. Piedra	probable
Laguna Bonita, LC	800 x 1750	none obvious	yes
Laguna Cuate (west), LC	1450 x 3050	none obvious; NE-SW migrating vent along buried fault	yes
Laguna Cuate (east), LC	960 x 2400	none obvious; NE-SW migrating vent along buried fault	yes
Laguna Fria, LC	320 circle	none obvious	uncertain
Laguna Cruz, LC	800 x 1300	none obvious; present on south end (?)	yes
Laguna Redonda, LC	560 circle	lag gravel/boulders on SW shore (?)	yes
Laguna Largo, CP	650 x 1750	none obvious, vague deposits; on NE-trending fault	probable
Laguna del Padre, LC	320 x 550	none obvious; low spot at flow front	uncertain
Unnamed depression, LC	320 circle	none obvious; lag gravel on N shore, pond N of C. Colorado	uncertain
Laguna de Damacio, LC	800 x 1100	none obvious; deposits buried around shoreline	yes
Unnamed depression, LC	550 x 700	none obvious; buried on NE shore, pond S of L. Damacio	uncertain
Laguna (unnamed), LC	1100 x 1350	lag gravel/boulders on eastern shore, lake in southern quad	yes
Laguna de Frances, LC	400 x 1450	none obvious; fault-controlled sag pond	no
Laguna Telesfor, LC	650 x 800	none obvious; low spot between flows	uncertain
Laguna Blanquita, LC	330 x 500	none obvious; low spot between flow lobes	no
Laguna Vieja, LC	500 x 950	none obvious	probable
Laguna Cañoneros, LC	1200 x 2550	double vent; deposits along S drain	yes
Laguna Bandeja, LC	500 x 800	lag gravel/boulders on margins	yes
Laguna Reyes, LC	650 x 1120	lag gravel/boulders on margins	probable
Laguna Encina, LC	800 x 1300	none obvious; beds on NW shore (?), E edge of map	yes
Llanito Frio Tanks, CP	550 x 900	lag gravel/boulders on margins	probable
Unnamed vent, LS	800 x 1450	deposits obvious on eastern Horace Mesa	yes

^aCP—Cerro Pelon, LC—Laguna Cañoneros, LS—Lobo Springs

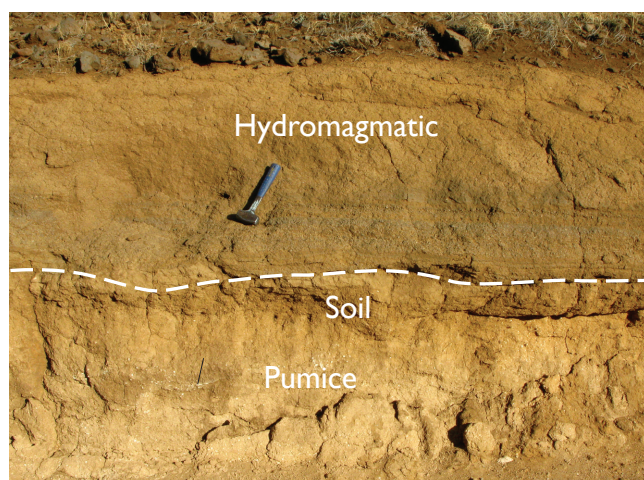


FIGURE 46. The view looks to the east at the drainage wall on the south end of Laguna Cañoneros showing plane parallel beds of basaltic hydromagmatic deposits overlying pumice-rich soil. Similar trachydacite pumice found to the south is dated at 2.70 Ma. *Photo by J.R. Lawrence.*



FIGURE 47. The view looks to the northwest at the upper cliff face along southeast Horace Mesa: 1) pinkish upper ignimbrite of Grants Ridge rhyolite tuff (3.26 Ma), 2) trachydacite tuff (ca. 2.75 Ma), 3) bedded and cross-bedded hydromagmatic surge, 4) massive, poorly bedded hydromagmatic deposits, and 5) massive debris flows of QTvs.



FIGURE 48. A panoramic view that looks southwest towards Lagunas Cuates with a younger, overlying lava flow (unit **Qftb**, 2.28 Ma) flooding between the basins. Cerro Redondo's scoria cone (unit **Qfocr**, 1.90 Ma) and Mount Taylor are on the skyline. *Photo by J.R. Lawrence.*

constrained by an overlying flow of basanite (unit **Tbal**, 2.58 Ma; Fig. 26) and an underlying soil containing trachydacite pumice (≥ 2.70 Ma). We can provide a minimum age on some of the other maars from the age of overlying lava flows. For example, the age of the two Laguna Cuates maars is older than the basaltic flow that floods between them (>2.28 Ma, unit **Qftb**, Fig. 48). Using the same logic, Laguna Reyes is >2.14 Ma (age of overlying unit **Qfatb**), Laguna de Damacio is >2.26 Ma (age of overlying lava from Cerro Aguila), etc. The hydromagmatic deposits exposed beneath the east side of the scoria cone just east of Seboyeta Canyon (unit **Totb**, subunit **Toth**) formed at 2.83 Ma.

The maar craters are circular to oblong, usually elongated in a northeast-southwest direction. A few craters appear to be double-maars with adjacent vents located on northeast-southwest trends. The largest is the western crater of Lagunas Cuates, which is 3×1.5 km (Fig. 48). The smallest craters, such as Laguna Fria, have diameters ≤ 320 m. An unusual characteristic of most maars in the Mount Taylor area is a virtual lack of exposed crater rampart and flanking hydromagmatic deposits typical of tuff rings and tuff cones (Wohletz and Sheridan, 1983; Lorenz, 1986). Except for remnant craters, the maar volcanoes are surrounded and buried by younger lava flows and scoria cones. In this respect, the Mesa Chivato maars resemble eroded scoria cones and volcanic plugs (necks) surrounded by younger lavas in the Camargo volcanic field, Mexico (Aranda-Gómez et al., 2010). Based on field relations and $^{40}\text{Ar}/^{39}\text{Ar}$ dates, the Mount Taylor region maar volcanoes formed between 1.9 and 3.2 Ma (Goff et al., 2014a, b). As in the case of Laguna Cañoneros hydromagmatic beds, we did not attempt to date primary magmatic fragments because of small grain size, alteration and weathering, and contamination with foreign lithics.

Our generalized model in Figure 49 explains the development and resulting field relations of the partially buried maars. The initial tuff cone/ring is fed from an underlying basaltic diatreme and is built on an older surface of lava with or

without soil. Relatively soon thereafter, a younger eruption of lava surrounds the cone/ring before it has completely eroded. With time hydromagmatic beds continue to erode, widening and filling the crater. We believe that the crater-fill deposits are complicated mixtures of eroded hydromagmatic debris, eolian silt, and organic-rich lacustrine beds. Near crater walls, blocks of eroded younger basalt create coarse talus breccia mixed with marginal crater fill. Primary hydromagmatic beds are preserved where covered by younger lava and exposed along streams that drain the craters. Today, Mount-Taylor-region maars are mostly dry, but occasionally contain shallow ponds or small lakes (Goff et al., 2014a, b).

A link between a now-eroded maar and its underlying diatreme (Valentine and White, 2012) is exposed in Seboyeta Canyon cutting southern Mesa Chivato (unit **Tmbi**, Fig. 50). The diatreme contains abundant blocks of Cretaceous rocks ≤ 1 m long (Fig. 51). A dike cutting the diatreme is dated at 3.07 Ma (magnetic polarity is reverse). The elevation difference between diatreme and flanking basalt-covered mesas is 400 m. Presumably, each Mount Taylor region maar is connected to a basaltic root at similar depths.

The Plio-Pleistocene boundary was a period of dramatic global climate change from warmer and wetter to drier and cooler conditions (Zachos et al., 2001; 2008, fig. 2). Changing climate conditions were no different in New Mexico (Morgan and Lucas, 1999). Apparently, the Mount Taylor region maars formed during wetter conditions predominating in the Pliocene, which were normal before 2.5 Ma when groundwater sources were more voluminous. During this time period, the high mesas were broader and rapid canyon cutting had not ensued (Love and Connell, 2005). However, maar activity may have continued until almost 1.9 Ma within the limitations of our mapped stratigraphy and dates. Consequently, a maar-diatreme sequence like Laguna Cañoneros presents an opportunity to drill about 400 m of crater-fill deposits and diatreme root to investigate maar processes and climate change from present to the Plio-Pleistocene boundary.

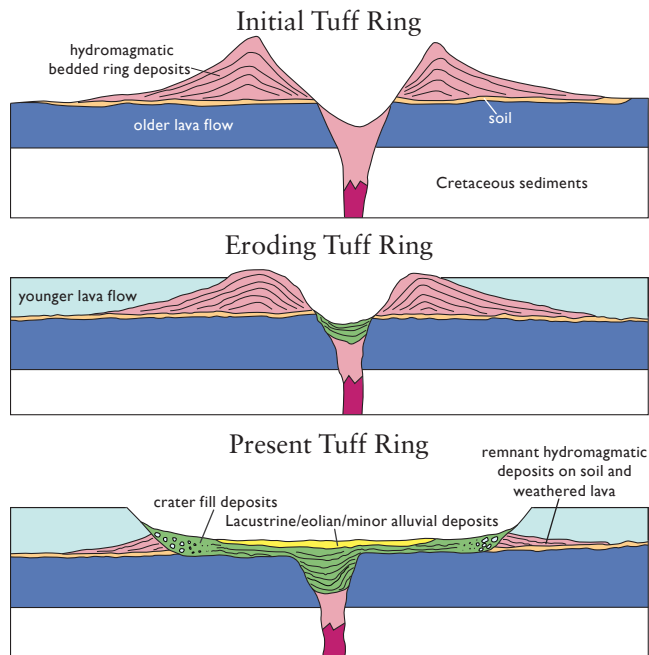


FIGURE 49. Idealized tuff ring evolution in cross section of older maar crater such as Laguna Cañoneros (Fig. 26; see Table 3 for the actual dimensions of maar craters). The magma, shown in red, that formed the maar erupted through Cretaceous rocks, shown in white, and older lava flows, shown in dark blue, that may be covered with soil, shown in tan. The bedded tuff ring deposits, shown in pink, associated with the formation of the maar were probably ≤ 80 m high. Later on, the eroded tuff ring deposits were flooded by younger lava flows, in light blue. Erosion of the tuff ring caused backfilling of the preexisting vent with crater-fill deposits, shown in green (unit **QTvm**), and young lacustrine and/or eolian deposits, shown in yellow (unit **Qlm**).

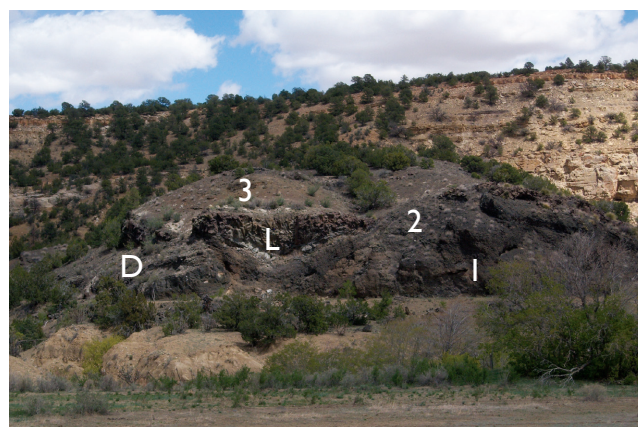


FIGURE 50. The view looks to the east at the Seboyeta Canyon diatreme (**Tmbi**); 1) scoria, 2) hydromagmatic, L) lava infill, 3) hydromagmatic, D) dikes cutting lava and scoria. Cliffs in background are Cretaceous sandstone and siltstone (Gallup Sandstone and Dilco Coal Member).



FIGURE 51. A large block of "cooked" Cretaceous sandstone about 1 m long is exposed on the west side of diatreme.

Water Resources

Because of its elevation, Mount Taylor has relatively high rainfall and snowfall, and this water eventually feeds numerous cold springs throughout the upper flanks and Amphitheater of the volcano. Around the lower flanks, cold springs are primarily limited to the contact between the volcanic rocks, usually lava flows, and underlying Cretaceous sediments. Many of these larger springs are found where streams and ravines have cut canyons across this contact. Examples include the springs at or near the heads of Seboyeta,

Bear, Encinal, Seco, Rinconada, La Mosca, San Mateo, El Rito, and Lobo Canyons. Most of these springs have flow rates of <150 L/min. A few cold springs of low flow rate also occur at similar contact horizons north and northeast of Mount Taylor on the margins of Mesa Chivato. Within Mesa Chivato, the best horizons to exploit water are at the top of Cretaceous rocks or lava flow boundaries. We did not measure flow rates, measure temperatures, or collect samples for chemical analysis of any cold springs in the map area.

Hydrothermal Alteration and Mineralization

Weak hydrothermal alteration is found in many of the volcanic units flanking Mount Taylor. Generally, the alteration is pale red to pink in color and consists of combinations of clay, silica, carbonate, and Fe- and Mn-oxides found in fractures, cavities, and vugs. Two small areas of brick-red alteration are found in the Gibson Coal Member on the west side of upper Rinconada Basin (Fig. 7). The alteration consists of Fe- and Mn-oxides in shale and may have been produced by coal fires rather than hydrothermal fluids. A 3-m-thick coal bed is found within this

area. Fe- and Mn-oxides and travertine deposits are found on Cretaceous units in the exposed southern core of San Fidel Dome (Fig. 52) and just southeast of Devil Canyon dome. The San Fidel Dome area also contains faulted silicified limestone beds (Fig. 53), and some of the Cretaceous rocks seem to be slightly metamorphosed to hornfels. The hornfelsed rocks and hydrothermal deposits are probably caused by the intrusion of shallow magma, as mentioned previously.



FIGURE 52. Photograph showing a 0.5-m-wide rib of Fe- and Mn-oxides and carbonate cutting Cretaceous rocks in the southern core of San Fidel Dome; second author for scale.

Within the Mount Taylor Amphitheater, the hydrothermal alteration is relatively weak and inconsistent, although locally pervasive. Maximum alteration rank is low-grade propylitic (silica, calcite, Fe- and Mn-oxides, chlorite, illite/smectite). Widespread silicification and minor Fe- and Mn-oxide alteration extend throughout the lower northwest wall and areas within and surrounding the eastern rhyolites (unit *Tre*). Significant Fe- and Mn-oxide alteration occurs in Cretaceous rocks near the east margin of the gabbro intrusion (*Qxgi*) and within gravels of *QTVs* adjacent to a prominent dike (*Thbi*) on the northeast side of the youngest trachydacite plug (*Tqtd*). This area of sediments includes zones that resemble

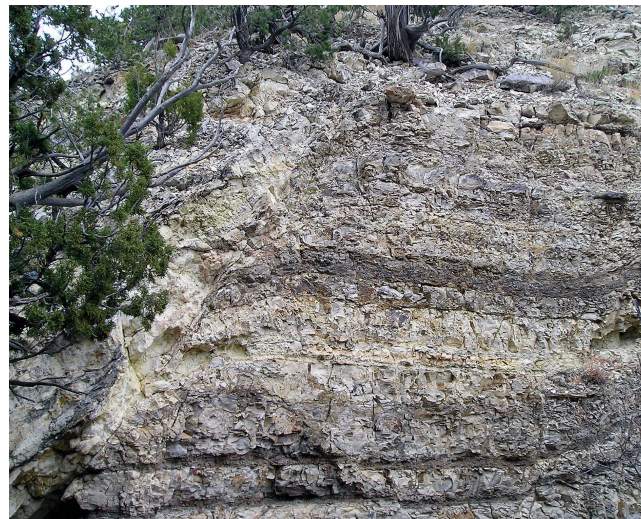


FIGURE 53. The view looks north at a faulted and silicified exposure of Bridge Creek Limestone (unit *Kmb*) in the southern core of San Fidel Dome.

intrusion breccia (Perry et al., 1990) and contains a few large blocks of Cretaceous rocks. Some of the Cretaceous rocks exposed in the eastern Amphitheater appear to be slightly hornfelsed but thin section examination reveals only slight silicification and addition of carbonate. Silica veins where observed are thin wisps of chalcedony and opal. We found no bonanza quartz veins accompanied by pyrite and/or other sulfides anywhere in the map area. Additionally, we found no clear evidence for deposition or replacement of epidote that generally indicates hydrothermal alteration at temperatures $\geq 220^\circ\text{C}$ (Stimac et al., 2015, fig. 46.5).

Geothermal Potential

The geothermal potential of the Mount Taylor region has never been adequately evaluated. A blanket assessment of geothermal potential in the southern Colorado Plateau states: “Although young volcanic features of northern Arizona and New Mexico are possible geothermal targets, the (Colorado Plateau) province has little identified geothermal potential” (Mariner et al., 1982, p. 36). The area around Mount Taylor has measured temperature gradients of $25\text{--}35^\circ\text{C}/\text{km}$ and estimated heat flow of ≤ 2.5 HFU (heat flow units) equivalent to about ≤ 100 mW/m^2 (Nathenson et al., 1982). Additionally, there are no identified hot or warm springs in the Mount Taylor region from which geothermal activity is inferred, and subsurface reservoir temperatures are estimated. Finally, the age and volume of volcanic rocks in the Mount Taylor region are too old and too small (>1.3 Ma and ≤ 100 km^3) to indicate much if any high-temperature geothermal potential ($T \geq 200^\circ\text{C}$; Duffield and Sass, 2003, p. 6).

The first author conducted several discussions with retired uranium miners at local bars and the Grants, New Mexico Mining Museum (2007–2013). These men worked around Mount Taylor up until the early 1980s and claimed

that warm temperatures and warm waters occurred in Jurassic rocks deep in the mines, nominally as deep as 1,500 m. Water as hot as 40°C emerges from the San Mateo mine (Mount Taylor mine; J. C. Witcher, geothermal specialist, personal communication, 2016). As noted above, alteration minerals exposed in Mount Taylor Amphitheater do not indicate particularly high past temperatures (probably $\leq 160^\circ\text{C}$; Stimac et al., 2015, fig. 46.5) but obviously, magmatic temperatures of about 850°C were achieved in the contact zones between intrusions and Jurassic–Cretaceous rocks at depth. The intrusive character of the magma and their high injection temperatures probably disrupted and fractured host rocks creating enhanced permeability around intrusion margins (e.g., map cross section B–B’ and Fig. 54; Stimac et al., 2015). After central magmatic activity ceased around 2.5 Ma, erosion of the Amphitheater created a large basin for water recharge. Thus, the subsurface of the Amphitheater might be a good location for finding geothermal fluids suitable for space heating or other low-temperature applications in fractured igneous and sedimentary rocks at depths $\geq 1,500$ m.

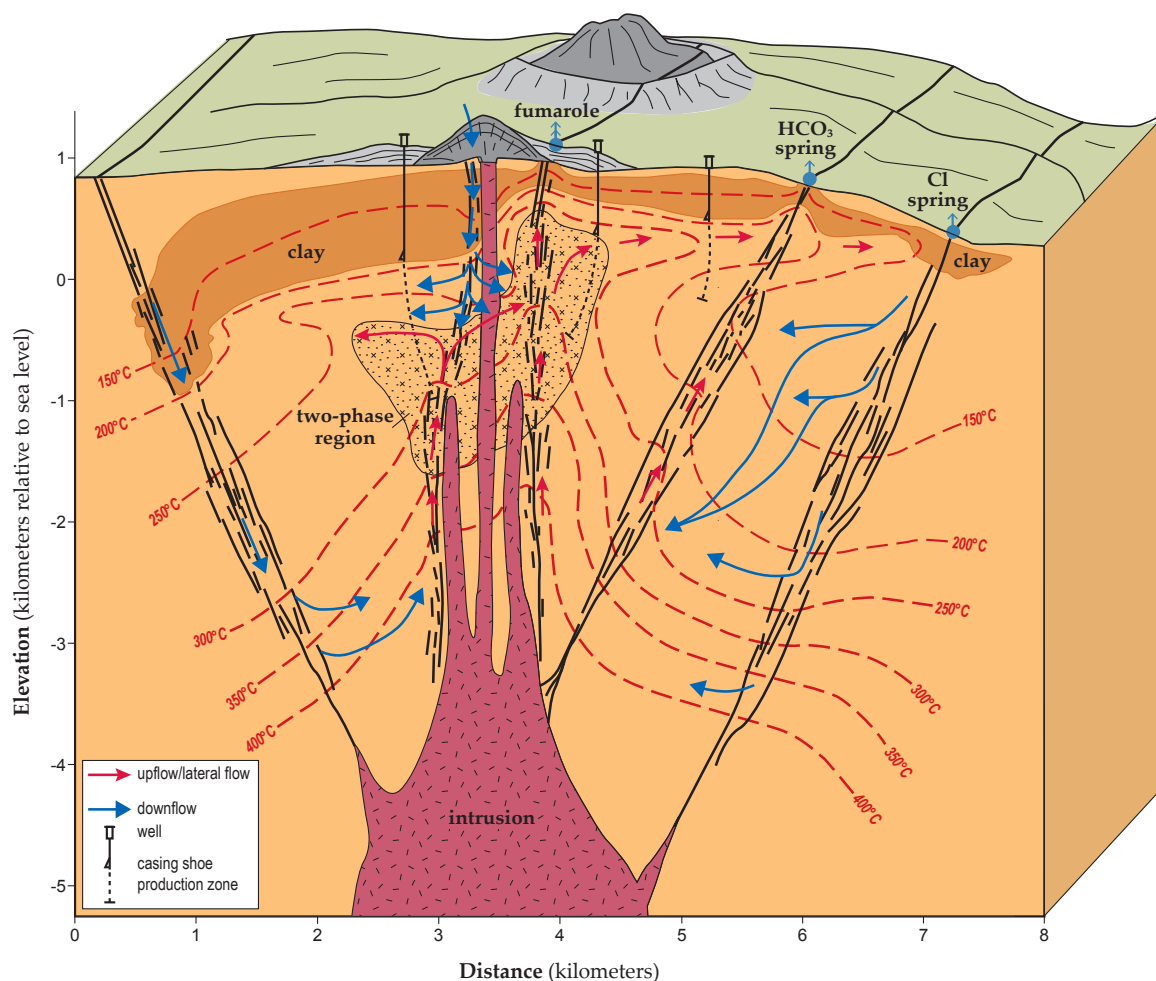


FIGURE 54. A conceptual model of a geothermal system associated with a series of domes of rhyolitic and dacitic composition (from Stimac et al., 2015, fig. 46.4B). This model stresses the interaction of crustal structure and intrusion to localize fluid flow along highly fractured zones. In the Mount Taylor case, the magmatic regime should be visualized as a broad “spine” of multiple intrusions and radial dikes. Because centralized magmatic activity at Mount Taylor ceased at 2.5 Ma, current subsurface temperatures are considerably lower than those depicted in this model. Instead, present subsurface temperatures probably mimic the regional temperature gradient of roughly 30° C/km. As a result, low-temperature geothermal fluids could circulate in the fractured rocks created by earlier intrusive activity at depths of about 2 km.

Conceptual Model of Volcano Evolution

The evolution of the Mount Taylor volcano conceptual model was developed through the examination of the cross sections on the map, Fig. 9, and Fig. 54. The growth of Mount Taylor volcano began around 3.7 Ma and culminated at 2.5 Ma in a more-or-less east to west trending, structurally controlled spine of trachyandesite, trachydacite, and alkali rhyolite intrusions laced with radiating dikes. Intrusion temperatures were nominally about 850°C. The many maar volcanoes around Mount Taylor provide ample evidence that the late Pliocene was relatively wet in northern New Mexico. Thus, ample water circulated into the subsurface of the volcano to create a small hydrothermal system. The intrusion of multiple magmas, the release of acidic volatiles, and concurrent hydrothermal alteration weakened the summit area of the original volcano. This eventually led to the extensive erosion of the core of the volcano forming the proto-amphitheater. Small volume mafic eruptions within and on the flanks of the volcano continued until 1.26 Ma. Some of this activity prolonged destabilization

of the edifice (e.g., the intrusion of the 1.97 Myr gabbro plug), and further enhanced erosion of the Amphitheater. Directed blast explosions (e.g., Mount St. Helens) and Pleistocene glaciation had no influence on formation of the Amphitheater.

Peripheral volcanic centers developed around Mount Taylor, particularly to the southwest and northeast. The Grants Ridge rhyolite center erupted from 3.50–3.18 Ma producing a widespread sequence of pyroclastic deposits and multiple rhyolite intrusions. Although the younger rhyolites contain impressive deuteric alteration minerals, such as topaz, we see no evidence that the Grants Ridge center produced a hydrothermal system. The Mesa Chivato area contains rocks similar in age and composition to the floor rocks at Mount Taylor (Phase I and early Phase II). However, this style of volcanism was not sustained beyond 2.75 Ma at the latest, and Mesa Chivato never developed a stratovolcano similar to Mount Taylor. Other peripheral centers to Mount Taylor are relatively insignificant in terms of size to produce hydrothermal systems.

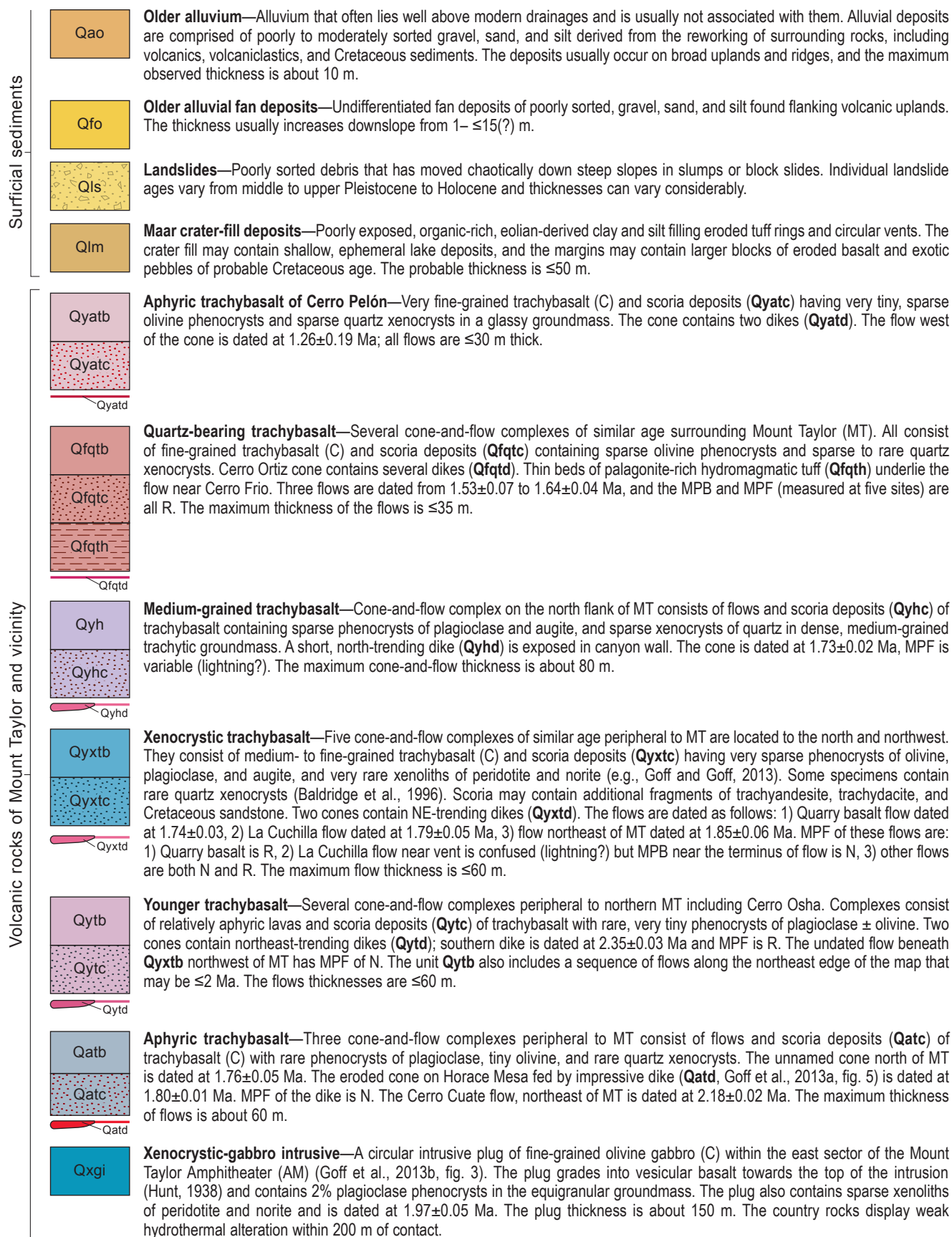
Description of Map Units

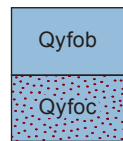
Note: Descriptions of map units are listed in approximate order of increasing age. Volcanic units are primarily subdivided into two geographic groups: Mount Taylor and southwestern Mesa Chivato. Formal stratigraphic names of Cretaceous units are described by Sears et al. (1941), Lipman et al. (1979), Dillinger (1990), and Skotnicki et al. (2012). Field identification of volcanic rocks is based on hand specimens, petrography and chemical data published by Hunt (1938), Baker and Ridley (1970), Lipman and Moench (1972), Lipman and Mehnert (1979), Crumpler (1980a, 1980b, 1982), Perry et al. (1990), and this report. Names of volcanic units are based on the above chemical data and the alkali-silica diagram of Le Bas et al. (1986). See Goff et al. (2008) for a contemporary description of the rocks and geology in the Mount Taylor area. A “C” in the rock description means at least one chemical analysis is available for the unit in question. Radiometric $^{40}\text{Ar}/^{39}\text{Ar}$ dates are from the NM Tech/NMBGMR laboratory (Socorro) unless otherwise stated. We measured magnetic polarities of some basalt specimens by Brunton compass (MPB). All other polarities were obtained with a portable fluxgate magnetometer (MPF). Correlations of magnetic polarities with age follow Table 2 from Gee and Kent (2007); N = normal polarity and R = reverse polarity; MT = Mount Taylor; AM = Mount Taylor amphitheater.

CENOZOIC

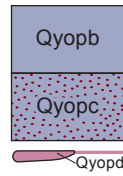
QUATERNARY

Surficial sediments	d	Disturbed land and/or artificial fill —Areas of modern excavation and associated deposits of compacted, very fine to very coarse-sand (often with minor pebbles), silt, and clay around open-pit mines, mine adits, dams, and reservoirs. Numerous, small check dams were not included.
	Qa	Modern stream alluvium —Deposits of gravel, sand, silt, and minor clay in swales associated with modern streams; mostly Holocene in age. The maximum thickness of various alluvial deposits is uncertain but may exceed 15 m.
	Qay	Younger alluvium —Alluvium that lies above modern drainages, underlying surfaces adjacent to modern drainages that are located approximately 5–15 m above local base level. The maximum observed deposit thickness about 15 m.
	Qfy	Younger alluvial fan deposits —Undifferentiated deposits of poorly-sorted gravel, sand, and silt emerging from some type of hillslope channel, usually in upland settings. The thickness of the deposit usually increases downslope from <1–≤15(?) m.
	Qf5	Alluvial fan deposits in basins flanking Mount Taylor —Poorly sorted fan lobe deposits of gravel, sand, and silt emerging from streams draining mountain uplands filling basin margins. The deposits are often intermixed with colluvium in mountain front settings. The youngest fan deposits are inset into older deposits, ranging in age from middle(?) Pleistocene (Qf1) (only found capping isolated Cretaceous and/or colluvial-covered mesas) to upper Pleistocene to lower Holocene (Qf2–Qf4) to Holocene to modern (Qf4–Qf5). The fans generally decrease in thickness with distance from the mountain front, and range from ≥20 m to <1 m thick.
	Qf4	
	Qf3	
	Qf2	
	Qf1	
	Qt4	Alluvial stream terrace deposits —Generally strath terraces comprised of moderately to well-sorted alluvial gravel, sand, and silt found above stream alluvial bottoms. Strath elevations increase in height with age, ranging from ≈30–50 m above streams for middle(?) Pleistocene terraces (Qt1); to ≈12–25 m for upper Pleistocene terraces (Qt2–Qt3); to ≈2.1–4.5 m for uppermost Pleistocene to lower Holocene terraces (Qt4). The thicknesses range from 2 to ≈15 m.
	Qt3	
	Qt2	
	Qt1	
	Qes	Eolian and/or alluvial sheetwash deposits —Windblown deposits of silt and fine sand, commonly reworked by sheetwash, often into a fining-upwards sequence. Alluvial pebbly sand to silt is on various surfaces, but most commonly basaltic-capped plateau flanks surrounding the main volcanic edifice. The thickness is typically ≤1 m.
	Ql	Shallow lake deposits —Fine-grained, poorly exposed deposits of medium- to fine-grained sand, silt, and clay filling shallow, small diameter basins on lava flow surfaces and sag ponds along fault traces. The thickness is ≤5 m. Generally, the ponds contain water only during rainy seasons.
	Qc	Colluvium —Poorly sorted slopewash and mass-wasting deposits from local sources; mapped only where extensive or where covering critical relations. Colluvium thickness can locally exceed 15 m.

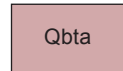




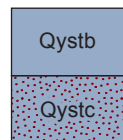
Fine-grained olivine trachybasalt—A single cone-and-flow complex north of MT, which consists of fine-grained trachybasalt and a scoria deposit (**Qyfoc**) with abundant tiny phenocrysts of olivine. The unit is not dated and has a maximum thickness of ≤ 50 m.



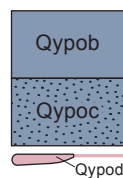
Olivine plagioclase trachybasalt—Two cone-and-flow complexes north of MT, which consist of slightly porphyritic trachybasalt and scoria deposits (**Qyopc**). Both cones contain northeast-trending dikes (**Qyopd**). Specimens are relatively aphyric, containing tiny rare phenocrysts of olivine \pm augite, and sparse small phenocrysts of plagioclase. The northerly cone contains rare fragments of gabbro and Cretaceous sandstone. The unit is not dated, and the maximum thickness about 60 m.



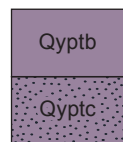
Basaltic trachyandesite—An eroded cone and short flow of basaltic trachyandesite (C) on the north flank of MT. Phenocrysts consist of plagioclase, augite, and hypersthene \pm rare olivine. The unit is not dated and the thickness is ≤ 100 m.



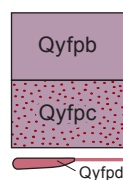
Spotted trachybasalt—Lava flows and scoria deposit (**Qystc**) northeast of Cerro Osha containing a distinctive trachybasalt that is mottled on weathered surfaces. The deposit contains phenocrysts of plagioclase and tiny phenocrysts of olivine. The unit is not dated, and the maximum thickness is about 120 m.



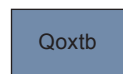
Plagioclase olivine trachybasalt—Cone-and-flow complex northeast of MT, which consists of flows and scoria deposit (**Qypoc**) of distinctive, medium-grained trachybasalt (C), containing abundant plagioclase, olivine, and augite phenocrysts. The cone contains north-northeast-trending dikes (**Qypod**). The flow is dated at 2.29 ± 0.06 Ma, and the MPF is R. The maximum thickness is about 100 m.



Porphyritic gabbro-bearing trachybasalt—Two cone-and-flow complexes on north and southwest flanks of MT. They consist of medium- to fine-grained trachybasalt (C) and scoria deposits (**Qyptc**) containing sparse small phenocrysts of plagioclase, olivine, and augite. Locally, the unit contains gabbroic xenoliths (Goff et al., 2013b). The north complex is dated at 2.30 ± 0.13 Ma, and the MPF is R. The maximum thickness of the flows is < 25 m.

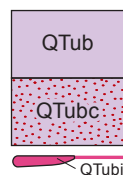


Fine-grained plagioclase trachybasalt—A cone-and-flow complex northeast of MT, which consists of fine- to medium-grained, trachytic trachybasalt (C) and scoria deposits (**Qyfpc**) having tiny plagioclase and olivine phenocrysts. The dike (**Qyfpd**) cuts the flow south of the cone. The cone is dated at 2.37 ± 0.14 Ma. The cone thickness is about 150 m.



Older xenolith-bearing trachybasalt—A medium-grained porphyritic trachybasalt, in central Horace Mesa, which contains phenocrysts of olivine, plagioclase, and augite, and very rare xenoliths of gneiss and peridotite; The unit is not dated, and the thickness is < 40 m.

TERTIARY—Pliocene



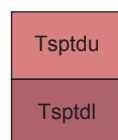
Trachybasalt and basalt: undivided—A lumped unit that consists of mafic rocks south of MT loosely equivalent to the “upper basalt” of Lipman and Moench (1972). The unit groups many flows, scoria cones (**QTubc**), and dikes (**QTubi**) of variable composition and texture. Most are trachybasalt (C); at least two flows and one cone complex contain peridotite and gabbro xenoliths. Two flows are dated at 2.22 ± 0.06 and 2.75 ± 0.03 Ma, respectively but most flows are probably Pliocene. The MPF of three flows is N; and another flow is R. The thickness is highly variable.



Volcaniclastic sedimentary rocks—Debris flows, hyperconcentrated flows, and fluvial deposits shed from the MT stratovolcano during its growth. The flows and deposits underlie and interlayer with a multitude of flows, domes, and cones peripheral to MT. The unit is interlayered with many tuffs (**Twst**, **Trt**, **Ttdt**). The basal contact is gradational with older fluvial deposits (**Tvss**). Most deposits are Pliocene, and the maximum thickness is > 200 m.



Porphyritic enclave- and quartz-bearing trachyandesite—Trachyandesite to trachydacite flows (C) on the southwest margin of the AM, which have abundant volcanic enclaves up to 50 cm in diameter in the devitrified matrix. The northeast part of the unit appears to be intrusive. The lavas contain 10–15% phenocrysts of large sanidine, plagioclase, augite, hornblende, biotite, and conspicuous resorbed quartz. The flows are dated at 2.50 ± 0.07 Ma, and the MPF is R. The maximum thickness is > 200 m.



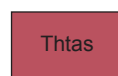
Porphyritic trachdacite of Spud Patch—A satellite eruption of devitrified to glassy trachdacite flows (C) that erupted north of MT is composed of upper (Tsptdu) and basal (Tsptdl) map units. They both contain 15–20% phenocrysts of large sanidine, plagioclase, augite, hornblende, and biotite with enclaves of intermediate composition volcanic rocks. The upper unit dated at 2.53 ± 0.06 Ma. The MPF (measured at three sites) is R. The maximum thickness is roughly 200 m.



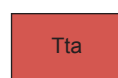
Porphyritic quartz-bearing trachdacite of Amphitheater—An irregular-shaped intrusion of porphyritic trachdacite to alkali rhyolite (C) in the western part of the AM containing phenocrysts of sanidine, plagioclase, augite, hornblende, biotite, and minor quartz in a devitrified trachytic groundmass. The unit contains dikes (Tqtdi) of similar composition and texture with sparse enclaves of mafic volcanic rocks. Unit dates range from 2.54 ± 0.02 to 2.58 ± 0.02 Ma, and the MPF (measured at two sites) is R. The thickness exceeds 200 m.



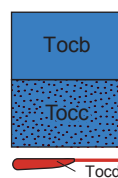
Hornblende trachyandesite—A lumped unit of porphyritic trachyandesite satellite vents (Thtav) and various flows (C) southwest of, and on the south margin of MT. The vents and flows display rare-to-sparse megacrysts of resorbed hornblende (≤ 5 cm) in a devitrified groundmass. The phenocrysts consist of plagioclase, augite, magnetite, olivine, hypersthene, and hornblende, and may contain plagioclase-pyroxene clots. The satellite eruption is dated at 2.60 ± 0.10 Ma, the flow beneath the summit is dated at 2.70 ± 0.02 Ma, and the other flows are older. The MPF of both dated sites is N. The thickness is ≤ 275 m.



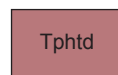
Summit hornblende trachyandesite—Several flows comprising the summit and west margin of MT. The flows contain phenocrysts that consist of plagioclase, augite, hypersthene, hornblende, sparse biotite, and minor sanidine in devitrified groundmass. They contain rare, small (≤ 10 mm) hornblende megacrysts. The flows are dated at 2.73 ± 0.01 Ma, and the MPF is confused (lightning?). The thickness of the exposed flows is >215 m.



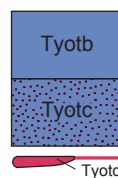
Trachyandesite: undivided—Multiple flows of porphyritic lavas found on the flanks of MT. Phenocrysts consist of plagioclase, clinopyroxene, and magnetite \pm hypersthene. Various flows are not dated, however, the knob south of MT summit is dated at 2.66 ± 0.31 Ma, the MPF (measured at two sites) is N. The thickness of the flows is ≤ 100 m.



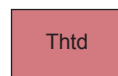
Augite-megacrystic basalt—Fine-grained basalt (C) and scoria deposits (Tocc) that are located several km southwest of MT, which contain sparse resorbed megacrysts of augite (≤ 1 cm). Included phenocrysts consist of olivine, plagioclase, augite, and magnetite. A fissure and dike (Tocc) extend from the northeast side of the eroded scoria cone. The unit is dated at 2.62 ± 0.01 Ma, and MPF is confused (lightning?). The maximum thickness is about 100 m.



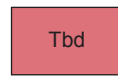
Porphyritic-hornblende trachdacite of San Jose Canyon—Satellite dome-and-flow complex roughly 15 km south of MT is equivalent to the porphyry of San Jose Canyon (Lipman et al., 1979). The flow is characterized as flow-banded porphyritic lava with large phenocrysts of plagioclase and smaller phenocrysts of hornblende and augite. The flow contains mafic enclaves of plagioclase, augite, hornblende, opaque oxides, and tiny olivine (?). The unit is dated at 2.63 ± 0.10 Ma. The thickness is about 55 m.



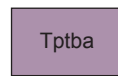
Trachybasalt of Cerro Colorado (La Jara Mesa)—Weakly porphyritic trachybasalt and scoria deposits (Tyotc) containing sparse small phenocrysts and cumulate clusters of plagioclase, olivine, and trace augite. The cone contains northeast-trending dikes (Tyotd) that are dated at 2.64 ± 0.01 Ma, and the MPF is N. The thickness is ≤ 30 m.



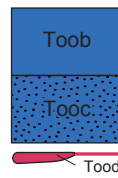
Hornblende trachdacite—Satellite eruption northwest of MT that is composed of massive to sheeted, porphyritic trachdacite (C) containing phenocrysts of plagioclase, augite, and minor hornblende. The unit is dated at 2.66 ± 0.02 Ma, and MPF is N. The thickness is nearly 200 m.



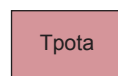
Porphyritic-biotite trachdacite—Massive to sheeted, porphyritic trachdacite (C) on the northeast margin of the AM containing phenocrysts of sanidine, augite, biotite, sparse hornblende, rare quartz, and opaque oxides in devitrified groundmass. The unit is dated at 2.66 ± 0.01 Ma, and MPF is N. The thickness is about 350 m.



Porphyritic basaltic trachyandesite—Massive, stubby flow with broad dike on the north margin of the AM. The flow consists of porphyritic basaltic trachyandesite (C) containing phenocrysts of augite, plagioclase, and rare olivine. The unit is not dated and has a maximum thickness of about 110 m.



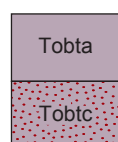
Olivine-rich basalt—Flows and scoria deposits (Tooc) of basalt (C) found northeast of MT that contain conspicuous olivine, plagioclase, and augite phenocrysts. The eroded cone is cut by north-northeast-trending dike (Tood) and the cone is dated at 2.67 ± 0.12 Ma. The maximum thickness is about 50 m.



Porphyritic-olivine trachyandesite—Satellite eruption northeast of the AM consisting of a highly porphyritic trachyandesite to trachdacite (C), which contains abundant large phenocrysts of plagioclase and tiny phenocrysts of olivine, augite, plagioclase, and sparse biotite in a very fine-grained, devitrified groundmass. The lavas contain sparse enclaves of plagioclase-augite that are

≤12 cm in diameter. Two flows are dated: the flow near the vent is dated at 2.68 ± 0.04 Ma, and the flow near the toe is 2.67 ± 0.01 Ma. The thickness is about 75 m.

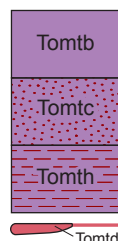
Tbhtd	Porphyritic-biotite-hornblende trachydacite: undivided —A lumped unit consisting of a satellite dome, a small plug, and several flow-and-intrusive complexes that are located on the northwest, southwest, east, and west margin of MT and the northwest wall of AM. All consist of massive to sheeted trachydacite (C) containing phenocrysts of plagioclase, sanidine, hornblende, biotite, and augite in trachytic groundmass. The satellite dome is dated at 2.66 ± 0.01 Ma, and the MPF is N. The plug is dated at 2.68 ± 0.03 Ma, and the MPF is N. The flow east of the intrusive complex in the bottom of the upper Rinconada Canyon is dated at 3.26 ± 0.20 Ma, and the MPF is N. The Rinconada Canyon flow is dated at 2.72 ± 0.04 Ma, and the MPF is N. The thickness of these deposits is variable.
Tbhd	Very porphyritic-biotite-hornblende trachydacite —North-northwest-trending flow, dike, and plug complex in the north wall and margin of the AM, which consists of porphyritic trachydacite (C) containing large phenocrysts of plagioclase and smaller biotite, hornblende, rare sanidine, quartz, and opaque oxides in a trachytic devitrified groundmass. The dike is dated at 2.67 ± 0.01 Ma. The maximum thickness is about 150 m.
Ttdc	Coarse porphyritic trachydacite —A satellite dome-and-flow complex on two hills east-southeast of the AM, which consists of coarsely porphyritic trachydacite containing large sanidine, augite, and sparse magnetite phenocrysts in a devitrified groundmass. The complex is dated at 2.70 ± 0.04 Ma. The thickness is about 210 m.
Tpbt	Porphyritic-biotite trachydacite of "La Mosca" —A massive to sheeted, porphyritic trachydacite (C) containing phenocrysts of sanidine, plagioclase, augite, and biotite in granular to trachytic, devitrified groundmass, which contains rare plagioclase-augite-biotite clots. The unit also contains a prominent, north-northwest-trending intrusion (Tpbt) of similar composition. The intrusion is dated at 2.71 ± 0.03 Ma, and its thickness is about 500 m.
Tpbt	
Tbta	Platy trachyandesite: undivided —A platy to massive, slightly porphyritic trachyandesite (C) containing phenocrysts of plagioclase, augite, and olivine in a trachytic devitrified groundmass. The unit contains rare quartz xenocrysts; contains plagioclase-augite-olivine clots. The eroded cone (Tbtac) lies on ridge to the east and may be the source of trachyandesite flows to the west. The undivided units are not dated. The thickness is about 170 m.
Tbtac	
Tsetdu	Sugary enclave trachydacite —Porphyritic, glassy to devitrified trachydacite (C) northwest of "La Mosca" that is composed of two map units: 1) a basal unit (Tsetdl) containing 15–20% phenocrysts of plagioclase, augite, hornblende and biotite, and 2) an upper unit (Tsetdu), which has similar phenocrysts that are set in a sugary matrix. Both units contain conspicuous mafic enclaves. The upper unit is dated at 2.71 ± 0.06 Ma, and the MPF is N. The thickness is about 250 m.
Tsetdl	
Tbtd	Slightly porphyritic-biotite trachydacite —Platy flows of slightly porphyritic trachydacite (C) on the north margin of the AM, which contains 2–4% small plagioclase, biotite, and augite phenocrysts. The unit is not dated and the flow thickness is about 215 m.
Tppta	Porphyritic trachyandesite: undivided —A lumped unit of massive to sheeted, porphyritic trachyandesite flows (C) from multiple vents having phenocrysts of plagioclase, augite, hornblende, rare olivine, and opaque oxides in a devitrified groundmass. Some flows have small hornblende megacrysts. The unit may contain thin beds of QTvs . Lava from the north AM rim is dated at 2.63 ± 0.07 Ma; other flows are older. The thickness is about 330 m.
Ttd	Trachydacite: undivided —Porphyritic trachydacite flows in small canyons southeast of Horace Mesa and east-northeast of the AM. The flows contain 15–20% crystals of biotite, plagioclase, hornblende, and sparse quartz, and contains rare megacrysts of augite. One flow is dated at 2.79 ± 0.14 Ma. The thickness is about 40 m.
Tpcta	Porphyritic-augite trachyandesite —Massive to sheeted flows of trachyandesite in the north margin of the AM with conspicuous megacrysts of augite. The flows contain phenocrysts of plagioclase, augite, and rare olivine. The unit is not dated and the thickness is about 50 m.
Tppta	Porphyritic-biotite trachyandesite —Massive flows of trachytic, devitrified trachyandesite that are located north of the AM containing large plagioclase, conspicuous biotite, augite, and sparse olivine phenocrysts. The unit is not dated and the thickness is ≥ 160 m.
Thrtd	Porphyritic-hornblende-rich trachydacite —Distinctive, massive, porphyritic trachydacite (C) located on the south rim of AM, which contains abundant phenocrysts of hornblende, plagioclase, augite, magnetite, sparse biotite, and sparse sanidine in a devitrified groundmass. The unit also contains small plagioclase-magnetite-augite clots. The unit is not dated and the thickness is ≤ 200 m.
Togtb	Older gabbro-bearing trachybasalt —Medium-grained trachybasalt (C) and scoria deposits (Togtc) on southern Horace Mesa containing phenocrysts, which consist of abundant small olivine, plagioclase, and augite. The deposits contain rare cumulate clots of plagioclase-olivine-augite. The unit is not dated and the thickness is about 35 m.
Togtc	



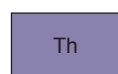
Aphyric basaltic trachyandesite—Flows and scoria deposits (**Tobtc**) of basaltic trachyandesite (C) at the head of Lobo Canyon. The unit contains tiny phenocrysts of plagioclase, augite, and olivine in a glassy, aphyric groundmass. The unit also contains rare quartz xenocrysts. The unit is not dated, and the thickness is about 75 m.



Hydromagmatic trachybasalt—Beds of granular, quenched, glassy trachybasalt on the southeast cliffs of Horace Mesa. The trachybasalt contains small phenocrysts of olivine, plagioclase, and augite. The glass in the unit shows minor palagonite alteration. The beds are planar to wavy and contain lithic clasts of volcanic rocks. The source of the eruption is probably from shallow crater to the north (**QIm**, e.g., Goff et al., 2014a,b). The unit is not dated, and the thickness is about 10 m.



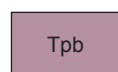
Older megacrystic trachybasalt—Several cone-and-flow complexes surrounding MT that are of a similar age and mineralogy. The complexes consist of fine-grained trachybasalt (C), scoria deposits (**Tomtc**), and dikes (**Tomtd**) containing conspicuous, large (≤ 1.5 cm) megacrysts of augite, plagioclase, and olivine (e.g., Lipman et al., 1979). Phenocrysts in the flow consist of plagioclase, olivine, augite \pm hypersthene, and may contain quartz xenocrysts. The complex on La Jara Mesa contains hydromagmatic deposits (**Tomth**). The eroded cone south of MT contains rare blocks of fine- to medium-grained olivine gabbro (Goff et al., 2013b). The flow near Cerro Pelón is dated at 2.64 ± 0.10 Ma. The La Jara Mesa flow is dated at 2.77 ± 0.06 Ma. The Rinconada flow is dated at 2.79 ± 0.06 and 2.78 ± 0.03 Ma. The MPF of all sites is N. The maximum thickness is about 80 m.



Older fine-grained trachybasalt—A small plug-like body and associated flows of massive olivine trachybasalt in the lower east walls of the AM and the west side of Water Canyon contain small phenocrysts of olivine and augite; plug contains fragments of altered rhyolite. The unit is not dated, and the thickness is about 35 m.



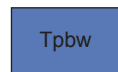
Porphyritic-plagioclase trachydacite—A massive, thick flow of trachydacite (C) south of the AM contains 15–20% large phenocrysts (≤ 2.5 cm) of plagioclase and smaller phenocrysts of augite, biotite, magnetite, and minor sanidine in a fine-grained trachytic groundmass. The flow is dated at 2.78 ± 0.05 Ma and the MPF is N. The thickness is about 200 m.



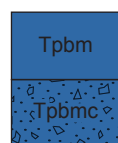
Plagioclase basalt—Classic “big feldspar or plagioclase basalt” of Baker and Ridley (1970), Lipman et al. (1979), and Perry et al. (1990). The basalt consists of massive to vesicular trachybasalt (C) flows on the north and south flanks of the AM. The flows contain 10–20% laths of plagioclase (≤ 2.5 cm) and smaller phenocrysts of plagioclase, olivine, and augite in glassy matrix. The flows to the south are dated at 2.76 ± 0.06 Ma; the north flows are dated at 2.79 ± 0.04 Ma. The thickness is about 150 m.



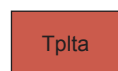
Plagioclase basalt of Cañon Seco—One of several highly porphyritic, plagioclase-phyric mafic lavas previously called “plagioclase basalt.” The massive to vesicular flow of basaltic trachyandesite (C) is found in Cañon Seco area south of the AM. The flow contains phenocrysts of large plagioclase and smaller olivine and augite in a medium-grained matrix. The unit is not dated, and the thickness is about 100 m.



Plagioclase basalt of Water Canyon—A massive, highly porphyritic, plagioclase-phyric mafic lava exposed in the northeast wall of the AM, in walls of Water Canyon, and adjacent areas to the west. The flow consists of trachyandesite (C) containing phenocrysts of large plagioclase but smaller phenocrysts of augite and rare olivine in a medium-grained groundmass. The unit is not dated, and the thickness is about 100 m.



Plagioclase basalt south of San Mateo—Massive to vesicular basaltic trachyandesite (C) and scoria deposits (**Tpbmc**) having abundant large phenocrysts of plagioclase and much smaller phenocrysts of olivine and augite. The unit is not dated, and the thickness is about 75 m.



Porphyritic plagioclase-rich trachyandesite—Massive flows on the mesa to the south of San Mateo and a poorly exposed flow north of Cerro Aguila. The flows consist of highly porphyritic trachyandesite (C) containing large phenocrysts of plagioclase and smaller phenocrysts of augite, olivine, and magnetite. The flow south of San Mateo is dated at 2.86 ± 0.04 Ma. The maximum thickness is about 75 m.



Porphyritic enclave-bearing trachydacite—Thick flows of porphyritic trachydacite (C) on the west margin of the AM having conspicuous mafic enclaves up to 50 cm in diameter, especially in the lower flows. They contain sanidine, plagioclase, augite, hypersthene, and biotite phenocrysts in a devitrified groundmass. The flows are dated at 2.81 ± 0.04 Ma and the MPF is N. The thickness is about 250 m.

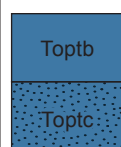


Coarse-porphyritic trachyte—Very coarse-grained porphyritic lavas in the southwest wall of the AM and beneath the west flank of MT. The flows consist of trachyte (C) with roughly 50% large (≤ 3 cm) phenocrysts of sanidine in a felty, trachytic matrix of sanidine, plagioclase, augite, and magnetite. The flow erodes like weathered syenite. The lava on the west flank is dated at 2.82 ± 0.08 Ma. The thickness is about 80 m.



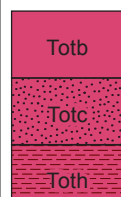
Biotite-hornblende trachyte—A plug-like body of slightly porphyritic trachyte (C) on the south flank of MT, which contains small phenocrysts of sanidine, biotite, hornblende, and magnetite in trachytic groundmass of plagioclase and hornblende (?). The plug contains small mafic enclaves, and is dated at 2.83 ± 0.04 Ma. The thickness is about 200 m.

Ttdu	Upper biotite trachydacite —A massive flow southeast of the AM of slightly porphyritic trachydacite with 2–4% phenocrysts of small plagioclase, augite, and biotite in a devitrified trachytic matrix. The unit is not dated, and has a maximum thickness of about 100 m.
Ttdl	Lower biotite trachydacite —A massive flow beneath and resembling Ttdu . Volcaniclastic gravel (QTvs) separates the upper and lower biotite trachydacite units. The lower flow contains conspicuous mafic enclaves, and contains at least one dike (Ttdld). The unit is not dated, and the thickness is about 150 m.
Ttdld	
Tbtdl	Porphyritic-biotite trachydacite —A thick, massive flow exposed in the lower northeast wall of the AM contains abundant phenocrysts of plagioclase, augite, biotite, and hornblende(?) in a devitrified groundmass. The unit is not dated, and the thickness is about 120 m.
Tplu	Porphyritic intermediate-composition volcanic rocks: undivided —Poorly exposed flows in the walls of the AM. The float generally contains phenocrysts of plagioclase, augite, hornblende, and/or biotite. The thickness is ≤ 300 m.
Tpmtd	Porphyritic mixed lava —A unit several km south of MT described as “distinctive bulbous flow or intrusion” (Lipman et al., 1979), which consists of porphyritic trachydacite mixed with variable amounts of fine-grained, slightly porphyritic, basaltic enclaves. The trachydacite phenocrysts are sanidine, plagioclase, augite, hornblende, and rare quartz. The mafic component contains plagioclase, augite, hypersthene, and olivine phenocrysts. The unit is not dated, and the thickness is about 280 m.
Tvsb	Basaltic-rich volcaniclastic gravels —Fluvial deposits containing primarily subrounded- to rounded-clasts of basalt, trachybasalt, and subordinate intermediate composition volcanic rocks. The deposits contain minor cobbles of rhyolite, chert, and Precambrian crystalline rocks. The unit is unique to the southwest part of Horace Mesa. The thickness is ≤ 25 m.
Tvss	Volcaniclastic sandstone —Fine- to coarse-grained fluvial sandstone containing small clasts and grains of quartz, plagioclase, olivine, augite, chert, pumice, and various types of mafic and intermediate composition volcanics. The unit may contain thin-beds of trachydacite or rhyolite tuffs, which are too thin to map. The sandstone occupies shallow channels cut into the earliest lava flows and underlies and interlayers with QTvs . The thickness is ≤ 35 m.
Tootb	Older olivine trachybasalt —Flows and scoria deposits (Tootc) of borderline basalt/trachybasalt (C) with conspicuous olivine and sparse plagioclase and augite phenocrysts. The unit has a reported date of 2.89 ± 0.07 Ma (Perry et al., 1990), and was redated twice at 2.86 ± 0.13 and 2.94 ± 0.12 Ma from two different sites. The MPF for all sites is N, and the thickness is > 50 m.
Tootc	
Ttdt	Trachydacite tuffs —Beds of trachydacite (C) pumice fall, pyroclastic flow, and reworked pumice scattered all around MT. The tuffs contain phenocrysts of plagioclase, augite, biotite \pm hornblende \pm sanidine in a eutaxitic groundmass. Four dates range from 2.700 ± 0.002 to 2.79 ± 0.09 Ma. The maximum tuff thickness is ≤ 15 m.
Twst	Tuffs of Water and San Mateo Canyons: undivided —Bedded tuffs and tephros of rhyolite to trachydacite composition with interlayered volcaniclastic sands and gravels. The tuffs consist of pyroclastic fall and flow deposits that are ≤ 4 m thick. Rhyolitic tuffs are most common toward base of the unit. Five dates were obtained for the unit, which range from 2.74 ± 0.03 to 3.04 ± 0.12 Ma. The maximum thickness is about 200 m.
Tls	Landslide deposit —Unsorted debris that forms a discontinuous layer in the upper part of Marquez Canyon. The deposit consists of angular trachydacite blocks, which are 3–4 m in diameter on top of boulder- to cobble-sized volcaniclastic debris. The unit is intercalated within Twst . The thickness is 6–12 m.
Trt	Rhyolitic tuffs —Beds of rhyolitic (C) pumice fall and reworked pumice from separate sites all round MT. Continuous beds are exposed in the cliffs above San Mateo and may include thin beds of Grants Ridge Tuff in the bottom of the cliff exposures. The tuffs contain phenocrysts of quartz, sanidine, biotite, and augite. A bed south of San Mateo is dated at 3.08 ± 0.20 Ma. The thickness of the individual beds is usually < 3 m.
Tre	East Amphitheater biotite rhyolite —A massive to flow-banded, fine- to medium-grained, biotite rhyolite (C). The unit probably consists of multiple intrusions where porphyritic varieties contain quartz, sanidine, biotite, augite, and plagioclase. Some types of intrusions contain only sparse quartz, sanidine, and biotite. Locally, the unit displays intense silicification. The rhyolite is dated at 2.91 ± 0.04 Ma. The thickness is about 200 m.
Trw	West Amphitheater biotite rhyolite —Flow-banded to spherulitic to massive rhyolite (C) containing small phenocrysts of quartz, sanidine, biotite, augite, plagioclase, and minor hornblende. The unit may show hydrothermal alteration from later intrusions. The rhyolite is dated at 3.03 ± 0.11 Ma (Perry et al., 1990), and the thickness is about 200 m.
Ttr	Fine-grained trachyte —An eroded and dissected plug of fine-grained trachyte (C) in the eastern part of the AM, which contains rare-small phenocrysts of plagioclase in a trachytic groundmass. The plug is dated at 3.14 ± 0.01 Ma, and the thickness is about 120 m.
Tbaa	Amphitheater basanite —Two flows of fine-grained to aphyric basanite (C) that are exposed in the eastern part of the AM and Water Canyon, which contain extremely small phenocrysts of iddingsitized olivine in a glassy to devitrified groundmass. The flows are dated at 3.22 ± 0.04 Ma, and the thickness is about 65 m.
Toab	Older alkali basalt —Multiple flows of fine- to medium-grained, olivine basalt (C; Lipman and Moench, 1972), which contains small phenocrysts of olivine and very rare phenocrysts of plagioclase and augite. The basalt is most common in Water Canyon and the eastern part of the AM. A small plug and flow are also found in upper Rinconada Canyon. Two dates have been obtained



for different locations and are from 3.16 ± 0.03 to 3.21 ± 0.12 Ma. The MPF (measured at the two sites) is N and R, respectively. The flow thickness is ≤ 35 m.

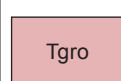
Older porphyritic trachybasalt—Flows and scoria deposits (**Toptc**) of medium-grained, porphyritic basalt/trachybasalt that are located in the southwest part of Horace Mesa (C) and upper cliff of Lobo Canyon. The flows contain conspicuous olivine and plagioclase phenocrysts. This unit is not dated, and the MPB is N. The thickness is about 35 m.



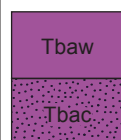
Older trachybasalt: undivided—A lumped unit consisting of older, primarily fine-grained to aphyric trachybasalt and scoria deposits (**Totc**) surrounding MT and underlying most of southern Mesa Chivato. Some scoria cones contain dikes (**Totd**). One cone near the east edge of the map is partially underlain by hydromagmatic deposits (**Toth**). Most flows contain some olivine phenocrysts. The flow in the upper Seboyeta Canyon is dated at 2.83 ± 0.02 Ma, and the MPB is N. Two flows northwest of MT are dated at 3.20 ± 0.05 and 3.31 ± 0.08 Ma, and the younger flow has MPB of R. The flow in the southwest part of Horace Mesa has a date of 3.24 ± 0.09 Ma (Laughlin et al., 1993). The maximum thickness of the unit is about 45 m.



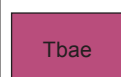
Grants Ridge rhyolite tuff—Bedded, rhyolitic, pyroclastic fall, flow, and surge deposits. The upper pyroclastic beds have abundant aphyric obsidian clasts (C). Pumice clasts (C) are glassy to slightly devitrified with very rare phenocrysts of tiny sanidine. Lithics consist of Precambrian granite and gneiss, chert, sandstone, limestone, and rare basanite. The tuff is dated at 3.26 ± 0.04 (obsidian) and 3.33 ± 0.07 Ma (sanidine in pumice). The maximum thickness is about 110 m.



Grants Ridge rhyolite center—Multiple eruptions of sparsely porphyritic rhyolite (C) containing phenocrysts of sanidine, plagioclase, rare quartz, and very sparse biotite. Lavas are massive to flow-banded. The unit contains some spherulitic zones. Locally, it contains mariolitic cavities with quartz, alkali feldspar, hematite, garnet, and topaz. The northern, lower flank of the dome contains sparsely porphyritic obsidian. The devitrified zone on the southeast side is dated at 3.18 ± 0.01 Ma, and the MPF is N. The obsidian is dated at 3.498 ± 0.003 Ma. The maximum thickness of the complex is >100 m.

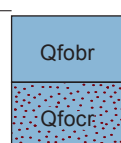


West olivine basanite—A fine-grained, massive to sheeted basanite (C) with tiny microphenocrysts of iddingsitized olivine and sparse magnetite. Commonly, the basanite has a spotted appearance on weathered surfaces. A vent of scoria and spatter (**Tbac**) is exposed at the head of Lobo Canyon. The unit is dated at 3.64 ± 0.15 Ma, and the MPF is R. The thickness is about 40 m.

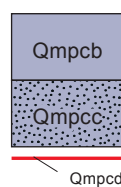


East olivine basanite—A fine-grained, nearly aphyric basanite (C) with small phenocrysts of plagioclase and iddingsitized olivine. Weathered surfaces are distinctly to vaguely spotted. The upper part of the unit is massive to rubby, while the lower part is columnar. It is dated at 3.72 ± 0.02 Ma, and the MPF is R. The thickness is about 45 m.

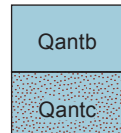
QUATERNARY



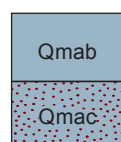
Porphyritic-olivine basalt of Cerro Redondo—A massive to vesicular, fine-grained basalt (C) and scoria deposits (**Qfocr**), which contain 15% phenocrysts of olivine, plagioclase, and augite near the vent. The basalt also contains 1–2% olivine phenocrysts near the flow terminus. There is a dike-like mass in the summit of the cone, which is dated at 1.90 ± 0.03 Ma, and the MPB is N (measured at three sites). The thickness is about 35 m.



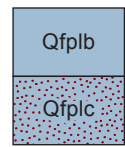
Medium-grained, plagioclase- and augite-phyric trachybasalt—Massive flows and scoria deposits (**Qmpcc**) located southwest of Laguna Redonda, which consists of trachybasalt with phenocrysts of plagioclase and augite. The cone contains an eroded dike (**Qmpcd**) that is trending N40E. The unit not dated. The MPB of the dike is R, and the MPB of the flow is N. The thickness is about 40 m.



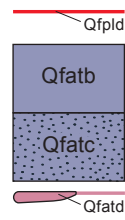
Gabbro-bearing olivine trachybasalt—A porphyritic-olivine trachybasalt flow (C) and scoria deposits (**Qantc**) on the northeast edge of the map containing enclaves of gabbro, anorthosite, and minor peridotite (Goff et al. 2013b). The phenocrysts consist of olivine and scattered augite and plagioclase. The unit not dated, and the MPB is N, suggesting an age between 1.77 and 1.95 Ma. The thickness is about 45 m.



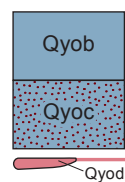
Medium-grained, aphyric trachybasalt—Flows and scoria deposits (**Qmac**) of trachybasalt underlying the east side of Cerro Redondo. The flows have trachytic texture caused by aligned plagioclase microphenocrysts, and contain tiny phenocrysts of augite and olivine. The unit is not dated, and the MPB is R suggesting an age >1.95 Ma (Gee and Kent, 2007). The thickness is about 60 m.



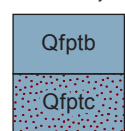
Fine- to medium-grained, plagioclase-phyric trachybasalt—Fine- to medium-grained trachybasalt (C) and scoria deposits (**Qfplc**) on the northeast edge of the map with conspicuous trachytic texture, which contains small phenocrysts of plagioclase, augite, and olivine. The cone contains a northeast-trending, poorly exposed dike (**Qfpld**). The unit is dated at 2.13 ± 0.01 Ma, and the MPB is R. The thickness is about 75 m.



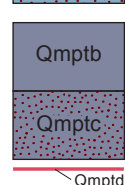
Younger fine-grained, aphyric trachybasalt—Extremely fine-grained, aphyric trachybasalt (C) and scoria deposits (**Qfatc**) containing no phenocrysts. The cone contains northeast-trending dikes (**Qfatd**). The unit is dated at 2.14 ± 0.02 Ma, and the MPB is N. The thickness is about 100 m.



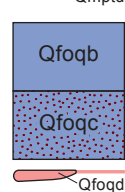
Younger olivine trachybasalt—Massive flows and scoria deposits (**Qyoc**) of fine-grained trachybasalt (C) containing 2–4% olivine phenocrysts. The flows may have a felty texture. The three cones contain several north-northeast-trending dikes (**Qyod**). The unit may contain plagioclase and augite megacrysts. The western flow is dated at 2.18 ± 0.06 Ma. Overall thickness is about 70 m.



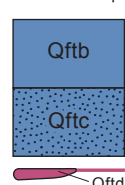
Fine-grained, plagioclase-phyric trachybasalt—Flows and scoria deposits (**Qfptc**) northeast of Cerro Cuate; consist of fine-grained trachybasalt with trachytic texture. The unit contains rare phenocrysts of augite and olivine. The unit is not dated, and the thickness is about 65 m.



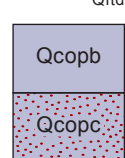
Medium-grained, plagioclase-phyric trachybasalt—Flows and a small scoria cone (**Qmptc**) located near the northeast edge of the map. The flows consist of medium-grained, plagioclase-phyric trachybasalt with tiny phenocrysts of augite and olivine. The cone contains a north-trending dike (**Qmptd**). The unit is not dated, and the thickness is about 40 m.



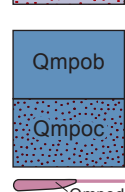
Fine-grained, quartz-bearing olivine basalt of Cerro Aguila—Flows and scoria deposits (**Qfoqc**) of fine-grained basalt/trachybasalt (C) having small phenocrysts of olivine and sparse xenocrysts of quartz. The scoria cone has several arcuate and linear dikes (**Qfoqd**). The lava southeast of the cone is dated at 2.25 ± 0.01 Ma, and the MPB is R; the dike in the cone is dated at 2.27 ± 0.01 Ma. The maximum thickness is about 85 m.



Younger fine-grained, plagioclase trachybasalt—Flows and scoria deposits from two cones (**Qftc**) located west and southwest of Cerro Cuate, which consist of very similar, aphyric, aphanitic trachybasalt having a felted groundmass of very fine-grained plagioclase, augite, and minor olivine. The south cone has several dikes (**Qftd**). The flow is dated at 2.28 ± 0.07 Ma, and the thickness is about 50 m.



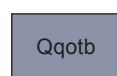
Porphyritic-augite-olivine basalt—Flows of very distinctive, medium- to coarse-grained, porphyritic basalt (C) and the associated scoria cone (**Qcopc**), which is located west of Cerro Cuate. The flows contain abundant phenocrysts (5–15%) of augite, olivine, and plagioclase, and may contain trace xenocrystic quartz. Weathered surfaces are often speckled. The unit is dated at 2.31 ± 0.06 Ma, the MPB is R, and the thickness is about 30 m.



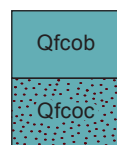
Medium-grained, sparsely porphyritic-olivine trachybasalt—Flows and scoria deposits (**Qmpoc**) located southeast of Cerro Redondo, which consist of medium- to fine-grained trachybasalt with small sparse-phenocrysts of olivine and very sparse-small phenocrysts of plagioclase and augite. The cone contains a NE-trending dike (**Qmpod**). The unit is not dated, and the thickness is about 35 m.



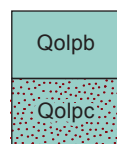
Fine-grained, aphyric trachybasalt south of Laguna Bandeja—Fine-grained, aphyric trachybasalt and scoria deposits (**Qafc**) with visible microlites of plagioclase. The flow contains no phenocrysts. The prominent scoria cone on the northeast edge of the map contains two dikes (**Qafd**). The scoria cone and flows are cut and incised by the spectacular maar of Laguna Bandeja. While the unit is not dated, the MPB = R (measured at one site), which suggests an age < 2.58 Ma (Gee and Kent, 2007). The thickness is about 50 m.



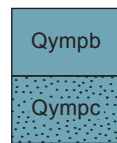
Quartz-bearing, olivine trachybasalt—A massive to vesicular trachybasalt (C) capping the small mesa east of Bear Canyon, Rio Paguata, which contains conspicuous olivine phenocrysts, possibly some disaggregated peridotite, and rare quartz xenocrysts. The unit is dated at 2.32 ± 0.01 Ma, and the MPB is confused (lightning?). The thickness is about 20 m.



Fine-grained, augite-bearing olivine basalt—Flows and scoria deposits (**Qfcoc**) located southeast of Cerro Redondo, which consist of fine-grained olivine basalt(?), containing sparse, large phenocrysts of augite. The cone contains a pond of basalt on the western summit and eroded, northeast-trending dikes (**Qfcod**) on the east summit. The unit is not dated, and the MPB is R suggesting an age >1.95 Ma (Gee and Kent, 2007). The maximum observed thickness is about 80 m.



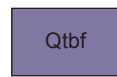
Olivine-rich plagioclase basalt—Flows and scoria deposits (**Qolpc**) of olivine-rich, porphyritic basalt (C) near the northeast edge of the map, which contains scattered, large phenocrysts of augite and plagioclase. The cone contains a northeast-trending dike (**Qolpd**), which is dated at 2.41 ± 0.02 Ma. The thickness is about 100 m.



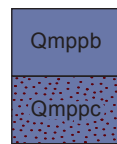
Younger medium-grained, plagioclase trachybasalt—Flows and scoria deposits (**Qympc**) located about 3 km southeast of Antelope Flats, which consist of medium-grained trachybasalt containing small, platy, interlocking microphenocrysts of plagioclase and tiny microphenocrysts of olivine and augite. The scoria contains rare fragments of Cretaceous sandstone. The unit is not dated, and the thickness is about 60 m.



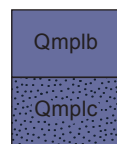
Fine-grained, plagioclase- and augite-phyric olivine basalt—Flows and scoria deposits (**Qfpoc**) of basalt (C) located east of Cerro Redondo, which contain conspicuous phenocrysts of plagioclase, augite, and olivine in a fine-grained groundmass. The south cone contains several dikes (**Qfpod**). The unit is not dated, and the MPB is R suggesting an age >2.15 but <2.58 Ma (Gee and Kent, 2007). The maximum thickness is about 65 m.



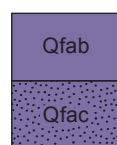
Fine-grained trachybasalt—A flow with 1–3% phenocrysts of olivine, augite, and plagioclase in an aphanitic matrix, which is located northeast of Cerro Chivato. The flow contains rare quartz xenocrysts. The unit not dated, and the thickness is about 15 m.



Plagioclase-phyric trachybasalt of Cerro Colorado (Mesa Chivato)—Flows and scoria deposits (**Qmppc**) of medium-grained trachybasalt. Fresh surfaces display a shimmery reflection of aligned plagioclase microlites. The flow contains rare phenocrysts of plagioclase. The unit is not dated, and the MPB is R. The thickness is about 45 m.



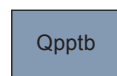
Medium-grained, plagioclase-phyric olivine trachybasalt of Cerro Frio—Medium-grained, sparsely porphyritic trachybasalt (C) and scoria deposits (**Qmplc**) containing plagioclase phenocrysts ≤ 3 cm long and smaller phenocrysts of plagioclase, olivine, and augite. The unit is dated at 2.44 ± 0.01 Ma, and the MPB (measured at two sites) is R. A similar looking, faulted flow lies just east of Laguna Bonita in the northeast part of the map. While the age of this similar flow is unknown, it may be younger than Cerro Frio. The maximum thickness of flows is about 35 m.



Fine-grained, aphyric trachybasalt southeast of Cerro Redondo—Flows and scoria deposits (**Qfac**) located southeast of Cerro Redondo, which consist of very fine-grained, aphyric trachybasalt containing visible microphenocrysts of plagioclase and olivine. The cone contains a northeast-trending dike (**Qfad**) and a sill-like body. The unit is not dated, and the maximum thickness is about 35 m.

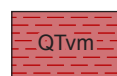


Fine-grained, quartz- and xenolith-bearing olivine trachybasalt—Fine-grained, sporadically flow-banded, nearly aphyric trachybasalt (C) located north of Silver Dollar Mesa, which contains sparse quartz xenocrysts. The trachybasalt also contains very rare, ≤ 4 cm, dunite xenoliths and augite megacrysts. The unit is not dated, and the MPB is R. The maximum thickness is about 20 m.

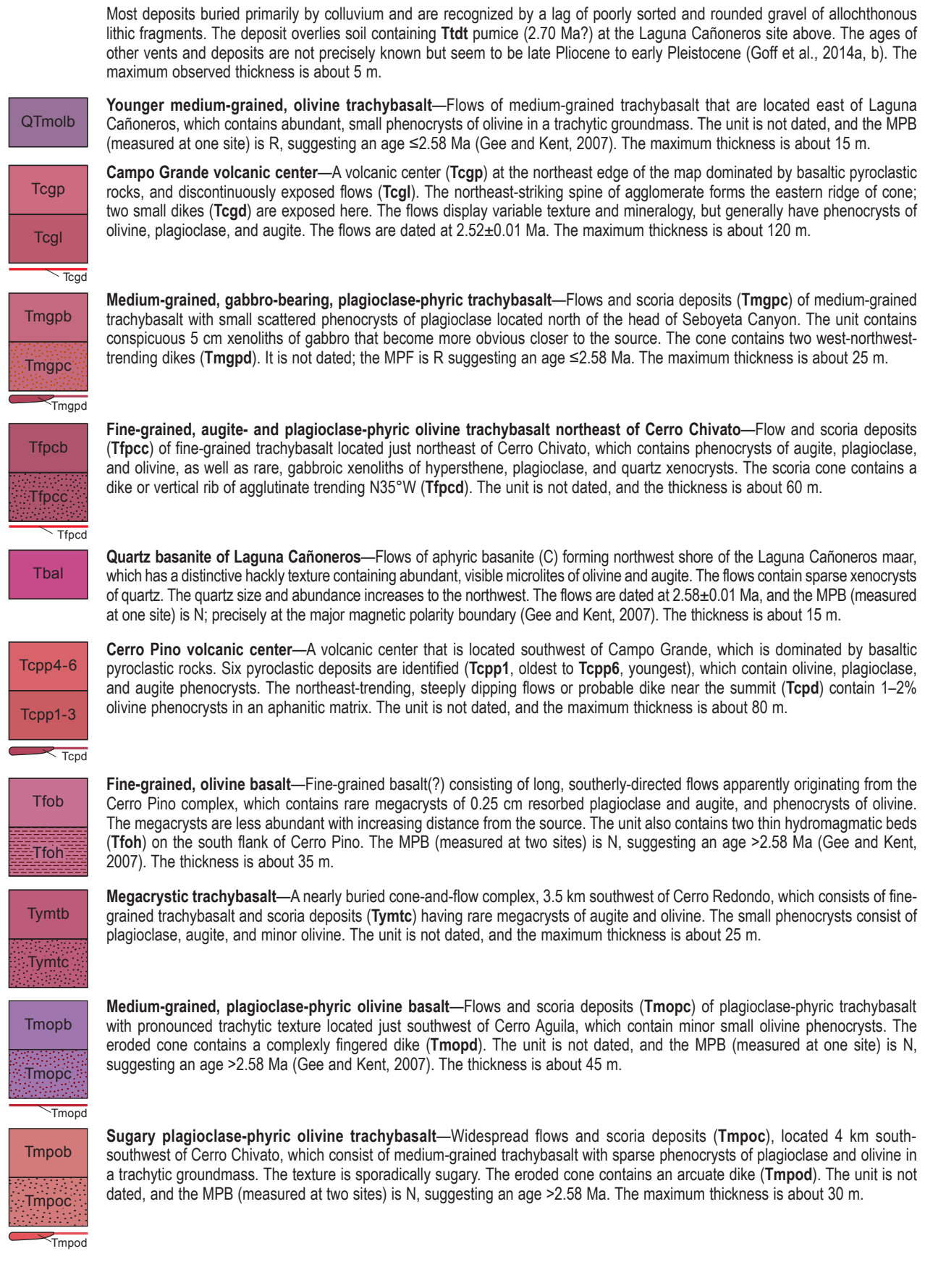


Plagioclase-phyric trachybasalt of Silver Dollar Mesa—Flows of fine- to medium-grained, slightly porphyritic trachybasalt (C) in a trachytic groundmass covering the southern end of Silver Dollar Mesa. They contain 0.5–1.5 cm plagioclase phenocrysts and smaller phenocrysts of plagioclase, olivine, and augite. The flows are dated at 2.49 ± 0.06 Ma, and the MPB is confused (measured at two sites - lightning?). The maximum thickness is about 35 m.


TERTIARY—Pliocene



Hydromagmatic deposits from maar eruptions—Consists of poorly exposed hydromagmatic deposits derived from the explosive interaction of shallow groundwater with magma during eruption. The best exposures occur in the modified drainage on the south end of the Laguna Cañoneros maar where the deposits consist primarily of plane-parallel base surge beds containing a mixture of quenched basaltic (hydroclastic) shards and fragments, sideromelane, yellow-brown palagonite, and lithic fragments.





	Tolpyb Porphyritic-olivine-augite basalt —Aphanitic to fine-grained flows located east-northeast of Cerro Pino, with 1–3% phenocrysts of olivine, augite, and plagioclase that are 3–7 mm in diameter and contains 1–2% augite xenocrysts that are 1 cm across. The unit is not dated, and the thickness is $t \leq 25$ m.
	Tttb Trachybasalt —A fine-grained flow of variable texture, located in the northeast corner of the map, which contains small olivine and augite phenocrysts. The unit is not dated, and the maximum thickness is about 10 m.
	Tpp Porphyritic basalt with plagioclase phenocrysts —Porphyritic fine-grained basalt flows, located north-northeast of Cerro Pino near the edge of the map, which contain 5–12% plagioclase phenocrysts that are ≤ 5 mm in diameter and trace augite, and olivine phenocrysts that are ≤ 3 mm in diameter. The unit is not dated, and the thickness is ≥ 30 m.
	Tpctb Porphyritic augite-phyric trachybasalt —Distinctive flow located in the northeast corner of the map, with 15% augite phenocrysts that are 2–4 mm in diameter and lesser amounts of plagioclase in an equigranular matrix. The unit is not dated, and the thickness is about 3 m.
	Older fine-grained, aphyric trachybasalt —Flows and scoria deposits (Taptc), on the east edge of the map, which consist of fine-grained trachybasalt with rare, small, phenocrysts of olivine and elongated plagioclase microlites. The cone contains impressive assortment of bombs and a north-trending dike (Taptd). The unit is not dated, and the thickness is about 65 m.
	
	Taptd
	Tmctb Medium-grained, augite-phyric olivine trachybasalt —A medium-grained, slightly-porphyritic trachybasalt, located on the west side of Bear Canyon and Rio Paguete, which contains abundant, small phenocrysts of augite, plagioclase, and olivine. The unit sporadically displays a spotted appearance on weathered surfaces. The K-Ar age is 2.65 ± 0.15 Ma (Lipman and Mehnert, 1979), the MPB is N, and the thickness is about 35 m.
	Tmcpb Medium-grained, augite- and plagioclase-phyric olivine trachybasalt —Flows of medium-grained, sparsely-porphyritic trachybasalt with phenocrysts of plagioclase and augite. The flows are exposed along the upper Rio Paguete, south of Cerro Ortiz. The unit is not dated, the MPB is R, and the thickness is about 25 m.
	Tfvb Fine-grained, vesicular trachybasalt —Several small flows of vesicular, aphyric to fine-grained trachybasalt located in the northeast corner of the map, with $< 1\%$ of olivine that are < 2 –4 mm in diameter and trace augite and plagioclase that are < 2 mm in diameter. The unit is not dated, and the thickness is < 3 m.
	Fine-grained, augite-phyric olivine trachybasalt —Massive to platy flows originating from the eroded cone (Tfctc) and covering southern Chupadero Mesa. They consist of fine- to medium-grained, slightly-porphyritic trachybasalt (C) containing phenocrysts of plagioclase that are ≤ 1.5 cm long and phenocrysts of augite that are very sparse. The flows are dated at 2.65 ± 0.02 Ma, and the MPB is N. The maximum thickness is about 20 m.
	
	Ttdt Porphyritic trachydacite tuffs —Beds of trachydacite to rhyolitic pumice (C) and pumice-rich sediments that are scattered through the southern Mesa Chivato area. The pumice is highly vesicular, containing small, phenocrysts of plagioclase, augite \pm biotite, hornblende, sanidine, and quartz. The sources are presumably from Mount Taylor. The date on the bed on Chupadero Mesa is 2.700 ± 0.002 Ma. The dates on similar deposits, to the west, range from 2.71 to 2.76 Ma (determined from four samples). Individual beds are ≤ 2 m thick.
	Fine-grained, augite-porphyritic olivine basalt —Distinctive flows of fine-grained, porphyritic basalt with conspicuous megacrysts of augite and small phenocrysts of plagioclase and olivine. The flows originate from a scoria cone (Tfcpoc) containing northeast-trending dikes (Tfcpod). The unit is not dated, and the MPB (measured at one site) is N. The unit underlies Ttdt . The maximum thickness is about 20 m.
	
	Tfcpod
	Aphyric olivine basanite of Seboyeta Creek —Flows of very fine-grained, aphyric basanite (C) with tiny microphenocrysts of plagioclase, olivine, and augite. The flows originate from the eroded scoria cone (Tbasc), and are dated at 2.68 ± 0.04 Ma. The unit underlies Tfcpob . The thickness is about 40 m.
	
	Medium-grained, plagioclase-phyric trachybasalt —Massive to sheeted flows and scoria deposits (Tmplc). The flows form a cliff in upper Seboyeta Canyon. They consist of medium-grained, porphyritic trachybasalt (C) with phenocrysts of plagioclase and very small phenocrysts of olivine and augite. The cone contains a north-northwest-trending dike (Tmpld). The unit is dated at 2.70 ± 0.02 Ma, and the MPB (measured at three sites) is N. The thickness is about 15 m.
	
	Tmpld
	Fine-grained, quartz- and xenolith-bearing trachybasalt —A flow of fine-grained trachybasalt, located at the northeast end of Silver Dollar Mesa, with rare, quartz xenocrysts and very rare xenocrysts of pyroxene gabbro that are 0.5–2 cm in diameter. The gabbro is medium-grained and equigranular. The eroded vent (Tfqqc) is mostly stripped of scoria. The unit is not dated, and the thickness is about 15 m.
	

Volcanic rocks of southwest Mesa Chivato

	Medium-grained, augite-phyric olivine trachybasalt of Encinal Creek —Medium-grained, slightly porphyritic trachybasalt flows (C) with sparse megacrysts of augite and small phenocrysts of olivine. A flow forms a distinctive cliff along Encinal Creek near the southwest margin of Silver Dollar Mesa. The K-Ar date is 2.93 ± 0.12 Ma (Laughlin et al., 1993), and the MPF is N. The thickness is about 20 m.
	Medium-grained, olivine trachybasalt of Bear Canyon —Flows of medium-grained trachybasalt (C) containing about 3% olivine phenocrysts that are ≤ 1 mm in diameter in a slightly trachytic groundmass. The flows originate from a small exhumed cinder cone (Tmotc) on the west side of Bear Canyon, upper Rio Paguete. The unit is not dated, and the MPB is N. The thickness is about 35 m.
	Medium-grained, augite- and plagioclase-phyric olivine trachybasalt —Massive to sheeted flows and scoria deposits (Tcpoc), located on Encinal Mesa, which consist of medium-grained porphyritic trachybasalt with phenocrysts of plagioclase, olivine, and sparse augite. The unit is not dated, and the MPF is R, suggesting an age between 3.04–3.11 Ma. The maximum thickness is about 20 m.
	Older fine-grained, olivine trachybasalt of Red Mesa —Massive flows of fine-grained trachybasalt with sparse phenocrysts of olivine, plagioclase, and augite. The flow forms a cliff on the mesa east of Seboyeta Creek. The unit is not dated, and the MPF is R. The thickness is about 15 m.
	Basalt diatreme of Seboyeta Canyon —A complex diatreme consisting primarily of three cycles of alternating massive hydromagmatic beds overlain by layers of coarse pyroclastic breccia and welded basaltic scoria (Goff et al., 2014b). Two dikes, trending S30°W, cut the northeast side of the diatreme. The hydromagmatic beds contain ≤ 1 -m-long fragments of Cretaceous sandstone and rounded chert. The lava, dikes, scoria, and hydromagmatic fragments all consist of fine-grained basalt (C) containing conspicuous complex megacrysts of augite and hornblende. The unit is dated at 3.07 ± 0.09 Ma, and the MPF is R. The thickness is about 50 m.
	Fine-grained trachyte of Cerro Chivato —A strongly foliated trachyte dome (C) in the northeast part of the map area, which contains sparse phenocrysts of plagioclase in a fine trachytic groundmass of plagioclase, augite, and hornblende(?). An intrusion breccia is present on the south margin of the dome. The unit is dated at 3.16 ± 0.02 Ma, and the thickness is about 120 m.
	Porphyritic hornblende trachybasalt —Massive to vesicular flows of trachybasalt (almost basanite, C) containing 1–3% hornblende phenocrysts in a fine-grained matrix with phenocrysts of plagioclase, olivine, and augite. The flows form faulted slopes north of Cerro Pino. They are dated at 3.16 ± 0.01 Ma and the MPB is N. The maximum thickness is about 20 m.
	Hackly olivine basanite —An aphanitic flow of basanite(?) overlying Totb (described previously) in the northeast map area, with pronounced hackly and spotted textures. The flow contains $\ll 1\%$ of very small, iddingsitized olivine microphenocrysts. The unit is not dated, and the thickness is about 10 m.
	East olivine basanite —A fine-grained, nearly aphyric basanite (C) with rare, small phenocrysts of plagioclase and iddingsitized-olivine. On weathered surfaces, the basanite can be distinctly to vaguely spotted. The upper part of the unit is massive to rubbly; the lower part is columnar. The unit is dated at 3.72 ± 0.02 Ma, and the MPF is R. The thickness is about 45 m.

Small dikes and intrusions located throughout map

	Biotite trachydacite dikes: undivided —Massive, porphyritic to coarse-porphyritic, trachydacite dikes (C) found within and on the flanks of MT and the AM (Goff et al., 2013a). The dikes contain phenocrysts of plagioclase, biotite, augite \pm sanidine. They commonly form tall fins. A dike cutting the northwest AM wall is dated at 2.66 ± 0.01 Ma; a tall dike cutting the southeast AM wall is dated at 2.69 ± 0.03 Ma. The dikes' maximum width is roughly 30 m, the height ≤ 50 m, and the exposed longest length is ≤ 1 km.
	Hornblende trachydacite dikes: undivided —Massive, porphyritic trachydacite dikes (C) found within and on the flanks of MT and the AM (Goff et al., 2013a), which contain phenocrysts of plagioclase, augite, and hornblende \pm sanidine. One dike is dated at 2.77 ± 0.02 Ma; its exposed length is ≤ 0.7 km.
	Hornblende-biotite trachydacite dikes: undivided —Massive, porphyritic to coarse-porphyritic, trachydacite dikes (C) found within and on the flanks of MT and the AM, which contain phenocrysts of plagioclase, augite, hornblende, and biotite \pm sanidine. A curving dike in the eastern part of the AM is dated at 2.64 ± 0.06 Ma, and the MPF is N. The exposed length is ≤ 0.8 km.
	Trachyandesite dikes: undivided —Massive, porphyritic, trachyandesite dikes (C) found mostly on flanks and the AM walls of MT, which contain phenocrysts of plagioclase, augite \pm hypersthene \pm olivine. Most dikes of this type are ≤ 10 m wide, ≤ 15 m tall and ≤ 60 m long, however, the exception is the large dike-and-plug complex south of San Mateo; the latter dike is dated at 2.79 ± 0.03 Ma.
	Trachydacite dike —A poorly exposed dike trending east-west on the southwest part of Horace Mesa, which consists of fine-grained trachydacite with very sparse, small phenocrysts of plagioclase. The unit not is dated. The dike width is ≤ 30 m, and the length is ≤ 200 m.
	Mafic dikes: undivided —Linear spines and fins identified only on air photos, which cut rocks of basaltic composition in the northeast part of the map. The dikes are not dated, and they are ≤ 15 m wide.
	Porphyritic nephelinite dike —Spotty, porphyritic, 1-m-wide nephelinite dike (C) located just west of the San Fidel Dome (Goff et al., 2013a), with $>20\%$ olivine phenocrysts with minor augite and sparse plagioclase phenocrysts. The dike trends nearly east-west, and is too altered to date.
	Augite-megacrystic trachybasalt dikes and plug —Fine-grained, trachybasalt (C) dikes containing megacrysts of augite and small phenocrysts of augite and plagioclase, and may contain small xenocrysts of quartz. The dikes trend nearly east-west cutting



prominent north-south-trending folded Cretaceous rocks along the east edge of the map (Goff et al., 2013a). Other similar dikes are in Lobo Canyon; and all dikes are too altered to date. The dikes are ≤ 2 m wide, with the plug being about 30 m wide.

Plagioclase basalt dikes—About four dikes of porphyritic plagioclase basalt cutting the AM floor and the southeast rim. The dikes contain large plagioclase, small olivine, and augite phenocrysts. The dikes are not dated. The widths are ≤ 25 m, and the lengths are ≤ 150 m.



Olivine basalt and trachybasalt dikes—Many dikes ≤ 3 m-wide and ≤ 350 m-long, identified mostly in the Rinconada Basin area (Goff et al., 2013a), consist of basalt and trachybasalt (C), with small-phenocrysts of olivine and rare plagioclase and augite. The dikes are too altered to date.



Olivine gabbro intrusives—Medium- to fine-grained allotriomorphic-granular gabbro bodies and blocks (C) consisting mostly of plagioclase, augite, olivine, and opaque oxides (Goff et al., 2013b). Geochemically, the intrusions vary from gabbro to monzodiorite (Cox et al., 1979). The unit forms a circular, 50-m-in-diameter, intrusion on an isolated hill west of Rinconada Canyon. Forms two, sill-like bodies exposed northeast of MT. Blocks of gabbro are found in scoria cone deposits of unit **Tomtc**, east of Rinconada Canyon, and are ≤ 1 m long. One sill is dated at 2.68 ± 0.07 Ma. A gabbro block, mentioned above and located in the scoria cone, is dated at 3.10 ± 0.24 Ma.



Olivine basanite dike of Picacho Peak—A fine-grained, basanite (C) dike on the south margin of the map contains small olivine, plagioclase, and augite microphenocrysts, and rare quartz xenocrysts. The dike trends northeast away from Picacho Peak plug (Lipman and Moench, 1972). The plug is dated at 4.49 ± 0.08 Ma. The magnetic polarity (laboratory measurement) is R (Hallett et al., 1997). The length of the dike is ≤ 350 m.

MESOZOIC

(Listed by Formational names; these units interfinger; see Correlation Chart 5a)

CRETACEOUS

Mesaverde Group



Menefee Formation—Golden to yellow-orange, medium- to thin-bedded sandstone, black to gray to brown shale and siltstone with carbonized wood fragments, and minor coal. Petrified-wood fragments are common. The Menefee only occurs in the northeast part of the map and in the east-central AM. The maximum exposed thickness is ≥ 45 m.



Point Lookout Sandstone, Hosta Tongue—A fine-grained, cross-bedded, quartz sandstone with rare darker lithic grains, which forms prominent light-gray cliffs. The maximum exposed thickness is about 45 m.

Crevasse Canyon Formation



Gibson Coal Member—An interbedded, light-orange, very fine-grained, quartz sandstone and dark shale in massive to thinly bedded layers, which are ≤ 4 m thick. The shale commonly contains dark-brown to black, lignite coal in seams, which are ≤ 2 m thick. Locally contains light-gray fragments of fossilized wood. The maximum exposed thickness is < 50 m.



Dalton Sandstone Member—The member consists of two prominent sandstone layers: a lower, yellowish-orange layer and an upper white layer with an intervening shale bed. The basal sandstone often has thin beds containing abundant pelecypod casts and molds. The maximum exposed thickness is ≤ 25 m.



Stray Sandstone Member—The member consists of two prominent, reddish-orange, sandstone layers with an intervening shale bed, forming a distinct couplet. The top of the unit is a thin (< 1 m) conglomerate with pebbles to cobbles of quartzite, chert, and quartz. The Stray pinches out to the southeast. The maximum exposed thickness (≤ 40 m) is located in the Lobo Canyon area.

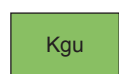


Dilco Coal Member—Interbedded, black to brown siltstone, thin- to medium-bedded, tan, brown, and olive-green sandstone, and black coal. The sandstones are cross-bedded to ripple-laminated. The coal beds are < 0.5 m thick, usually in the lower part of the unit. The maximum exposed thickness (≤ 150 m) is located in the Lobo Canyon area.

Gallup Sandstone



Main Body—A yellowish-gray, white, or golden-yellow, medium- to thick-bedded, cross-bedded sandstone. The sandstone is intercalated with carbonaceous shale. Locally, the unit contains fossiliferous (*Innocermid*) beds near the top. Exposed thickness increases to the southwest in the Lobo Springs quadrangle, where it reaches a maximum of ≤ 25 m (Goff et al., 2008).



Upper tongue (combined with Km in cross sections)—A white, medium-bedded, cross-bedded to tabular sandstone that is locally capped by well-cemented, fractured, planar-cross-bedded sandstone that is weathered brown. The upper and lower contacts are gradational with the Mancos Shale. The maximum exposed thickness is in the Lobo Springs quadrangle and is ≤ 30 m (Goff et al., 2008).



Lower tongue (combined with Km in cross sections)—A white, medium-bedded, cross-bedded to tabular sandstone that is locally capped by well-cemented, fractured, planar-cross-bedded sandstone that is weathered brown. The top of the unit is locally conglomeratic with sandstone clasts and sharks teeth. The upper and lower contacts are gradational with the Mancos Shale. The maximum exposed thickness is in the southwest part of the map and is ≤ 15 m (Goff et al., 2008).

Mancos Shale

Kmsa	Satan Tongue —An interbedded dark shale and less abundant very fine-grained quartz sandstone, which is exposed in Seboyeta Canyon and the eastern floor of the AM. The Satan Tongue pinches out and interlayers with the Point Lookout Sandstone to the northwest (Sears et al., 1941). The maximum observed thickness is about 65 m.
Kmm	Mulatto Tongue —A golden-yellow, thin-bedded, tabular to ripple-laminated sandstone and black shale. Burrows and scattered pelecypod molds are common in the sandstone beds. The upper and lower contacts are gradational with the Dalton and Stray sandstones. The maximum exposed thickness (≤ 50 m) is in the southwest part of the map (Goff et al., 2008).
Km	Main Body —A black to dark-brown shale and silty shale, intercalated with finely laminated to cross-bedded, thinly bedded sandstone. The sandstones are well-sorted, fine-grained, quartz arenites. The upper and lower contacts are gradational. Small tongues of the Main Mancos are interbedded within the Gallup Sandstone units. The maximum exposed thickness of the Main Mancos is beneath the Gallup Sandstone and is ≤ 50 m.
Kmb	Bridge Creek Limestone (combined with Km in cross sections) —A finely laminated, fossiliferous, light-gray limestone, interbedded with thin, black shale below the Main Body of the Mancos Shale. The Bridge Creek was identified only in the San Fidel Dome in the southwest part of the map (Goff et al., 2008). The unit is correlative with the Greenhorn Limestone. It contains abundant invertebrate fossils. The maximum exposed thickness is in the southwest part of the map, and is ≤ 25 m (Goff et al., 2008).

Dakota Formation

Kd	Dakota Formation: undivided —Alternating sandstones and shales of the Dakota Formation and the Mancos Shale. The Dakota unit identified in the uranium well logs near San Mateo (Reise, 1977, 1980) is inferred to be the lower Oak Canyon Sandstone Member (about 25 m thick). Aggregate thickness of the Dakota is about 100 m in the northwestern map area (Owen and Owen, 2003). The Dakota is also exposed in San Fidel Dome and near Paguata. Includes three thin sandstone units (≤ 20 m thick) in the southeast corner of the map (Twowells, Paguata, and Cubero members; Owen and Owen, 2003); also see the cross sections in Goff et al. (2008) and McCraw et al. (2009), and measured sections in Skotnicki et al. (2012).
----	--

JURASSIC**Morrison Formation**

Jmb	Brushy Basin Member —A grayish-green mudstone, interbedded with thin-lenticular beds of light-gray to yellowish-gray, fine- to medium-grained sandstone. There is very limited exposure in the extreme west central edge of the map. The maximum exposed thickness is about 10 m, and the maximum thickness in drill holes is about 40 m (Reise, 1977; Goff et al., 2012).
Jmw	Westwater Canyon Member —Light-gray and yellowish-gray and light-red, fine- to medium-grained sandstones, interbedded with thin, greenish-gray mudstones. There is very limited exposure in the extreme west central edge of map. The maximum exposed thickness is about 30 m, and the maximum thickness in drill holes is about 50 m (Reiss, 1977; Goff et al., 2012).
Jms	Salt Wash Member (cross sections only) —A dark-red, variegated (pink, brown, and gray) shale, and white quartz, cemented by lime sandstone. Some of the shale beds are calcareous and slabby. The unit contains imbricated, gypsiferous beds. The maximum thickness is about 100 m (Anderson and Lucas, 1995).
Jt	Todilto Formation: undivided (cross sections only) —Bedded, massive anhydrite and limestone identified only in State 36-1 well near the south edge of the map (San Fidel Dome; Goff et al., 2008). Because this is a widespread unit throughout west-central New Mexico, it is shown in the cross section. The thickness is assumed to be uniform at ≤ 25 m.
Je	Entrada Formation: undivided (cross sections only) —A massive, bedded to cross-bedded sandstone identified in State 36-1 well near the south edge of the map (San Fidel Dome). As defined here, includes only the Slick Rock Member (Lucas and Zeigler, 2003). Because this is a widespread unit throughout west-central New Mexico, it is shown in the cross section. The bottom of the unit was not penetrated.

Acknowledgments

The STATEMAP Program jointly supported by the US Geological Survey (USGS) and the New Mexico Bureau of Geology and Mineral Resources (NMBGMR) funded this geologic map. J. Michael Timmons (NMBGMR) provided logistical and tactical support. We thank Kate Zeigler (Zeigler Geologic Consulting), Donathon Krier (Los Alamos National Laboratory, retired), Adam Read (NMBGMR), C.A. Ferguson (Arizona Geological Survey), and Jim Risterer (Glorieta Geosciences, Inc.) for mapping assistance during the 2007–2013 field campaigns. Robert Andres (Oak Ridge National Laboratory, retired) helped with edge matching and magnetic polarity measurements during 2014. The cartography of the various editions of the six quadrangles that this map is based on was performed by David J. McCraw, Mark M. Mansell, Shannon Williams, Kelsey Seals, Phil L. Miller, and Elizebeth H. Roybal (NMBGMR). Phil L. Miller, David J. McCraw, Mark M. Mansell, and Brigitte Felix also did much of the cartography for this compilation map and report. The following people and entities are graciously thanked for providing access to fenced private property: Harry Lee, Jr. (Lee Ranch and Fernandez Co.); Jed Elrod and Robert Alexander (Silver Dollar Ranch and Laguna Pueblo); Buddy Elkins (Elkins Ranch); Kelley D'Amato (Lobo Ranch); Shawn Pit (Red Mesa Wind Farm); Lee Maestas (Seboyeta Cattle Association). Darwin Vallo (US Forest Service, Grants) offered valuable advice on logistics on Forest Service and BLM lands. William McIntosh and Lisa Peters (NMBGMR) provided our superb $^{40}\text{Ar}/^{39}\text{Ar}$ dates. Amy Trivett, Ginger McLemore (NMBGMR) and Rusty Reise (formerly Gulf Western Mining Co.) researched and provided well logs from various areas to improve our cross sections. Gordon Keating (LANL, now deceased) worked with the first author on several measured sections of Grants Ridge tuff. Nelia Dunbar (NMBGMR, now Director and State Geologist) assisted with the chemical identification of rhyolitic glasses by electron microprobe. Barry Kues (University of New Mexico) identified Cretaceous marine fossils in the Bridge Creek Limestone. David Mann (High Mesa Petrographics) crafted polished thin sections for petrographic analysis. John Wolff and Kamilla Fellah (Washington State University) provided chemical analyses of rocks. Additional chemical analyses were obtained from ALS USA, Inc. (Reno). Frank Truesdell (USGS, Hawaii Volcano Observatory) suggested a vendor (ASC Scientific, Carlsbad, CA) from which we obtained our fluxgate magnetometer. Duane Champion (USGS, Alaska Branch) gave us magnetic polarity charts. Frank Perry (LANL) and Larry Crumpler (NM Natural History Museum) offered some petrologic insights. Peer reviews by Frank Perry, Matt Zimmerer (NMBGMR), and John Stix (McGill University, Canada) improved our final map and text.

References

- ALS, 2014, Schedule of services and fees: ALS Geochemistry, Reno, NV, 44 p.
- Acocella, V., Cifelli, F., and Funciello, R., 2001, The control of overburden thickness on resurgent domes: Insights from analogue models: *Journal of Volcanology and Geothermal Research*, v. 111, p. 137–153.
- Aldrich, M.J., and Laughlin, A.W., 1984, A model for the tectonic development of the southeastern Colorado Plateau boundary: *Journal of Geophysical Research*, v. 89, p. 10,207–10,218.
- Anderson, D.J. and Lucas, S.G., 1995, Base of the Morrison Formation, Jurassic, of northwestern New Mexico and adjacent areas: *New Mexico Geology*, v. 17, p. 44–53.
- Aranda-Gómez, J.J., Housh, T.B., Luhr, J.F., Neyola-Medrano, C., and Rojas-Beltrán, M.A., 2010, Origin and formation of neck in a basin landform: Examples from the Camargo volcanic field, Chihuahua (México): *Journal of Volcanology and Geothermal Research*, v. 197, p. 123–132.
- Aubele, J.C., Crumpler, L.S., Loeber, K.N., and Kudo, A.M., 1976, Maars and tuff rings of New Mexico: *New Mexico Geological Society Special Publication 6*, p. 109–114.
- Bacon, C.R., 1986, Magmatic inclusions in silicic and intermediate volcanic rocks: *Journal of Geophysical Research*, v. 91, p. 6091–6112.
- Baldrige, W.S., Sharp, Z.D., and Reid, K.D., 1996, Quartz-bearing basalts: Oxygen isotope evidence for crustal contamination of continental mafic rocks: *Geochimica et Cosmochimica Acta*, v. 60, p. 4,765–4,772.
- Baker, I., and Ridley, W. I., 1970, Field evidence and K, Rb, Sr data bearing on the origin of the Mt. Taylor volcanic field, New Mexico, USA: *Earth and Planetary Science Letters*, v. 10, p. 106–114.
- Bassett, W.A., Kerr P.F., Schaeffer, O.A., and Stoenner, R.W., 1963, Potassium-argon ages of volcanic rocks near Grants, New Mexico: *Geological Society of America Bulletin*, v. 74, p. 221–226.
- Brown, R.J., Blake, S., Thordarson, T., and Self, S., 2014, Pyroclastic edifices record vigorous lava fountains during emplacement of flood basalt flow field, Roza Member, Columbia River Basalt Province, USA: *Geological Society of America Bulletin*, doi: 10.1130/B30857.1, 17 pp.
- Bryan, K., and McCann, F.T., 1938, The Ceja del Rio Puerco—border feature of the Basin and Range province in New Mexico, Pt. II, *Geomorphology: Journal of Geology*, v. 46, p. 1–16.
- Channer, M.A., Ricketts, J.W., Zimmerer, M., Heizler, M., and Karlstrom, K.E., 2015, Surface uplift above the Jemez mantle anomaly in the past 4 Ma based on $^{40}\text{Ar}/^{39}\text{Ar}$ dated paleoprofiles of the Rio San Jose, New Mexico, USA: *Geosphere*, v. 11, p. 1384–1400.
- Chapman, Wood, and Griswold, Inc., 1974, Geologic map of the Grants uranium region: New Mexico Bureau of Mines & Mineral Resources, Geologic Map 31, scale 1 inch = 2 miles.
- Christiansen, E.H., Burt, D.M., Sheridan, M.F., Wilson, R.T., 1983, The petrogenesis of topaz rhyolites from the western United States: *Contributions to Mineralogy and Petrology*, v. 83, p. 16–30.
- Clark, F.W., 1910, Analyses of rocks and minerals from the laboratory of the United States Geological Survey, 1880–1908: *U.S. Geological Survey Bulletin 419*, p. 123.
- Cobos, R., 2003, A dictionary of New Mexico & southern Colorado Spanish: Museum of New Mexico Press, Santa Fe, 258 pp.
- Cohen, K.M., Finney, S.C., Gibbard, P.L., and Fan, J.X., 2013, The ICS international chronostratigraphic chart: *Episodes*, v. 36, p. 199–204.
- Crumpler, L.S., 1977, Alkali basalt-trachyte suite and volcanism, northern part of the Mount Taylor volcanic field, New Mexico: M.S. thesis, University of New Mexico, Albuquerque, 131 p. w/ 1:32,000 scale geologic map.
- Crumpler, L.S., 1980a, Alkali basalt through trachyte suite and volcanism, Mesa Chivato, Mount Taylor volcanic field, New Mexico, Part I: *Geological Society of America Bulletin*, v. 91, p. 253–255.
- Crumpler, L.S., 1980b, Alkali basalt through trachyte suite and volcanism, Mesa Chivato, Mount Taylor volcanic field, New Mexico, Part II: *Geological Society of America Bulletin*, v. 91, p. 1,293–1,313.
- Crumpler, L.S., 1982, Volcanism in the Mount Taylor region, *in* Albuquerque Country II: New Mexico Geological Society, Guidebook 33, p. 291–298.

- Crumpler, L., and Goff, F., 2012, The geology of Mount Taylor, a large, young composite volcano, west central New Mexico: Geological Society of America, Rocky Mountain Section, Field Trip Guide, May 7 and 8, 21 p. (available from the authors).
- Crumpler, L., and Goff, F., 2013, Third day road log: Trip 1—A brief tour of Mount Taylor, in Zeigler, K., Timmons, J.M., Timmons, S., and Semken, S., eds., *Geology of Route 66 Region: Flagstaff to Grants: New Mexico Geological Society, 64th Annual Field Conference, Guidebook*, p. 59–65.
- Cox, K.G., Bell, J.D., and Pankhurst, R.J., 1979, *The interpretation of igneous rocks*: London, Allen and Unwin, 450 p.
- Dillinger, J. K., 1990, Geologic map of the Grants 30' x 60' quadrangle, west-central New Mexico: U.S. Geological Survey, Coal Investigations Map C-118-A, 1 sheet, 1:100,000 scale (color).
- Duffield, W.A., and Sass, J.H., 2003, Geothermal energy—clean power from the Earth's heat: U.S. Geological Survey Circular 1,249, 36 pp.
- Dunbar, N.W., Kelley, S.A., Goff, F., and McIntosh, W.C., 2013, Rhyolitic pyroclastic deposits at Mount Taylor: Insight into early eruptive processes of a major composite volcano, in Zeigler, K., Timmons, J.M., Timmons, S., and Semken, S., eds., *Geology of Route 66 Region: Flagstaff to Grants: New Mexico Geological Society, 64th Annual Field Conference, Guidebook*, p. 72–74.
- Dutton, C.E., 1885, Mount Taylor and the Zuni Plateau: U.S. Geological Survey, 6th Annual Report, p. 105–198.
- Eichelberger, J.C., 1980, Vesiculation of mafic magma during replenishment of silicic magma reservoirs: *Nature*, v. 288, p. 446–450.
- Ellis, R.W., 1935, Glaciation in New Mexico: University of New Mexico Bulletin, Geological Series, v. 5, 31 p.
- English, J.M., and Johnston, S.T., 2004, The Laramide Orogeny: What were the driving forces: *International Geology Review*, v. 46, p. 833–838.
- Fellah, K., 2011, Petrogenesis of the Mount Taylor volcanic field and comparison with the Jemez Mountain volcanic field, New Mexico: M.S. thesis, Washington State University, Pullman, WA, 92 p.
- Fellah, K., Wolff, J.A., Goff, F., 2009, Geochemistry of volcanic rocks from the Mt. Taylor volcanic field and comparison with the nearby Jemez Mountains: Geological Society of America, Abstract and Poster, 2009 Portland Annual Meeting, 18–21 October, paper 33–10.
- Fisher, R.V., and Schmincke, H.-U., 1984, *Pyroclastic Rocks*: Springer-Verlag, Berlin, 472 p.
- Gardner, J.H., 1909, The coal field between Gallup and San Mateo, New Mexico: U.S. Geological Survey Bulletin 341, p. 364–378.
- Gee, J.S., and Kent, D.V., 2007, Source of oceanic magnetic anomalies and the geomagnetic polarity timescale, *Treatise on Geophysics*, v. 5: Elsevier, London, p. 455–507.
- GeoMetrics, 1979, Aerial gamma ray and magnetic survey, Raton Basin project, Albuquerque quadrangle [1° x 2°], Final Report, Volume II: Bendix Field Engineering Corporation, Grand Junction, Colorado, GJBX-116 (79). <http://pubs.usgs.gov/of/2009/1129/US/albuquerque>.
- Goff, F., and Goff, C.J., 2013, The Quarry lava flow, a peridotite-bearing trachybasalt at Mount Taylor volcano, New Mexico, in Zeigler, K., Timmons, J.M., Timmons, S., and Semken, S., eds., *Geology of Route 66 Region: Flagstaff to Grants: New Mexico Geological Society, 64th Annual Field Conference, Guidebook* p. 67–69.
- Goff, F., and Gardner, 2004, Late Cenozoic geochronology of volcanism and mineralization in the Jemez Mountains and Valles caldera, north central New Mexico, in Mack, G.H. and Giles, K.A., eds. *The Geology of New Mexico*: New Mexico Geological Society, Special Publication 11, p. 295–312.
- Goff, F., Kelley, S.A., Zeigler, K., Drakos, P., and Goff, C., 2008, Geologic map of the Lobo Springs 7.5-minute quadrangle map, Cibola County, New Mexico: New Mexico Bureau of Geology & Mineral Resources Open-File Geologic Map 181, 1:24,000 (<http://geoinfo.nmt.edu/publications/maps/geologic/ofgm/details.cfm?Volume=181>).
- Goff, F., Kelley, S.A., Lawrence, J.R., and Goff, C.J., 2012, Geologic map of the Cerro Pelón 7.5-minute quadrangle, Cibola and McKinley counties, New Mexico: New Mexico Bureau of Geology and Mineral Resources, Open-File Geologic Map 202, 1:24,000 (at: <http://geoinfo.nmt.edu/publications/maps/geologic/ofgm/details.cfm?Volume=202>).
- Goff, F., Wolff, J.A., and Fellah, K., 2013a, Mount Taylor dikes, in Zeigler, K., Timmons, J.M., Timmons, S., and Semken, S., eds., *Geology of Route 66 Region: Flagstaff to Grants: New Mexico Geological Society, 64th Annual Field Conference, Guidebook*, p. 159–165.
- Goff, F., Wolff, J.A., McIntosh, W., and Kelley, S.A., 2013b, Gabbroic shallow intrusions and lava-hosted xenoliths in the Mount Taylor area, New Mexico, in Zeigler, K., Timmons, J.M., Timmons, S., and Semken, S., eds., *Geology of Route 66 Region: Flagstaff to Grants: New Mexico Geological Society, 64th Annual Field Conference, Guidebook*, p. 143–151.
- Goff, F., Kelley, S.A., Lawrence, J.R., and Goff, C.J., 2014a, Geologic map of the Laguna Cañoneros 7.5-minute quadrangle, Cibola and McKinley counties, New Mexico: New Mexico Bureau of Geology and Mineral Resources, Open-File Geologic Map 244, 1:24,000 (<https://geoinfo.nmt.edu/publications/maps/geologic/ofgm/details.cfm?volume=244>).
- Goff, F., Lawrence, J.R., and Goff, C.J., 2014b, Plio-Pleistocene maar-diatremes, Mesa Chivato, New Mexico, USA in Carrasco-Núñez, G., Aranda-Gómez, J.J., Ort, M.H., Silva-Corona, J.J., eds., 5th International Maar Conference, Abstracts Volume: Juriquilla, Oro. México, Universidad Nacional Autónoma de México, Centro de Geociencias, p. 20–21.
- Hallet, R.B., 1994, Volcanic geology, paleomagnetism, geochronology and geochemistry of the Rio Puerco Necks, west-central New Mexico: PhD dissertation, New Mexico Institute of Mining and Technology, Socorro, 340 p.
- Hallet, R.B., Kyle, P.R. and McIntosh, W.C., 1997, Paleomagnetic and ⁴⁰Ar/³⁹Ar age constraints on the chronologic evolution of the Rio Puerco volcanic necks and Mesa Prieta, west-central New Mexico: Implications for transition zone magmatism: *Geological Society of America Bulletin*, v. 109, p. 95–106.
- Hoblitt, R.P., Miller, C.D., and Vallance, J.W., 1981, Origin and stratigraphy of the deposit produced by the May 18 directed blast, in Lipman, P.W., and Mullinaux, D.R., eds., *The 1980 eruptions of Mount St. Helens*, Washington: U.S. Geological Survey, Professional Paper 1250, p. 401–419.
- Hunt, C.B., 1938, Igneous geology and structure of the Mount Taylor volcanic field, New Mexico: U.S. Geological Survey, Professional Paper 189-B, p. 51–80.
- Hunt, C.B., 1956, Cenozoic geology of the Colorado Plateau: U.S. Geological Survey, Professional Paper 279, 99 p.
- Iddings, J.P., 1888, On the origin of primary quartz in basalt: *American Journal of Science*, v. 136, p. 208–221.
- Irvine, T.N., and Baragar, W.R.A., 1971, A guide to the chemical classification of the common volcanic rocks: *Canadian Journal of Earth Science*, v. 8, p. 523–548.
- Johnson, D.W., 1907, Volcanic necks of the Mount Taylor region, New Mexico: *Geological Society of America Bulletin*, v. 18, p. 303–324.
- Keating, G.N., and Valentine, G.A., 1998, Proximal stratigraphy and syn-eruptive faulting in rhyolitic Grants Ridge Tuff, New Mexico, USA: *Journal of Volcanology and Geothermal Research*, v. 81, p. 37–49.
- Keating, G.N., Valentine, G.A., Krier, D.J., and Perry, F.V., 2008, Shallow plumbing systems for small volume basaltic volcanoes: *Bulletin of Volcanology*, v. 70, p. 563–582.
- Kelley, V.C., 1963, Geology and technology of the Grants uranium region: New Mexico Bureau of Mines & Mineral Resources, Memoir 15, p. 563–582.
- Kelley, S., Dunbar, N., McIntosh, W., and Goff, F., 2013, Third day road log: Trip 2—Tuffs of San Mateo Canyon, in Zeigler, K., Timmons, J.M., Timmons, S., and Semken, S., eds., *Geology of Route 66 Region: Flagstaff to Grants: New Mexico Geological Society, 64th Annual Field Conference, Guidebook*, p. 70–72.,

- Kerr, P.F., and Wilcox, J.T., 1963, Structure and volcanism, Grants Ridge area: New Mexico Bureau of Mines & Mineral Resources, Memoir 15, p. 205–213.
- Komuro, H., Fujita, Y., and Kodama, K., 1984, Numerical and experimental models on the formation mechanism of collapse basins during the Green Tuff orogenesis of Japan: *Bulletin of Volcanology*, v. 47, p. 649–666.
- Kuiper, K.F., Deino, A., Hilgen, H.J., Krijgsman, W., Renne, P.R., and Wijbrans, J.R., 2008, Synchronizing rock clocks of earth history: *Science*, v. 320, p. 500–504.
- Laughlin, A.W., Aldrich, M.J., Ander, M.E., Heiken, G.H. and Vaniman, D.T., 1982, Tectonic setting and history of late Cenozoic volcanism west-central New Mexico: *in* Grambling, Jeffrey, Wells, Steven G., and Callahan, Jonathan F., A., New Mexico Geological Society, 33rd Annual Field Conference, Guidebook, p. 279–284.
- Laughlin, A.W., Perry, F.V., Damon, P.E., Shafiqullah, M., WoldeGabriel, G., McIntosh, W., Harrington, C.D., Wells, S.G., and Drake, P.G., 1993, Geochronology of Mount Taylor, Cebollita Mesa, and Zuni-Bandera volcanic fields, Cibola County, New Mexico: *New Mexico Geology*, v. 15, p. 81–92.
- Le Bas, M.J., Le Maitre, R.W., Streckeisen, A., and Zanettin, B., 1986, A chemical classification of volcanic rocks based on the total alkali-silica diagram: *Journal of Petrology*, v. 27, p. 745–750.
- Lipman, P. W., and Mehnert, H. H., 1979, Potassium-argon ages from the Mount Taylor volcanic field, New Mexico: U.S. Geological Survey, Professional Paper 1124-B, 8 p.
- Lipman, P. W., and Moench, R. H., 1972, Basalts of the Mt. Taylor volcanic field, New Mexico: *Geological Society of America Bulletin*, v. 83, p. 1335–1344.
- Lipman, P.W., Pallister, J.S., and Sargent, K.A., 1979, Geologic map of the Mount Taylor quadrangle, Valencia [now Cibola] County, New Mexico: U.S. Geological Survey, Map GQ-1523, 1:24,000 scale (color).
- Lorenz, V., 1986, On the growth of maars and diatremes and its relevance to the formation of tuff rings: *Bulletin of Volcanology*, v. 48, p. 265–274.
- Love, D.W., and Connell, S.D., 2005, Late Neogene drainage development on the southeastern Colorado Plateau, New Mexico: *New Mexico Museum of Natural History and Science Bulletin* 28, p. 151–169.
- Luedke, R.G., and Smith, R.L., 1978, Map showing distribution, composition, and age of late Cenozoic volcanic centers in Arizona and New Mexico: U.S. Geological Survey, Miscellaneous Investigations Series Map I-1091-A.
- Mariner, R.H., Brook, C.A., Reed, M.J., Bliss, J.D., Rapport, A.L., and Lieb, R.J., 1982, Low-temperature geothermal resources in the western United States, *in* Reed, M.J., ed. *Assessment of low-temperature geothermal resources in the United States—1982*: U.S. Geological Survey Circular 892, p. 31–40.
- Marti, J., Ablay, G.J., Redshaw, L.T., and Sparks, R.S.J., 1994, Experimental studies of collapse calderas: *Journal of the Geological Society (London)*, v. 151, p. 919–929.
- Mayo, E.B., 1958, Lineament tectonics and some ore districts of the southwest: *Transactions American Institute of Metallurgical Engineers*, v. 211, p. 1169–1175.
- McCraw, D.J., Read, A.S., Lawrence, J.R., Goff, F., and Goff, C.J., 2009, Geologic map of the San Mateo quadrangle, McKinley and Cibola counties, New Mexico. NM Bureau of Geology and Mineral Resources Open-File Map OF-GM 194, 1:24,000 (<http://geoinfo.nmt.edu/publications/maps/geologic/ofgm/details.cfm?Volume=194>).
- McLemore, V.T., 2011, The Grants uranium district: Update on source, deposition, exploration: *The Mountain Geologist*, v. 48, p. 23–44.
- McLemore, V.T., Broadhead, R.F., Barker, J.M., Austin, G.S., Klein, K., Brown, K.B., Murray, D., Bowie, M.R., and Hingtgen, J.S., 1986, A preliminary mineral-resource potential of Cibola County, northwestern New Mexico: New Mexico Bureau of Mines and Mineral Resources, Open-File Report OFR 230, 403 p.
- McLemore, V.T., Hill, B., Khalsa, N., and Lucas Kamat, S.A., 2013, Uranium resources in the Grants uranium district, New Mexico: An update, *in* Zeigler, K., Timmons, J.M., Timmons, S., and Semken, S., eds., *Geology of Route 66 Region: Flagstaff to Grants*: New Mexico Geological Society, 64th Annual Field Conference, Guidebook, p. 117–126.
- Meyer, G.A., Muir Watt, P., and Wilder, M., 2014, Was Mount Taylor glaciated in the Late Pleistocene? An analysis based on field evidence and regional equilibrium line altitudes: *New Mexico Geology*, v. 36, p. 32–39.
- Moench, R.H., 1963, Geologic map of the Seboyeta quadrangle, New Mexico: U.S. Geological Survey, Map GQ-207, 1:24,000 scale (color).
- Moench, R.H., and Schlee, J.S., 1967, Geology and uranium deposits of the Laguna district, New Mexico: U.S. Geological Survey, Professional Paper 519, 117 p.
- Molenaar, C.M., 1974, Correlation of the Gallup Sandstone and associated formations, upper Cretaceous, eastern San Juan and Acoma basins, New Mexico, *in* Siemers, C. T., Woodward, L. A., Callender, J. F., eds., *Ghost Ranch, New Mexico Geological Society Guidebook*, 25th Field Conference, p. 251–258.
- Morgan, G.S., and Lucas, S.G., 1999, Pliocene (Blancan) vertebrates from the Albuquerque Basin, north-central New Mexico, *in* Pazzaglia, F. J., Lucas, S.G., eds., *Albuquerque Geology, New Mexico Geological Society*, 50th Annual Field Conference, Guidebook p. 363–370.
- Nathenson, M., Guffanti, M., Sass, J.H., and Munroe, R.J., 1982, Regional heat flow and temperature gradients, *in* Reed, M.J., ed. *Assessment of low-temperature geothermal resources in the United States—1982*: U.S. Geological Survey Circular 892, p. 9–16.
- Nicholls, J., Carmichael, I.S.E., and Stomer, J.C., 1971, Silica activity and Ptotal in igneous rocks: *Contributions to Mineralogy and Petrology*, v. 33, p. 1–20.
- Olsen, K.H., Keller, G.H., and Stewart, J.N., 1979, Crustal structure along the Rio Grande rift from seismic refraction profiles, *in* Riecker, R.E., ed., *Rio Grande Rift: Tectonics and Magmatism*: American Geophysical Union, Washington, D.C., p. 127–143.
- Olsen, K.H., Baldrige, W.S., and Callender, J.F., 1987, Rio Grande rift: An overview: *Tectonophysics*, v. 143, p. 119–139.
- Osburn, G.R., Kelley, S.A., and Goff, F., 2010. Geologic map of the Mount Taylor quadrangle, Cibola County, New Mexico, New Mexico Bureau of Geology and Mineral Resources Open-File Map, 1:24,000 (<http://geoinfo.nmt.edu/publications/maps/geologic/ofgm/details.cfm?Volume=186>).
- Owen, D.E., and Owen, D.E., Jr., 2003, Stratigraphy of the Dakota Sandstone and intertongued Mancos Shale along the southern flank of the San Juan Basin, west-central New Mexico, *in* Lucas, S.G., Semken, S.C., Berglof, W.R., and Ulmar-Scholle, D.S., eds., *Geology of the Zuni Plateau, New Mexico Geological Society*, 54th Annual Field Conference Guidebook, p. 325–330.
- Pei, M.A., 1968, *The New World Spanish-English and English-Spanish Dictionary*. Signet, New American Library, New York, 1226 p.
- Perry, F.V., Baldrige, W.S., DePaolo, D.J., and Shafiqullah, M., 1990, Evolution of a magmatic system during continental extension: The Mount Taylor volcanic field, New Mexico: *Journal of Geophysical Research*, v. 95, p. 19,327–19,348.
- Pierce, K.L., 2004, Pleistocene glaciations of the Rocky Mountains, *in* Gillespie, A.R., Porter, S.C., and Atwater, B.F., eds. *The Quaternary Period in the United States*. *Developments in Quaternary Science* 1: Elsevier, Amsterdam, p. 63–76.
- Poland, M.C., Moats, W.P., and Fink, J.H., 2008, A model for radial dike emplacement in composite cones based on observations at Summer Coon volcano, Colorado, USA: *Bulletin of Volcanology*, v. 70, p. 861–875.
- Price, L.G., ed., 2010, *The Geology of Northern New Mexico's Parks, Monuments and Public Lands*, New Mexico Bureau of Geology and Mineral Resources, 385 p.

- Reise, W.C., 1977, Geology and geochemistry of the Mount Taylor uranium deposit, Valencia County, New Mexico: MS thesis, University of New Mexico, Albuquerque, 119 p. w/maps and sections.
- Reise, W.C., 1980, The Mount Taylor uranium deposit, San Mateo, New Mexico: Ph.D. thesis, University of New Mexico, Albuquerque, 643 p. w/maps and sections.
- Santos, E.S., 1966, Geologic map of the San Mateo quadrangle, McKinley and Valencia [now Cibola] Counties, New Mexico: U.S. Geological Survey, Map, GQ-517, 1:24,000 scale (color).
- Santos, E.S., 1970, Stratigraphy of the Morrison Formation and structure of the Ambrosia Lake district, New Mexico: U.S. Geological Survey, Bulletin 1272-E, 30 p.
- Schrader, F.C., 1906, The Durango-Gallup coal field of Colorado and New Mexico: U.S. Geological Survey, Bulletin 285, p. 241-258.
- Sears, J.D., Hunt, C.B., and Hendricks, T.A., 1941, Transgressive and regressive Cretaceous deposits in southern San Juan Basin, New Mexico: U.S. Geological Survey, Professional Paper 193-F, p., 101-121.
- Shackley, M.S., 1998, Geochemical differentiation and prehistoric procurement of obsidian in the Mount Taylor volcanic field, northwest New Mexico: *Journal of Archaeological Science*, v. 25, p. 1073-1082.
- Shimer, H.W., and Blodgett, M.E., 1908, The stratigraphy of the Mount Taylor region, New Mexico: *American Journal of Science*, 4th series, v. 25, p. 53-67.
- Simpson, J.H., 1850, Journal of a military reconnaissance from Santa Fe, N. Mexico to the Navajo country: 31st Congress, 1st session, S. Ex. Doc. 64, p. 56-138, 146-148.
- Skotnicki, S.J., Drakos, P.G., Goff, F., Goff, C.J., and Riesterer, J., 2012, Geologic map of the Seboyeta 7.5-minute quadrangle, Cibola County, New Mexico: New Mexico Bureau of Geology and Mineral Resources, Open-file Geologic Map 226, 1:24,000 (<http://geoinfo.nmt.edu/publications/maps/geologic/ofgm/details.cfm?Volume=226>).
- Smith, R.L., and Luedke, R.G., 1984, Potentially active volcanic lineaments and loci in western conterminous United States, in *Explosive Volcanism: Inception, Evolution and Hazards*: National Academy Press, Washington, D.C., p. 47-66.
- Sosa, A., Thompson, L., Velasco, A.A., Romero, R., and Herrmann, R., 2014, 3-D structure of the Rio Grande rift from 1-D constrained joint inversion of receiver functions and surface wave dispersion: *Earth and Planetary Science Letters*, v. 402, p. 127-137.
- Stimac, J.A., and Pearce, T.H., 1992, Textural evidence of mafic-felsic magma interaction in dacitic lavas, Clear Lake, California: *American Mineralogist*, v. 77, p. 795-809.
- Stimac, J.A., Goff, F., and Goff, C.J., 2015, Chapter 46: Intrusion-related geothermal systems, in Sigurdsson, H., Houghton, B., McNutt, S.R., Rymer, H., and Stix, J., eds. *Encyclopedia of Volcanoes*, 2nd Edition: Academic Press, Elsevier, London, p. 799-822.
- Thaden, R.E., Santos, E.S., and Raup, O.B., 1967, Geologic map of the Grants quadrangle, Valencia County, New Mexico: U.S. Geological Survey, Map GQ-681, 1:24,000 scale.
- Thompson, G.A., and Zoback, M.L., 1979, Regional geophysics of the Colorado Plateau: *Tectonophysics*, v. 61, p. 149-181.
- Valentine, G.A., and White, J.D.L., 2012, Revised conceptual model for maar-diatremes: Subsurface processes, energetics, and eruptive products: *Geology*, v. 40, p. 1111-1114.
- Voight, B., Glicken, H., Janda, R.J., and Douglass, P.M., 1981, Catastrophic rock slide avalanche of May 18, in Lipman, P.W., and Mullineaux, D.R., eds. *The 1980 eruptions of Mount St. Helens*, Washington: U.S. Geological Survey, Professional Paper 1250, p. 347-377.
- Walter, T.R., and Troll, V.R., 2001, Formation of caldera periphery faults: an experimental study: *Bulletin of Volcanology*, v. 63, p. 191-203.
- Williams, H., Turner, F.J., and Gilbert, C.M., 1954, *Petrography*: W.H. Freeman and Co., San Francisco, 406 p.
- Wilson, M., 1989, *Igneous Petrogenesis*: Unwin Hyman, London, 466 p.
- WoldeGabriel, G., Keating, G.N., and Valentine, G.A., 1999, Effects of shallow basaltic intrusion into pyroclastic deposits, Grants Ridge, New Mexico, USA: *Journal of Volcanology and Geothermal Research*, v. 92, p. 389-411.
- Wohletz, K.H., and Sheridan, M.F., 1983, Hydrovolcanic explosions II. Evolution of basaltic tuff rings and tuff cones: *American Journal of Science*, v. 283, p. 385-413.
- Zachos, J., Pagani, M., Sloan, L., Thomas, E., and Billups, K., 2001, Trends, rhythms and aberrations in global climate, 65 Ma to present: *Science*, v. 292, p. 686-693.
- Zachos, J.C., Dickens, G.R., and Zeebe, R.E., 2008, An early Cenozoic perspective on greenhouse warming and carbon-cycle dynamics: *Nature*, v. 45, p. 279-283.
- Zeigler, K., Timmons, J.M., Timmons, S., and Semken, S., eds., 2013, *Geology of Route 66 Region: Flagstaff to Grants, New Mexico* Geological Society, 64th Annual Field Conference, Guidebook, Plates 6, 7, 8, 14, 15, and 16.

Appendix 1.

English Translations of Spanish Words used in Mount Taylor Region (Pei, 1968; Cobos, 2003)

Agua —Water	-ita, -ito —Diminutive suffix meaning little
Aguila —Eagle, to be sharp or “on the ball”	Jara —Clump, thicket, rockrose, branch of a tree, (Mexican slang) the cops
Arroyo —Intermittent stream, creek; shallow ravine	Laguna, -ita —Lake or pond; little lake
Bajío —Shoal, sandbank; lowland	Largo —Large
Bandeja —Tray, platter	Llano —Plain, large flat area or region
Bibo —Imbibe; literally “I drink” (Latin)	Lobo —Wolf
Blanco, -a —White, blank, fair (complexion)	Malpais —Lava beds; rough country (literally, bad country)
Blanquita —Little and white	Mesa —Table; flat-topped mountain or hill
Bonita, -o —Pretty, neat	Mosca —Fly; housefly
Campo —camp, country, field, outdoors	Negra, -o —Black
Cañon —Canyon	Ojo —Eye; spring (source of water)
Cañoneros —Gunboat; canoneers (artillerymen); those who live in canyons (slang)	Osha —Wild celery
Casa —House	Oso —Bear
Cebolla —Onion	Padre —Father, priest, (adjective) great, stupendous, terrific
Celosa —Jealous, suspicious, zealous (female)	Paguete —Place of herbs or medicinal plants (?)
Cerro —Hill	Pelón —Bald; bare
Chamiso, -a —Generic sagebrush, rabbitbrush	Picacho —Large pointed isolated hill; small peak
Chivato —Young male goat; billy goat	Piedra —Stone, rock
Chupadero —Anything that serves to pacify; teething ring; secret prison or corral	Pino —Pine tree
Chute —Long, narrow	Piñon —Short, squat pine tree of American southwest; source of edible pine nuts
Cibola —Seven golden cities of Cibola; buffalo country; coiled Pueblo bowl	Prieta —Dark, black (female)
Ciénega —Marshy or swampy land; small farm (New Mexico)	Pueblo —Communal structure for dwelling and defense; small town or village
Colorado —Red, reddish, embarrassed	Redondo, -a —Round
Cruz —Cross	Rey, Reyes —King, kings
Cuate, -tes —Twin, twins, friends	Rinconada —Corner, nook; small valley or basin; group of houses
Cubero —Cask or tub maker; cooper	Río —River, large stream
Cuchilla —Large knife; blade	Rito —Small river, stream
Damacio —No translation; a man’s name?	Sebo —Tallow, fat, suet
de —of	Seboyeta —Place of small onions (Anglicized from Cebolleta); Seboya family village
del —of the (masculine)	Seco —Dry
Diablo —Devil, Satan	Telesfor —Telesforo(?); telescope
Encina, -al —Oaks, place of evergreen oaks	Verde —Green, verdant, unripe
Frances —Frenchmen, French language, (adjective) French	Viejo -a —Old, ancient
Fria, Frio —Cold	
Grande —Big, large	

Appendix 2. Selected Chemical analyses of volcanic rocks, Mount Taylor region.*

Name	Basanites				Older Trachybasalts				Older Basalts				Mafic Diatreme and Dikes				
	W Basanite	Amp Basan	Qtz Basanite	Aphy Tbasalt	Hbd Tbasalt	Mxd Tbasalt	Mxd Tbasalt	Old Alk Bas	Oliv Basalt	Cpx Basalt	Diatreme	Tbas dike	Neph dike	Map Unit	Sample No.	Source	Quad
	Tbac	Tbaa	Tbal	Toth	Tpthb	Tomtb	Toob	Toab	Toob	Toob	Tmbi	Ttcbi	Trnpi				
	F12-40A	F12-40A	F13-09A	F09-46	F13-33A	F08-113	F09-22	F07-48	F09-22	09KF-44	F12-03W	F07-43	F07-40				
	Fellah	ALS	ALS	Fellah	ALS	Fellah	Fellah	Fellah	Fellah	Fellah	Wolff	Fellah	Fellah				
	Lobo Spgs	Mt Taylor	Lag Canon	Cerro Pelón	Lag Canon	Cerro Pelón	Cerro Pelón	Lobo Spgs	Cerro Pelón	Lobo Spgs	Seboyeta	Lobo Spgs	Lobo Spgs				
Major Oxides, wt%																	
SiO ₂	44.37	43.6	45.4	47.85	48.59	50.19	46.67	46.39	46.67	47.28	46.99	50.13	41.82				
TiO ₂	4.202	4.38	3.27	3.54	3.05	2.091	3.09	3.466	3.09	3.025	3.022	3.414	3.349				
Al ₂ O ₃	14.27	14.4	15.82	17.21	17.43	15.98	15.34	16.03	15.34	16.15	15.55	18.54	8.72				
Fe ₂ O ₃	—	14.7	14.15	—	13.53	—	—	—	—	—	—	—	—				
FeO	15.43	—	—	11.72	—	9.97	12.96	12.79	12.96	12.33	12.22	7.54	12.15				
MnO	0.218	0.27	0.18	0.164	0.21	0.149	0.175	0.176	0.175	0.168	0.171	0.19	0.191				
MgO	5.50	6.63	6.98	5.02	3.63	6.87	7.95	6.78	7.95	6.69	7.40	2.72	14.72				
CaO	7.85	9.79	8.11	8.45	5.92	7.37	9.09	9.33	9.09	9.13	9.03	11.51	15.02				
Na ₂ O	4.60	2.90	3.66	3.84	4.24	4.57	3.09	3.39	3.09	3.45	3.16	3.99	1.91				
K ₂ O	2.35	2.45	1.70	1.57	2.44	2.06	1.11	1.17	1.11	1.24	1.57	1.34	1.33				
P ₂ O ₅	1.217	0.89	0.74	0.651	0.96	0.742	0.517	0.481	0.517	0.536	0.880	0.618	0.782				
Total	100.00	100.01	100.01	100.00	100.00	100.00	100.00	100.00	100.00	100.00	100.00	99.99	99.99				
Total Alk	6.95	5.35	5.36	5.41	6.68	6.63	4.20	4.56	4.20	4.69	4.73	5.33	3.24				
F	na	na	na	na	na	na	na	na	na	na	na	na	na				
Selected Trace Elements, ppm																	
Ba	888	719	571	610	945	915	423	417	423	450	581	697	890				
Ce	139	103	73.8	77	113.5	78	54	47	54	61	83	66	113				
Cr	5	90	60	2	10	167	179	103	179	126	135	250	544				
La	74	50.1	36.3	35	57.5	37	28	26	28	26	39	37	51				
Nb	90.0	68.1	50.0	48.0	78.1	45.8	34.5	31.2	34.5	36.9	47.1	39.5	59.2				
Ni	28	93	90	19	12	121	150	94	150	104	106	159	462				
Pb	6	<2	2	3	<2	4.3	2	2.4	2	2	4	4	4				
Rb	40	41.6	26	27	36.2	34	18	19	18	20	28	35	29				
Sr	1191	1095	824	927	917	918	651	673	651	730	908	818	1035				
Th	7	5.89	4.09	4	6.54	4.4	3	4	3	5	5	4	8				
U	4	1.69	1.14	1	1.32	1.3	1	0.8	1	3	2	1.9	1.8				
Zr	488	352	246	264	387	251	188	196	188	198	272	212	295				
Age (Ma)	3.64±0.15	3.22±0.04	2.58±0.01	3.20±0.05	3.16±0.01	2.64±0.10	2.67±0.12	3.21±0.12	2.67±0.12	2.62±0.01	3.07±0.09	2.9-2.7?	2.6?				
Magnetics	R	nd	N	R	N	N	nd	R	nd	nd	R	nd	nd				
Notes	scoria cone	AM	Mesa Chivato	on Cretaceous	Mesa Chivato	C Pelón area	N of C. Osha	Up. Rincon.	N of C. Osha	Hor Mesa	internal dike	N75°W	N80°E				
	na	na	na	na	na	na	na	na	na	na	na	na	na				
	na	na	na	na	na	na	na	na	na	na	na	na	na				

na — not available

nd — no data

Tbas or Tbasalt — trachybasalt

N — normal magnetic polarity

R — reverse magnetic polarity

Appendix 2, continued.

Name Map Unit Sample No. Source Quad	Older Rhyolites and Rhyolite Pumice						Trachytes			
	GR obsidian Tgro	GR rhyolite Tgro	GR pumice Tgrt	West rhyolite Trw	Pumice fall Trt	East rhyolite Tre	Pumice fall Trt	Ch Trachyte Ttrc	Am Trachyte Ttr	Bio Trachyte Tbht
	F07-68	09KF-01	09KF-83	09KF-04	NM5030G	F14-52	F08-37	F13-31	F08-21	09KF-53
	Fellah	Fellah	Fellah	Fellah	Dunbar/ALS	ALS	Fellah	ALS	Fellah	Fellah
	Lobo Spgs	Lobo Spgs	San Mateo	Mt. Taylor	San Mateo	Mt. Taylor	Mt Taylor	Lag Canon	Mt Taylor	Mt Taylor
Major Oxides, wt%										
SiO ₂	75.68	75.93	75.93	73.79	74.07	68.67	70.34	63.1	61.02	65.94
TiO ₂	0.030	0.036	0.029	0.276	0.13	0.24	0.152	0.33	0.521	0.464
Al ₂ O ₃	13.67	13.59	13.48	13.74	13.76	16.27	15.58	17.34	18.08	16.65
Fe ₂ O ₃	—	—	—	—	—	2.58	—	5.83	—	—
FeO	0.72	0.81	0.89	2.09	2.00	—	2.66	—	6.16	4.20
MnO	0.125	0.12	0.100	0.058	0.06	0.06	0.127	0.18	0.202	0.120
MgO	0.02	0.02	0.05	0.32	0.04	0.05	0.09	0.21	0.40	0.39
CaO	0.51	0.46	0.32	1.04	0.58	0.51	0.65	0.97	2.07	1.18
Na ₂ O	4.95	4.72	4.51	4.07	3.70	6.05	4.12	6.73	6.79	5.88
K ₂ O	4.28	4.30	4.69	4.53	5.71	5.51	6.25	4.91	4.06	5.04
P ₂ O ₅	0.007	0.014	0.010	0.088	0.02	0.05	0.031	0.42	0.695	0.139
Total	100.00	100.0	100.0	100.00	99.99	99.99	100.00	100.02	100.00	100.00
Total Alk	9.23	9.02	9.20	8.60	9.41	11.56	10.37	11.64	10.85	10.92
F	0.32-0.42 ⁺	0.09 ⁺	0.36 ⁺ (6)	na	0.21 ⁺ (10)	na	na	na	na	na
Selected Trace Elements, ppm										
Ba	2	23	20	413	564	232	60	1005	1360	1048
Ce	13	24	25	48	134	184	223	151.5	159	136
Cr	4	3	3	3	<10	<10	3	10	2	4
La	6	5	12	32	69.1	93.2	106	80	77	71
Nb	178	171	192	36.1	76.4	93.8	126	109	98.4	86.9
Ni	0	2	2	1	2	1	3	<1	0	5
Pb	58	59	54	19	42	15	21	7	9	14
Rb	523	509	465	119	125	114	159	73.6	75	121
Sr	4	7	5	150	63.9	11.3	9	87.1	691	146
Th	27	27	26	21	15.3	13.1	23	11	12	15
U	7.9	8	8	6	3.59	3.83	5.9	2.7	3.2	6
Zr	105	108	119	167	554	884	553	950	656	692
Age (Ma)	3.498±0.003	3.18±0.01	3.33±0.07	3.03±0.11	3.08±0.20	2.91±0.04	2.9?	3.16±0.02	3.14±0.01	2.83±0.04
Magnetics	nd	N	nd	nd	nd	nd	nd	nd	nd	nd
Notes	glass	lava	pumice	lava	La Mosca Canyon	silicified	overlies Tandesite	Cerro Chivato	East end of AM	South of AM

na — not available

nd—no data

Tbas or Tbasalt — trachybasalt

N — normal magnetic polarity

R — reverse magnetic polarity

Appendix 2, continued.

Name Map Unit Sample No. Source Quad	Early Trachyandesite/Trachydacite										Trachydacite Pyroclastic		
	Tdacite Tbhtd	Tandesite Tta	Tdacite Tplu	Tdacite Tbhtd	Encl Tdacite Tpetd	Tandesite Tpta	Oliv Tand Ttai	Ign pumice Twst	Ign pumice Ttdt	Pumice fall Ttdt/Trt			
	09KF-36 Fellah	F08-14 Fellah	09KF-12 Fellah	F14-56 ALS	09KF-15A Fellah	09KF-30 Fellah	F08-79 Fellah	F11-84 Wolff	F08-85 ALS	F11-51 ALS			
Lobo Spgs	Mt Taylor	Mt Taylor	Mt Taylor	Mt Taylor	Cerro Pelón	Mt Taylor	San Mateo	Seboyeta	San Mateo	Seboyeta			
Major Oxides, wt%													
SiO ₂	63.88	58.22	63.79	62.5	63.57	61.38	57.57	66.55	62.77	69.33			
TiO ₂	0.667	1.569	0.747	0.83	0.806	1.175	1.507	0.346	0.65	0.170			
Al ₂ O ₃	17.10	17.81	17.15	17.06	17.00	17.02	16.79	16.87	17.87	16.09			
Fe ₂ O ₃	—	—	—	6.13	—	—	—	—	5.95	3.37			
FeO	5.05	7.47	4.90	—	5.19	6.36	7.90	3.25	—	—			
MnO	0.134	0.130	0.086	0.09	0.147	0.120	0.178	0.097	0.15	0.12			
MgO	1.52	1.82	0.55	0.81	0.66	1.25	2.19	0.79	0.87	0.23			
CaO	2.40	4.52	2.54	2.79	2.49	3.60	4.72	3.00	2.69	0.82			
Na ₂ O	5.38	4.91	5.65	5.27	5.45	5.13	5.48	4.19	4.51	3.87			
K ₂ O	4.44	3.21	4.29	4.16	4.29	3.49	3.09	4.79	4.20	5.98			
P ₂ O ₅	0.232	0.634	0.294	0.38	0.391	0.478	0.574	0.132	0.340	0.02			
Total	100.00	100.00	100.00	100.02	100.00	100.00	100.00	100.00	100.00	100.02			
Total Alk	9.82	8.12	9.94	9.43	9.74	8.62	8.57	8.98	8.71	9.85			
F	na	na	na	na	na	na	na	na	na	na			
Selected Trace Elements, ppm													
Ba	1093	738	1072	1045	1156	923	934	542	719	799			
Ce	124	97	120	122	119	104	117	91	124	80.6			
Cr	5	5	2	10	2	1	19	3	<10	<10			
La	66	50	68	61.2	68	57	62	52	68.8	100.5			
Nb	69.3	61.2	74.8	71.0	73.0	56.7	68.8	67.2	93.4	121			
Ni	5	9	1	<1	3	5	11	1	1	3			
Pb	11	10	10	8	10	12	9	13	9	21			
Rb	100	78	106	103	100	97	54	139	92.9	139			
Sr	322	502	346	388	332	476	510	275	418	23.8			
Th	7	9	12	11.6	13	11	10	17	15.1	18.5			
U	4	3	5	3.35	5	5	2.2	3	3.89	4.97			
Zr	524	433	628	590	520	403	444.0	458	506	594			
Age (Ma)	3.26±0.20	≤3.1	≥2.9	≥2.85	2.81±0.04	>2.76	2.79±0.03	2.87±0.04	2.79±0.09	2.70±0.01			
Magnetics	N	nd	nd	nd	N	N	nd	nd	nd	nd			
Notes	Rinconada Canyon	SE wall AM	West wall AM	North wall AM	West of AM	NW wall AM	N10°E plug/dike	East wall Water Canyon	Salazar Canyon	Chupadero Mesa			

na — not available nd—no data Thas or Tbasalt — trachybasalt N — normal magnetic polarity R — reverse magnetic polarity

Appendix 2., continued.

Name Map Unit Sample No. Source Quad	Plagioclase (Big Feldspar) Basalt and Related										Late Trachyandesite/Trachydacite												
	"Plag Basalt" F14-34 ALS Mt Taylor	"Plag Basalt" F08-18 Fellah Mt Taylor	"Plag Basalt" 09KF-32 Fellah San Mateo	Por B/land JRL-Weird ALS Lag Canon	Por B/land JRL-Weird ALS Lag Canon	Sugary Enc F08-122 Fellah Cerro Pelón	Hbd Tand 09KF-17 Fellah Mt Taylor	Hbd Tand 09KF-18 Fellah Mt Taylor	Por Tdacite 09KF-24 Fellah Cerro Pelón	Hbd Tand 09KF-26 Fellah Cerro Pelón	Bio Tdacite 09KF-27 Fellah Cerro Pelón	"Plag Basalt" F14-34 ALS Mt Taylor	"Plag Basalt" F08-18 Fellah Mt Taylor	"Plag Basalt" 09KF-32 Fellah San Mateo	Por B/land JRL-Weird ALS Lag Canon	Por B/land JRL-Weird ALS Lag Canon	Sugary Enc F08-122 Fellah Cerro Pelón	Hbd Tand 09KF-17 Fellah Mt Taylor	Hbd Tand 09KF-18 Fellah Mt Taylor	Por Tdacite 09KF-24 Fellah Cerro Pelón	Hbd Tand 09KF-26 Fellah Cerro Pelón	Bio Tdacite 09KF-27 Fellah Cerro Pelón	
Major Oxides, wt%																							
SiO ₂	50.64	54.10	57.49	54.96	55.6	62.52	57.91	59.69	66.28	57.27	65.90	57.49	54.96	55.6	62.52	57.91	59.69	66.28	57.27	65.90	57.49	54.96	
TiO ₂	2.510	1.82	1.581	1.695	1.38	0.953	1.580	1.211	0.409	1.646	0.440	1.581	1.695	1.38	0.953	1.580	1.211	0.409	1.646	0.440	1.581	1.695	
Al ₂ O ₃	16.67	17.87	17.51	18.19	17.51	17.09	16.95	17.08	17.10	17.23	17.11	17.51	18.19	17.51	17.09	16.95	17.08	17.10	17.23	17.11	17.51	18.19	
Fe ₂ O ₃	—	9.21	—	—	8.78	—	—	—	—	—	—	—	—	8.78	—	—	—	—	—	—	—	—	
FeO	10.60	—	7.30	8.07	—	5.68	7.53	6.88	3.55	7.55	3.61	7.30	8.07	—	5.68	7.53	6.88	3.55	7.55	3.61	7.30	8.07	
MnO	0.172	0.16	0.137	0.159	0.20	0.108	0.156	0.151	0.090	0.143	0.065	0.137	0.159	0.20	0.108	0.156	0.151	0.090	0.143	0.065	0.137	0.159	
MgO	5.00	2.41	2.14	2.91	2.51	0.88	2.08	1.86	0.31	2.59	0.36	2.14	2.91	2.51	0.88	2.08	1.86	0.31	2.59	0.36	2.14	2.91	
CaO	7.74	6.39	5.21	6.03	4.98	2.83	4.71	3.89	1.49	5.08	1.83	5.21	6.03	4.98	2.83	4.71	3.89	1.49	5.08	1.83	5.21	6.03	
Na ₂ O	4.08	4.80	4.75	4.82	5.37	5.37	4.93	5.13	5.53	4.90	5.64	4.75	4.82	5.37	5.37	4.93	5.13	5.53	4.90	5.64	4.75	4.82	
K ₂ O	1.81	2.39	3.26	2.56	3.02	4.06	3.44	3.54	5.11	3.02	4.90	3.26	2.56	3.02	4.06	3.44	3.54	5.11	3.02	4.90	3.26	2.56	
P ₂ O ₅	0.776	0.88	0.617	0.602	0.67	0.506	0.719	0.574	0.123	0.576	0.147	0.617	0.602	0.67	0.506	0.719	0.574	0.123	0.576	0.147	0.617	0.602	
Total	100.00	100.03	100.00	100.00	100.02	100.00	100.00	100.00	100.00	100.00	100.00	100.00	100.00	100.00	100.00	100.00	100.00	100.00	100.00	100.00	100.00	100.00	100.00
Total Alk	5.89	7.19	8.01	7.38	8.39	9.43	8.37	8.85	10.64	7.92	10.54	8.01	7.38	8.39	9.43	8.37	8.85	10.64	7.92	10.54	8.01	7.38	
F	na	na	na	na	na	na	na	na	na	na	na	na	na	na	na	na	na	na	na	na	na	na	
Selected Trace Elements, ppm																							
Ba	584	703	715	872	1765	768	892	912	1160	735	1286	715	872	1765	768	892	912	1160	735	1286	715	872	
Ce	87	93	97	102	85.5	116	118	112	99	102	123	97	102	85.5	116	118	112	99	102	123	97	102	
Cr	93	10	12	35	30	3	0	14	3	36	3	12	35	30	3	0	14	3	36	3	12	35	
La	46	44.3	52	50	45.3	58	61	57	54	46	65	52	50	45.3	58	61	57	54	46	65	52	50	
Nb	45.0	51.8	56.0	61.8	43.5	67.2	65.5	69.9	64.9	58.7	61.3	56.0	61.8	43.5	67.2	65.5	69.9	64.9	58.7	61.3	56.0	61.8	
Ni	68	<1	10	31	16	0	3	11	3	28	3	10	31	16	0	3	11	3	28	3	10	31	
Pb	4	<2	8.9	7	<2	11	8	11	12	8	13	8.9	7	<2	11	8	11	12	8	13	8.9	7	
Rb	27	41.4	74	41	31.2	88	80	71	105	68	98	74	41	31.2	88	80	71	105	68	98	74	41	
Sr	680	706	514	703	690	427	543	525	196	587	234	514	703	690	427	543	525	196	587	234	514	703	
Th	4	5.3	9.6	7	4.07	13	10	12	11	8	9	9.6	7	4.07	13	10	12	11	8	9	9.6	7	
U	2	1.62	2.8	2	0.50	3.6	3	3	3	4	3	2.8	2	0.50	3.6	3	3	3	4	3	2.8	2	
Zr	271	338	404	395	271	406	444	438	554	394	529	404	395	271	406	444	438	554	394	529	404	395	
Age (Ma)	2.76±0.06	>2.75	<2.8?	<2.86;	2.75?	2.71±0.06	2.70±0.02	2.73±0.01	2.71±0.03	2.63±0.07?	>2.66	2.76±0.06	>2.75	<2.8?	2.71±0.06	2.70±0.02	2.73±0.01	2.71±0.03	2.63±0.07?	>2.66	2.76±0.06	>2.75	
Magnetics	confused	nd	nd	nd	nd	N	N	confused	nd	nd	nd	confused	nd	nd	N	N	confused	nd	nd	nd	nd	nd	
Notes	South flank "classic" Trachybasalt	Seco Canyon B/Tandesite	South rim AM Tandesite	San Mateo hill B/Tandesite	North of Cerro Aguila	NW flank Mt Taylor	Flow below summit flow	Summit, Mt Taylor	"La Mosca" intrusion	North rim AM >2.7 Ma	North rim AM	Summit, Mt Taylor	Flow below summit flow	North of Cerro Aguila	NW flank Mt Taylor	Flow below summit flow	Summit, Mt Taylor	"La Mosca" intrusion	North rim AM >2.7 Ma	North rim AM	Summit, Mt Taylor	Flow below summit flow	
na	— not available	nd	— no data	Tbas or Tbasalt	— trachybasalt	N	— normal magnetic polarity	N	— normal magnetic polarity	R	— reverse magnetic polarity	N	— normal magnetic polarity	Tbas or Tbasalt	— trachybasalt	N	— normal magnetic polarity	N	— normal magnetic polarity	R	— reverse magnetic polarity	N	— normal magnetic polarity

Appendix 2., continued.

Name Map Unit Sample No. Source Quad	Late Trachyandesite/Trachydacite				Late Satellite Eruptions				Late Amphitheatr Dikes			
	Por Td Tbd	Plag Td Tpid	Hbd Tand Thrtd	Td Td Tbhd	Oliv Tand Tpota	Bio Td Tbhd	San Jose Can Tphtd	Hbd Tand Thta	S wall dike Tbi	Bio Td Tbi	Tandesite Ttai	Hbd Td Thbi
09KF-28 Fellah Cerro Pelón	62.28	09KF-38 Fellah Mt Taylor	09KF-59 Fellah Mt Taylor	F07-47 Fellah Lobo Spgs	F11-68 Wolff Seboyeta	F08-81 Fellah Cerro Pelón	F07-72 Fellah Mt Taylor	09KF-03 Fellah Lobo Spgs	F08-26 Fellah Mt Taylor	09KF-14 Fellah Mt Taylor	09KF-21 Fellah Mt Taylor	F08-13 Fellah Mt Taylor
Major Oxides, wt%												
SiO ₂	63.77	62.28	59.35	64.37	62.04	62.72	64.65	60.83	64.69	67.98	61.88	62.78
TiO ₂	0.786	1.085	1.267	0.722	0.952	0.803	0.628	1.062	0.675	0.365	0.949	0.893
Al ₂ O ₃	16.83	16.44	17.65	16.62	17.19	17.60	18.88	16.61	17.06	16.49	17.24	17.69
Fe ₂ O ₃	—	—	—	—	—	—	—	—	—	—	—	—
FeO	5.51	5.92	6.85	4.93	5.92	5.29	2.43	6.46	4.83	2.93	6.41	5.12
MnO	0.124	0.121	0.150	0.116	0.123	0.136	0.039	0.157	0.103	0.067	0.163	0.123
MgO	0.67	1.28	1.37	0.89	1.03	0.83	0.17	1.84	0.26	0.26	0.86	0.41
CaO	2.58	3.12	4.05	2.48	3.21	2.95	2.72	3.50	1.84	0.97	2.59	2.67
Na ₂ O	5.50	5.09	5.29	5.35	5.29	5.59	5.96	5.11	5.41	5.54	5.80	5.64
K ₂ O	3.94	4.15	3.46	4.15	3.82	3.79	4.28	3.93	4.86	5.29	3.75	4.21
P ₂ O ₅	0.281	0.513	0.559	0.368	0.436	0.292	0.259	0.511	0.268	0.103	0.347	0.480
Total	100.00	100.00	100.00	100.00	100.00	100.00	100.00	100.00	100.00	100.00	99.99	100.02
Total Alk	9.44	9.24	8.75	9.50	9.11	9.38	10.24	9.04	10.27	10.83	9.55	9.85
F	na	na	na	na	na	na	na	na	na	na	na	na
Selected Trace Elements, ppm												
Ba	1068	844	829	761	912	972	767	889	1004	841	971	987
Ce	119	115	106	110	109	128	121	122	116	104	113	111
Cr	1	2	8	2	4	1	3	12	2	2	1	2
La	65	62	57	58	54	99	63	62	66	53	54	54
Nb	63.7	70.3	67.0	67.6	66.2	72.6	87.8	71.1	74.0	83.4	72.0	73.6
Ni	2	3	9	3	3	5	3	11	2	3	2	4
Pb	13	13	12	12	12	14	12	9	14	14	9	12
Rb	104	97	79	97	84	93	105	82	127	123	84	101
Sr	377	365	550	389	430	475	461	464	260	115?	402	453
Th	11	13	10	16	12	12	16	13	15	17	11	14
U	4	3	2	5	3	5	5	4	5	5	4	4
Zr	459	518	453	439	485	528	528	457	635	635	501	525
Age (Ma)	2.66±0.01	2.78±0.05	<2.75	2.68±0.03	2.67±0.01	2.66±0.01	2.63±0.10	2.60±0.10	2.69±0.03	2.66±0.01	<2.7	2.64±0.06
Magnetics	N	N	nd	N	nd	N	nd	N	nd	N	nd	N
Notes	North rim AM	Overlies "plag basalt"	Ridge top AM	Rinconada Canyon	Long flow NE flank	Dome NW flank	South margin of map	Flow west flank	N20°W	N30°W	N60°W	Curves

na — not available

nd — no data

Tbas or Tbasalt — trachybasalt

N — normal magnetic polarity

R — reverse magnetic polarity

Appendix 2., continued.

Name Map Unit Sample No. Source Quad	Last Mount Taylor Amphitheater and Flank Eruptions										Young Tbasalts flanking Mount Taylor and on SW Mesa Chivato														
	Amph plug Tqtd	Amph plug Tqtd	Amph plug Tqtd	Spud Patch Tsptdu	Encl Tdacite Teta	Bas Tand Qbta	Gab plug Qxgi	Frio Flow Qmplb	Oliv Tbasalt Qqotb	Gab Tbasalt Qyptb	Cer Aguila Qfoqb	Ol Tbasalt Qyob	Amph plug Tqtd	Amph plug Tqtd	Amph plug Tqtd	Spud Patch Tsptdu	Encl Tdacite Teta	Bas Tand Qbta	Gab plug Qxgi	Frio Flow Qmplb	Oliv Tbasalt Qqotb	Gab Tbasalt Qyptb	Cer Aguila Qfoqb	Ol Tbasalt Qyob	
	F14-50	F09Kf-10	F14-50	F09-60	F07-04	F08-109	F08-43	F12-15	F12-50A	F08-90	F13-39	F09-37	F14-50	F09Kf-10	F14-50	F09-60	F07-04	F08-109	F08-43	F12-15	F12-50A	F08-90	F13-39	F09-37	
	Mt Taylor	Mt Taylor	Mt Taylor	Fellah	Fellah	Fellah	Fellah	Wolff	ALS	Fellah	ALS	Fellah	Mt Taylor	Mt Taylor	Mt Taylor	Mt Taylor	Mt Taylor	Mt Taylor	Mt Taylor	Seboyeta	Seboyeta	Fellah	ALS	Fellah	
	Seboyeta	Seboyeta	Cerro Pelón	Cerro Pelón	Mt Taylor	Cerro Pelón	Mt Taylor	Seboyeta	Seboyeta	Cerro Pelón	Lag Canon	Cerro Pelón	Seboyeta	Seboyeta	Cerro Pelón	Cerro Pelón	Cerro Pelón	Cerro Pelón	Seboyeta	Seboyeta	Cerro Pelón	Lag Canon	Cerro Pelón	Cerro Pelón	
Major Oxides, wt%																									
SiO ₂	68.61	71.11	62.28	61.38	55.03	47.82	48.46	49.09	49.60	48.48	48.48	48.48	47.70	48.46	49.09	49.60	48.48	49.09	49.60	48.46	49.09	49.60	48.48	48.48	
TiO ₂	0.522	0.322	0.838	1.234	1.762	2.454	2.66	3.242	2.25	2.629	2.629	2.629	3.331	2.66	3.242	2.25	2.629	3.242	2.25	2.66	3.242	2.25	2.629	2.629	
Al ₂ O ₃	15.29	14.73	17.37	16.60	18.71	15.06	15.84	17.13	16.20	16.19	16.19	16.19	16.93	15.84	17.13	16.20	16.19	17.13	16.20	15.84	17.13	16.20	16.19	16.19	
Fe ₂ O ₃	—	—	—	—	—	—	—	—	—	—	—	—	—	—	—	—	—	—	—	—	—	—	—	—	
FeO	3.50	2.94	5.58	6.29	7.90	11.18	11.18	13.02	12.53	11.50	11.50	11.50	13.02	—	12.53	—	11.50	13.02	12.53	—	12.53	—	11.50	11.50	
MnO	0.088	0.060	0.162	0.116	0.175	0.169	0.17	0.180	0.18	0.174	0.174	0.174	0.180	0.17	0.184	0.18	0.174	0.180	0.18	0.17	0.184	0.18	0.174	0.174	
MgO	0.73	0.55	1.03	1.80	2.02	8.64	8.64	5.09	5.88	6.65	6.65	6.65	5.09	5.88	4.47	5.30	6.65	5.09	5.88	5.88	4.47	5.30	6.65	6.65	
CaO	2.13	1.85	2.91	4.38	5.86	9.18	9.18	7.75	8.10	7.65	7.65	7.65	7.75	8.10	7.03	7.65	8.48	7.75	8.10	8.10	7.03	7.65	8.48	8.48	
Na ₂ O	4.91	4.82	5.41	4.89	5.19	3.50	3.50	3.94	4.15	3.95	3.95	3.95	3.94	4.15	4.02	4.30	3.95	3.94	4.15	4.15	4.02	4.30	3.95	3.95	
K ₂ O	3.97	4.18	3.76	2.84	2.70	1.40	1.40	1.43	1.69	1.26	1.26	1.26	1.43	1.69	1.67	1.81	1.26	1.43	1.69	1.69	1.67	1.81	1.26	1.26	
P ₂ O ₅	0.254	0.141	0.652	0.467	0.647	0.601	0.601	0.625	0.92	0.677	0.677	0.677	0.625	0.92	0.645	0.83	0.677	0.625	0.92	0.92	0.645	0.83	0.677	0.677	
Total	100.00	99.97	100.00	100.00	100.00	100.00	100.00	100.00	100.00	100.00	100.00	100.00	100.00	100.03	100.00	100.02	100.00	100.00	100.00	100.03	100.00	100.02	100.00	100.00	100.00
Total Alk	8.88	9.06	9.17	7.72	7.89	4.90	4.90	5.37	5.84	6.11	5.21	5.21	5.37	5.84	5.69	6.11	5.21	5.37	5.84	5.84	5.69	6.11	5.21	5.21	
F	na	na	na	na	na	na	na	na	na	na	na	na	na	na	na	na	na	na	na	na	na	na	na	na	
Selected Trace Elements, ppm																									
Ba	595	687	796	666	804	697	655	556	832	576	576	576	556	655	624	832	576	556	624	655	624	832	576	576	
Ce	84	70.1	124	70	103	66	83.5	69	148.5	70	70	70	69	83.5	75	148.5	70	69	75	83.5	75	148.5	70	70	
Cr	3	10	5	4	28	250	150	2	110	132	132	132	2	150	6	110	132	2	6	150	6	110	132	132	
La	48	40.6	61	35	50	37	42.3	35	36.7	33	33	33	35	42.3	35	36.7	33	35	35	42.3	35	36.7	33	33	
Nb	54.6	54.1	63.7	45.0	57.7	39.5	50.1	41.9	45.1	39.9	39.9	39.9	41.9	50.1	43.3	45.1	39.9	41.9	43.3	50.1	43.3	45.1	39.9	39.9	
Ni	3	<1	6	4	22	159	89	33	67	106	106	106	33	89	22	67	106	33	22	89	22	67	106	106	
Pb	13	9	11	9	4	4	<2	2	<2	4	4	4	2	<2	5	<2	4	2	5	<2	5	<2	4	4	
Rb	100	101	82	62	50	35	32.5	23	29.8	17	17	17	23	32.5	30	29.8	17	23	30	32.5	30	29.8	17	17	
Sr	369	367	465	614	721	818	887	739	737	759	759	759	739	887	764	737	759	739	764	887	764	737	759	759	
Th	21	18.6	15	11	7	4	5.31	4	3.85	4	4	4	4	5.31	4	3.85	4	4	4	5.31	4	3.85	4	4	
U	5	5	3	3.2	2.2	1.9	1.33	0?	1.05	3?	3?	3?	0?	1.33	3?	1.05	3?	0?	3?	1.33	3?	1.05	3?	3?	
Zr	265	277	410	239	371	212	257	233	258	223	223	223	233	257	259	258	223	233	259	257	259	258	223	223	
Age (Ma)	2.54±0.02	2.55	2.53±0.06	2.50±0.07	2.2?	1.97±0.05	2.32±0.01	2.44±0.01	2.25±0.01	2.18±0.06	2.18±0.06	2.18±0.06	2.44±0.01	2.32±0.01	2.30±0.13	2.25±0.01	2.18±0.06	2.44±0.01	2.30±0.13	2.32±0.01	2.30±0.13	2.25±0.01	2.18±0.06	2.18±0.06	
Magnetics	R	nd	R	R	nd	nd	confused	R	R	confused	confused	confused	R	confused	R	R	confused	R	R	confused	R	R	confused	confused	
Notes	Summit west AM	North margin west AM	Dome/flow North flank	SW rim AM	North flank Mt Taylor	Last intrusion	Upper flow Bear Canyon	East Sec 16 tank	Flow north of Mt Taylor	Flow west of Cerro Pelón	Flow west of Cerro Pelón	Flow west of Cerro Pelón	Flow north of Mt Taylor	Flow north of Bear Canyon	Flow north of Mt Taylor	Flow north of Bear Canyon	Flow west of Cerro Pelón	Flow north of Mt Taylor	Flow north of Mt Taylor	Flow north of Bear Canyon	Flow north of Mt Taylor	Flow north of Bear Canyon	Flow west of Cerro Pelón	Flow west of Cerro Pelón	

na — not available

nd—no data

Tbas or Tbasalt — trachybasalt

N — normal magnetic polarity

R — reverse magnetic polarity

Appendix 2., continued.

Name Map Unit Sample No. Source Quad	Young Tbasalts flanking MT/SW MChiv			Young Basalts, SW Mesa Chivato			Young Xenolith-bearing Trachybasalts flanking Mount Taylor			
	Plg Tbasalt F13-01 ALS Lag Canon	Hor Msa Dike F07-55 Fellah Lobo Spgs	Cerro Pelón F08-114 Fellah Cerro Pelón	Ol Basalt F13-02 ALS Lag Canon	Mxtle Basalt F09-40 Fellah Cerro Pelón	Porph basalt F13-34 ALS Lag Canon	C Redondo C13-10 ALS Lag Canon	Quarry Tbas F08-74 Fellah San Mateo	Xeno Tbas F09-21 Fellah Cerro Pelón	Xeno Tbas F09-47 Fellah Cerro Pelón
	Qatd	Qyatl	Qolpb	Qocpb	Qfpod	Qfocr	Qyxtb	Qyxtb	Qyxtb	Qfqxb
SiO ₂	47.04	48.38	45.27	46.73	47.20	46.47	48.73	48.85	49.18	50.08
TiO ₂	3.14	2.257	2.48	2.931	2.81	2.42	2.096	2.092	1.990	2.188
Al ₂ O ₃	16.82	15.39	12.19	16.31	16.35	14.86	15.74	15.13	16.03	16.30
Fe ₂ O ₃	14.25	—	13.43	—	12.70	12.78	—	—	—	—
FeO	—	10.54	—	12.35	—	—	10.74	10.74	10.80	11.08
MnO	0.18	0.156	0.17	0.184	0.15	0.17	0.161	0.158	0.159	0.152
MgO	5.29	8.28	13.53	7.10	8.66	8.60	7.76	8.09	6.97	8.34
CaO	7.34	8.16	8.66	8.93	8.60	9.45	8.23	8.18	7.48	8.17
Na ₂ O	3.90	4.22	2.79	3.36	3.46	3.30	4.06	4.14	4.56	3.91
K ₂ O	1.45	1.87	1.03	1.17	1.25	1.31	1.76	1.84	2.10	1.72
P ₂ O ₅	0.57	0.741	0.45	0.947	0.62	0.64	0.709	0.771	0.736	0.631
Total	99.98	100.00	100.00	100.00	100.00	100.00	100.00	100.00	100.00	100.00
Total Alk	5.35	6.09	3.82	4.53	4.71	4.61	5.82	5.98	6.66	6.41
F	na	na	na	na	na	na	na	na	na	na

Major Oxides, wt%**Selected Trace Elements, ppm**

Ba	513	839	638	1119	622	574	870	775	919	828	873
Ce	60.1	77	49.7	71	103	63.8	76	80	88	81	59
Cr	20	221	520	173	150	270	202	234	143	236	103
La	28.5	39	22.4	37	26.2	32.3	41	33	37	43	31
Nb	40.5	46.3	30.2	36.0	33.7	40.0	41.9	45.1	52.0	47.3	40.9
Ni	26	154	458	105	103	161	140	137	121	168	86
Pb	2	4.2	6	3	<2	23	4.4	4	3	4	5
Rb	20.4	31	14.9	13	16.4	20	27	32	39	31	37
Sr	784	863	597	830	722	785	834	833	918	851	838
Th	2.91	4.3	2.88	3	2.71	3.64	4	3	5	4	5
U	0.87	1.4	0.72	3?	0.41	1.58	1.3	2	2	1	0?
Zr	199	244	146	182	189	187	225	246	290	238	221
Age (Ma)	2.13±0.01	1.80±0.01	2.41±0.02	2.31±0.06	2.1?	1.90±0.03	1.74±0.03	1.79±0.05	1.8?	1.85±0.06	1.75?
Magnetics	R	N	nd	R	R	N	R	N	N	R	R
Notes	Flow north quad edge	Dike at base of cone	Young flow Aphy Tbasalt	Flow west of cone	Dike in cone	Dike in cone summit	Distal part of flow	Distal Mesa Cuchilla	Amer. Canyon mid-flow	Near cone	Overlies QTvs

na — not available nd — no data Tbas or Tbasalt — trachybasalt N — normal magnetic polarity R — reverse magnetic polarity

Appendix 2., continued.

Young Qtz-bearing Tbasalts flanking Mount Taylor

Name	Qtz Tbasalt	Qtz Tbasalt	Qtz Tbasalt	Cerro Ortiz
Map Unit	Qfqtbb	Qfqtbb	Qfqtbb	Qfqtbb
Sample No.	F07-12	09KF-41	F08-115	flow 11, no. 10
Source	Fellah	Fellah	Fellah	L&M 1972
Quad	Lobo Spgs	Lobo Spgs	Cerro Pelón	Seboyeta

Major Oxides, wt%

SiO ₂	48.21	48.78	49.51	50.1
TiO ₂	2.228	2.118	1.968	1.9
Al ₂ O ₃	15.34	15.63	15.54	15.3
Fe ₂ O ₃	—	—	—	2.6
FeO	11.06	10.67	10.72	8.0
MnO	0.162	0.162	0.161	0.15
MgO	8.58	8.35	8.12	8.1
CaO	8.65	8.54	8.41	8.0
Na ₂ O	3.57	3.54	3.68	3.6
K ₂ O	1.65	1.66	1.42	1.7
P ₂ O ₅	0.553	0.560	0.475	0.56
Total	100.00	100.00	100.00	100.1
Total Alk	5.23	5.20	5.10	5.3
F	na	na	na	na

Selected Trace Elements, ppm

Ba	772	909	629	1000
Ce	60	70	52	—
Cr	225	224	234	250
La	26	31	29	86?
Nb	36.3	41.4	33.2	36
Ni	164	158	162	170
Pb	3.9	4	3.6	—
Rb	26	28	23.4	—
Sr	779	830	657	670
Th	3.2	4	3.6	—
U	1	1	1.3	—
Zr	199	212	186	220
Age (Ma)	1.6?	1.64±0.04	1.53±0.07	1.56±0.17
Magnetics	confused	R	R	R
Notes	NE Horace	NE Horace	Near Cerro	Date from
	Mesa	Mesa	Pelón	L&M (1979)
				S of F07-12

* Sample locations are keyed to map units. Major element analyses are normalized to 100 weight %.
 † F values from WoldeGabriel et al. (1999) and N. Dunbar (NMBGMR, unpublished data). Sample F07-68 shows range of two analyses.
 Sample 09KF-83 is an average of six analyses.
 Sample NM5030G is an average of ten analyses.

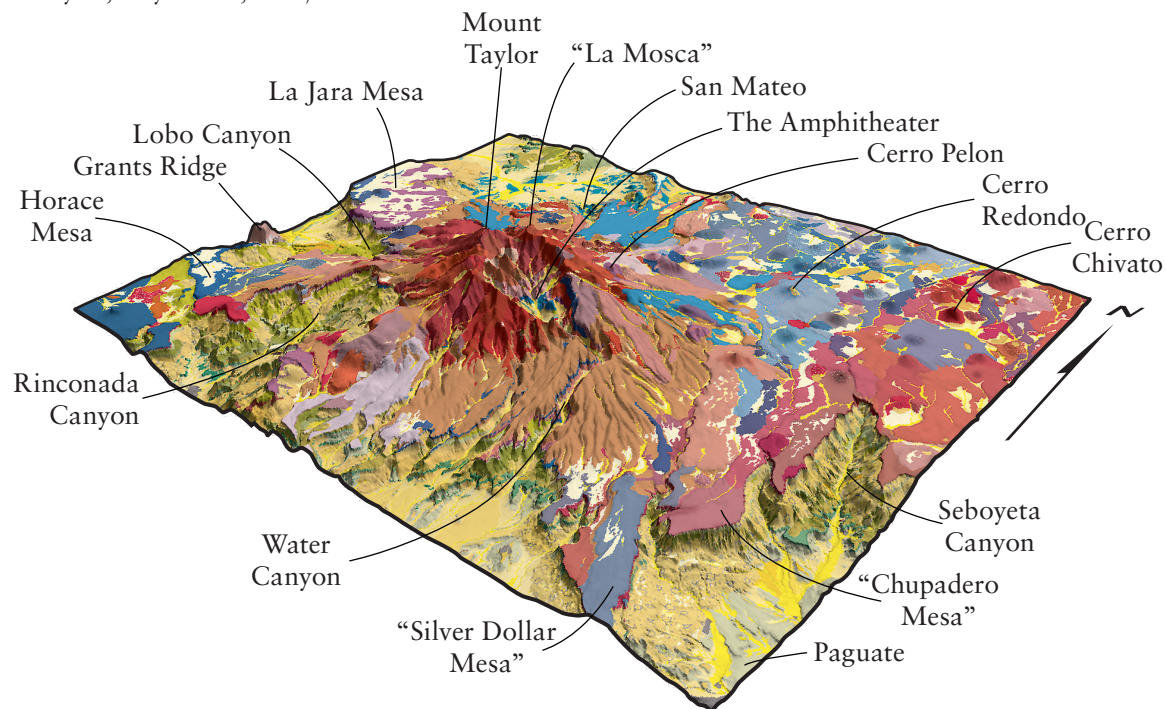
Appendix 3. Photo figures with UTM locations (NAD 83) and (NAD27)

FIGURE	EASTING (NAD83)	NORTHING (NAD83)	EASTING (NAD27)	NORTHING (NAD27)
3b	275550	3905104	275600	3904900
3c	282950	3904204	283000	3904000
6	257750	3893004	257800	3892800
7	255850	3894354	255900	3894150
10	277750	3895204	277800	3895000
11	258850	3910004	258900	3909800
12	267950	3901704	268000	3901500
15	262550	3903704	262600	3903500
16	262800	3905004	262850	3904800
17	266150	3900204	266200	3900000
18	262850	3903004	262900	3902800
19	268050	3900484	268100	3902800
20	267950	3906204	268000	3906000
21	250350	3900204	250400	3900000
22	251830	3905054	251880	3904850
23	256950	3897304	257000	3897100
24	256900	3897344	256950	3897140
25	261465	3890624	261515	3890420
26	282750	3912204	282800	3912000
27	279850	3904704	279900	3904500
29	273650	3894804	273700	3894600
30a	257450	3906804	257500	3906600
30b	260232	3900065	260282	3899861
31	265250	3910904	265300	3910700
32	258250	3901704	258300	3901500
34	249950	3903004	250000	3902800
35	258950	3891304	259000	3891100
36	259150	3891604	259200	3891400
38	267450	3901304	267500	3901100
40	254150	3890304	254200	3890100
40	258450	3890904	258500	3890700
41	256750	3895504	256800	3895300
42	275550	3906604	275600	3906400
45	266650	3901054	266700	3900850
46	282000	3911654	282050	3911450
47	254950	3896204	255000	3896000
48	275450	3914304	275500	3914100
50	282250	3899504	282300	3899300
52	260050	3891054	260100	3890850
53	260350	3891304	260400	3891100

Mount Taylor Physical Setting

Mount Taylor summit is located 20 km northeast of the small city of Grants (population about 9,200 in 2016) in west-central New Mexico (Fig. 2). The volcano forms a broad conical highland (Cover photo) cresting at an elevation of 3,445 m (11,301 ft) and is surrounded by several lava-capped mesas at elevations of roughly 2,440 m (8,000 ft). Lowest elevations are located along the Río Paguete at 1,838 m (6,030 ft) near the southeast corner of the map. Ponderosa pine, blue spruce, white pine, and aspen forest characterize the higher elevations, which can receive several meters of snow in winter. Piñon-juniper forest, sagebrush, and chamisa (rabbitbrush) are most common at lower elevations. Watercourses contain cottonwood and sycamore. The mountain areas are home to black bear, cougar, and elk, whereas deer, coyote, feral horses, and rattlesnakes are more common on the mesas and basins. While the regional climate is semi-arid, Mount Taylor and Mesa Chivato, however, are classified as boreal or warm temperate with high humidity and warm summers. Summer monsoons bring thunder, lightning, and bursts of rain from late June through August. Average yearly precipitation in Grants from weather records is 267 mm/year (10.5 in/year) while the Mount Taylor summit and Amphitheater receive more than 800–900 mm/year (31–35 in/year; Meyer et al., 2014).

The largest mesa is Mesa Chivato, which extends beyond the northeast corner of our map, but other significant mesas include La Jara to the west and Horace to the southwest. Mesa Chivato can be divided into several smaller mesas herein named Seboyetita Mesa, Chupadero Mesa, Silver Dollar Mesa and Encinal Mesa. The mesas are flanked or cut by several basins and canyons that expose primarily Cretaceous and older strata, but which also may expose capping layers of lavas and beds of silicic tuffs. The most significant canyon flanking the volcano is Water Canyon. It holds the largest perennial stream, which drains the eastern end of Mount Taylor Amphitheater before turning south. On the west is the basin that includes the village of San Mateo and the San Mateo (or Mount Taylor) uranium mine. Coal Mine basin and Lobo Canyon lie to the southwest between La Jara and Horace mesas. Rinconada basin and Rinconada Canyon lie to the south-southwest. Several smaller but relatively deep canyons such as Seco and Two Mile canyons also drain to the south. Encinal, Bear, Paguete, and Seboyeta canyons drain the southeast side of the volcanic highland. The only basin to the north is San Lucas Valley, which is normally dry.



Oblique view looking northwest to Mount Taylor (3,445 m, 11,301 ft) and southwest Mesa Chivato to the right, showing geology superimposed on elevation. Note the clustering of 3.2–2.5 Ma, intermediate to silicic domes and flows in the summit area (crimson reds to purples) and the large, coalesced, Plio-Pleistocene fan of volcanic debris (brown), formed by erosion of material from the summit amphitheater and shed to the east-southeast. Younger, 2.5–1.26 Ma mafic rocks (lava flows) (mostly blues, grayish-blues, and violets) drape the flanks of the volcano. The 3.16 Ma Cerro Chivato (crimson red dome in the northeast) is part of an older volcanic center in southwestern Mesa Chivato now largely flooded by younger, 1.9–2.5 Ma basaltic lavas. Cretaceous rocks (green and yellow-green), which underlie the volcanic pile, are well exposed in canyons draining south, as well as in the San Mateo area in the northwest.